

# Field Quantization in 5D Space-Time with $Z_2$ -parity and Position/Momentum Propagator

S. Ichinose<sup>1</sup> and A. Murayama<sup>2</sup>

November 11, 2018

<sup>1</sup> *Laboratory of Physics, School of Food and Nutritional Sciences, University of Shizuoka Yada 52-1, Shizuoka 422-8526, Japan; E-mail: ichinose@smail.u-shizuoka-ken.ac.jp*

<sup>2</sup> *Department of Physics, Faculty of Education, Shizuoka University, Shizuoka 422-8529, Japan; E-mail: a-murayama@mountain.ocn.ne.jp*

## Abstract

Field quantization in 5D flat and warped space-times with  $Z_2$ -parity is comparatively examined. We carefully and closely derive 5D position/momentum(P/M) propagators. Their characteristic behaviours depend on the 4D (real world) momentum in relation to the boundary parameter ( $l$ ) and the bulk curvature ( $\omega$ ). They also depend on whether the 4D momentum is space-like or time-like. Their behaviours are graphically presented and the  $Z_2$  symmetry, the "brane" formation and the singularities are examined. It is shown that the use of absolute functions is important for properly treating the singular behaviour. The extra coordinate appears as a *directed* one like the temperature. The  $\delta(0)$  problem, which is an important consistency check of the bulk-boundary system, is solved *without* the use of KK-expansion. The relation between P/M propagator (a closed expression which takes into account *all* KK-modes) and the KK-expansion-series propagator is clarified. In this process of comparison, two views on the extra space naturally come up: orbifold picture and interval (boundary) picture. Sturm-Liouville expansion ( a generalized Fourier expansion ) is essential there. Both 5D flat and warped quantum systems are formulated by the Dirac's bra and ket vector formalism, which shows the warped model can be regarded as a *deformation* of the flat one with the *deformation parameter*  $\omega$ . We examine the meaning of the position-dependent cut-off proposed by Randall-Schwartz.

PACS: PACS NO: 04.50.+h, 11.10.Kk, 11.25.Mj, 12.10.-g 11.30.Er,

Keywords: position/momentum propagator, Sturm-Liouville, deformation, singularity,  $Z_2$ -parity,  $\delta(0)$  problem, Randall-Schwartz, Bessel function, absolute value

# 1 Introduction

Since the discovery of the wall picture model of our space-time in 1999 by Randall and Sundrum[1, 2], eight years have passed. The model has surely brought a new tool to extend the standard model in the particle physics and in the cosmology. The mass hierarchy between the Weak scale and the Planck scale can be introduced more naturally than any other models before. The exponentially damping factor along the extra coordinate cause the mass scale so rapidly damp that the widely-ranging mass scales in nature could be naturally explained. Although it is still regarded as one of promising candidates as a beyond-standard model, some fundamental points below are not clear.

1. Stableness of the Randall-Sundrum(RS) model I
2. Renormalizability
3. Physical observables, BRS structure

The second and third ones are common problems in the higher dimensional (field theory) models. At the beginning stage of the model, it may be allowed to disregard them for the reason that it is an effective theory which should be derived from a more fundamental one such as the string theory, D-brane theory and M-theory. Recently, however, the above problems have gradually become serious because, inspired by the soon-coming LHC experiment, we are compelled to estimate the extra-dimensional effect in some physical quantities such as the B-physics experiments data, the electric dipole moment[3] and the hadron spectroscopy[4]. The problems cited above make these calculations have some ambiguity.

A source of (technical) difficulty of higher-dimensional models is the summation of all KK modes. In Ref.[5, 6, 7, 8], a new type propagator which takes into account *all* KK-modes was used. In the paper by Randall-Schwartz[9], it was closely examined and was called position/momentum(P/M) propagator. It was applied to the  $\beta$ -function calculation and the analysis of the unification of coupling in GUTs. We focus on the P/M propagator behavior and the relation to the familiar KK-expansion approach. In the analysis two kinds of standpoints about the extra axis naturally appear. They were pointed out by Hořava and Witten [10, 11] in the context of Calabi-Yau compactification of eleven-dimensional supergravity and  $E_8 \times E_8$  heterotic string affairs. One is called *orbifold* approach. We regard the extra space as  $S_1/Z_2$  by requiring, in the real space  $\mathbf{R}$ , the periodicity and  $Z_2$ -parity symmetry. The other view is called the *interval* approach. We simply regard the extra space a finite interval  $[0, l]$ . We will examine the two approaches comparatively.

Another difficulty is the lack of the clear systematic treatment of singular functions which have singularities at fixed points. We must handle functions involving  $\delta(x)$  and  $\epsilon(x)$  in relation to the symmetry requirement. We have been worried by the consistency with the field equation. We will develop a new method using the absolute function.

P/M propagator approach also gives us some new treatment about the regularization of divergences in quantization. It has a coordinate (position parameter), instead of a

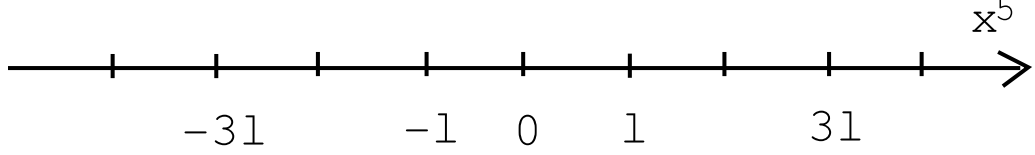
momentum, for the extra space description. In the original paper[9], the real world 4-momentum integral is regularized by the extra-space *position-dependent* cutoff. In fact the regularization successfully works in the Randall-Schwartz's paper and the finite  $\beta$ -function of the gauge coupling is obtained. This kind of regularization had never been taken before Ref.[9].

The content is organized as follows. We start by, in Sec.2, the 5D massless scalar field propagator on  $\mathcal{M} \times S^1/Z^2$ . It serves as the firm reference that is compared later with the warped case. For the quantization of 5D space-time, we introduce Dirac's bra and ket vector formalism in Sec.3. This is again the preparation for the quantization of the 5D warped space-time. In Sec.4, P/M propagator is explained carefully taking the simple model of Sec.2. A systematic treatment of the extra coordinate, in relation to the symmetrization of the P/M propagator, is explained. It is shown that, in Sec.5, the KK-expansion approach of Sec.2 and the P/M propagator approach of Sec.4 are related by the Fourier expansion. In Sec.6, the warped space-time is treated using the eigen-function expansion. Two alternative coordinates,  $y$  and  $z$ , are used. Through the Dirac's formalism analysis of the warped system, we see it is a deformation of the flat system with the deformation parameter (bulk curvature) $\omega$ . P/M propagator is obtained with much care for the  $Z_2$  symmetry and the singularity in Sec.7. The  $z$ -coordinate is used there. In Sec.8, the relation between the eigen-function expansion approach (Sec.6) and the P/M propagator approach (Sec.7) is clarified using the Sturm-Liouville expansion. As the visual output of the present analysis, we present the graphical display of the P/M propagators in Sec.9. We can clearly see how the characteristic scales and  $Z_2$ -symmetry appear, in particular, the distinct propagator behaviours between the flat and warped cases. The  $\delta(0)$ -problem, which generally appear in the bulk-boundary system, is solved, in Sec.10, using the results obtained before. We conclude in Sec.11. Three appendices are ready to supplement the text. App.A explains the Sturm-Liouville expansion in relation to the familiar Fourier expansion. In App.B, a general treatment of the propagator is given. In App.C, we display the propagator graphs for various interesting cases: 1) flat massless scalar with  $Z_2$ -parity even, Neumann-Neumann boundary condition (b.c.); 2) flat massless scalar with  $Z_2$ -parity odd, Dirichlet-Neumann b.c.; 3)  $z$ -representation, warped scalar with  $Z_2$ -parity odd, Dirichlet-Dirichlet b.c., space-like; 4) warped massless vector with  $Z_2$ -parity even, Neumann-Neumann b.c., space-like; 5)  $z$ -representation of 4); 6) warped massless vector with  $Z_2$ -parity even, Neumann-Neumann b.c., time-like.

## 2 5D propagator on flat geometry $\mathcal{M}_4 \times S^1/Z^2$

The simplest and most popular higher-dimensional model is 5D model with the circle as the one extra space-manifold. It began with the original ones by Kaluza[12] and Klein[13]. The bulk curvature vanishes, hence we call this model 'flat model' in comparison with 'warped model' later explained. We first consider the 5D massless scalar, on  $S^1/Z^2$ , interacting with

Figure 1: The extra space  $\mathbf{R} = (-\infty, \infty)$  in which the propagator is periodically (periodicity  $2l$ ) defined.



an external source  $J(X)$ .

$$S = \int d^5X \left( -\frac{1}{2} \partial_M \Phi \partial^M \Phi + J \Phi \right) , \quad (\eta^{MN}) = \text{diag}(-1, 1, 1, 1, 1) , \\ (X^M) = (x^m, x^5) \equiv (x, x^5) , \quad M, N = 0, 1, 2, 3, 5; \quad m, n = 0, 1, 2, 3. \quad (1)$$

The field  $\Phi$  and the source  $J$  have the properties:

$$(1) \text{ Periodicity} \quad \Phi(x, x^5) = \Phi(x, x^5 + 2l) , \quad J(x, x^5) = J(x, x^5 + 2l) , \\ (2) \text{ Z}_2\text{-property (5D parity)} \quad \Phi(x, x^5) = P\Phi(x, -x^5) , \quad J(x, x^5) = PJ(x, -x^5) , \quad (2)$$

where  $P = -1$  (odd) or  $+1$  (even). The above choice comes from the requirement that the 5D theory (1) is  $Z_2$ -invariant. The extra space manifold is shown in Fig.1. From the periodicity, we can express as

$$\Phi(x, x^5) = \sum_{n \in \mathbf{Z}} \phi_n(x) e^{i \frac{n\pi}{l} x^5} , \quad (3)$$

where  $\mathbf{Z}$  is the set of all integers. This is the Kaluza-Klein (KK) expansion. The  $Z_2$ -property (2) requires the above coefficients to be

$$\phi_n(x) = \mp \phi_{-n}(x) \quad \text{for} \quad P = \mp . \quad (4)$$

The plural signs  $P = \mp$  used in the paper mean that the upper sign case (lower sign case) corresponds to that of another quantities.

In particular,  $\phi_0 = 0$  for the odd case ( $P = -1$ ).<sup>1</sup> Then we obtain

$$\Phi(x, x^5) = \begin{cases} 2i \sum_{n=1}^{\infty} \phi_n(x) \sin\left(\frac{n\pi}{l} x^5\right), & P = -1 \\ \phi_0(x) + 2 \sum_{n=1}^{\infty} \phi_n(x) \cos\left(\frac{n\pi}{l} x^5\right), & P = +1 \end{cases} . \quad (5)$$

The odd and even functions w.r.t.  $x^5$  appear for  $P = -1$  case and for  $P = 1$  case respectively. Similarly for  $J(x)$ .

$$J(x, x^5) = \begin{cases} 2i \sum_{n=1}^{\infty} j_n(x) \sin\left(\frac{n\pi}{l} x^5\right), & P = -1 \\ j_0(x) + 2 \sum_{n=1}^{\infty} j_n(x) \cos\left(\frac{n\pi}{l} x^5\right), & P = +1 \end{cases} . \quad (6)$$

<sup>1</sup> There is *no* zero mode for the odd parity. This fact will be utilized in some places later.

Using the orthogonality relations:

$$\begin{aligned} \int_{-l}^l dx^5 \sin\left(\frac{m\pi}{l}x^5\right) \sin\left(\frac{n\pi}{l}x^5\right) &= \begin{cases} 0 & m \neq n \\ l & m = n (\neq 0) \\ 0 & m = n = 0 \end{cases}, \\ \int_{-l}^l dx^5 \cos\left(\frac{m\pi}{l}x^5\right) \cos\left(\frac{n\pi}{l}x^5\right) &= \begin{cases} 0 & m \neq n \\ l & m = n (\neq 0) \\ 2l & m = n = 0 \end{cases}, \end{aligned} \quad (7)$$

the equation (6) is "inverted" w.r.t.  $j_n$ .

$$P = -1 \quad , \quad j_n(x) = \frac{1}{2il} \int_{-l}^l dx^5 J(x, x^5) \sin\left(\frac{n\pi}{l}x^5\right), \quad n = 1, 2, 3, \dots \quad (8)$$

$$P = +1 \quad , \quad j_n(x) = \frac{1}{2l} \int_{-l}^l dx^5 J(x, x^5) \cos\left(\frac{n\pi}{l}x^5\right), \quad n = 0, 1, 2, 3, \dots \quad (9)$$

With above properties purely from the boundary conditions, let us solve the 5D field equation of (1).

$$\partial_M \partial^M \Phi(X) = -J(X) \quad . \quad (10)$$

Inserting (5) and (6), we obtain the 4D Klein-Gordon equation for the n-th Kaluza-Klein mode.

$$\{\partial_m \partial^m - \left(\frac{n\pi}{l}\right)^2\} \phi_n(x) = -j_n(x) \quad , \quad \begin{cases} n = 1, 2, \dots & P = -1 \\ n = 0, 1, 2, \dots & P = 1 \end{cases}, \quad (11)$$

where  $\partial_M \partial^M = \partial_m \partial^m + \partial_5 \partial_5$  ( $(\eta^{mn}) = \text{diag}(-1, 1, 1, 1)$ ) is used. <sup>2</sup> We note the massless mode appears for the even case ( $P=1$ ) and does not for the odd case ( $P=-1$ ).  $\phi_n(x)$  can be solved by the Feynman propagator.

$$\begin{aligned} \phi_n(x) &= \int d^4y \Delta_F^n(x - y) j_n(y) \quad , \\ \{\partial_m \partial^m - \left(\frac{n\pi}{l}\right)^2\} \Delta_F^n(x - y) &= -\delta^4(x - y), \quad \Delta_F^n(x) = \int \frac{d^4k}{(2\pi)^4} \frac{e^{-ikx}}{k^2 + \left(\frac{n\pi}{l}\right)^2 - i\epsilon} \quad , \end{aligned} \quad (12)$$

where  $k^2 = k_m k^m = -(k^0)^2 + (k^1)^2 + (k^2)^2 + (k^3)^2$ . Using (5), (12) and (9), we finally obtain

$$\begin{aligned} \Phi(X) &= \int d^4y \int_{-l}^l dy^5 \Delta_F(X, Y) J(Y), \quad (X^M) = (x^m, x^5), (Y^M) = (y^m, y^5), \\ \Delta_F(X, Y) &= \frac{1}{2l} \sum_{n \in \mathbf{Z}} \Delta_F^n(x - y) \frac{1}{2} (e^{-i\frac{n\pi}{l}(x^5 - y^5)} + P e^{-i\frac{n\pi}{l}(x^5 + y^5)}) \\ &= \int d^5K \frac{e^{-ik(x-y)}}{k^2 + (k^5)^2 - i\epsilon} \frac{1}{2} (e^{-ik^5(x^5 - y^5)} + P e^{-ik^5(x^5 + y^5)}) \quad , \end{aligned} \quad (13)$$

---

<sup>2</sup> The set of eigenvalues  $\{n\pi/l | n = 1, 2, 3, \dots\}$  for  $P = -1$  and  $\{n\pi/l | n = 0, 1, 2, \dots\}$  for  $P = 1$ , are the same except the zero mode. They are *equally* spaced. This is contrasting with the warped case appeared later (61).

where  $\int d^5 K \equiv \frac{1}{2l} \sum_{k^5} \int \frac{d^4 k}{(2\pi)^4}$ ,  $\{k^5\} \equiv \{\frac{n\pi}{l} | n \in \mathbf{Z}\}$ . Later we will come back here to confirm a result obtained by the new approach is correct. <sup>3</sup> 5D propagator  $\Delta_F(X, Y)$  satisfies

$$\partial_M \partial^M \Delta_F(X, Y) = -\frac{1}{2} (\delta^5(X - Y) + P \delta^5(X - \tilde{Y})) , \quad (14)$$

where  $(Y) = (y^m, y^5)$ ,  $(\tilde{Y}) = (y^m, -y^5)$  and  $\hat{\delta}(x^5 \mp y^5) \equiv \frac{1}{2l} \sum_{n \in \mathbf{Z}} \exp\{-i\frac{n\pi}{l}(x^5 \mp y^5)\}$  is the *periodic* delta function with the periodicity  $2l$ .

### 3 Dirac's bra and ket vector formalism

P.A.M. Dirac[14] introduced "bra and ket vector formalism" to formulate the quantum theory in the abstract way. The formalism clearly presents the orthogonality and the completeness relation between quantum states. In the completeness relation, Dirac's delta function generally appears. It is a singular function which should be properly treated. We show the 5D quantum field theory on  $Z_2$ -orbifold (flat case and warped case) can be naturally expressed in this formalism.

We introduce bra-vectors  $\langle K |$ ,  $\langle X |$ , and ket-vectors  $|K\rangle$ ,  $|X\rangle$ , in the Hilbert space of (abstract) quantum states labeled by 5D momentum  $K$  and by 5D coordinate  $X$ .

$$\begin{aligned} e^{iK \cdot X} &= \exp\{ik_m \cdot x^m + ik_5 x^5\} \equiv \langle K | X \rangle , \\ e^{-iK \cdot X} &= \exp\{-ik_m \cdot x^m - ik_5 x^5\} \equiv \langle X | K \rangle , \\ \langle K | X \rangle^* &= \langle X | K \rangle , \end{aligned} \quad (15)$$

where  $(K_M) = (k_m, k_5 = \frac{n\pi}{l})$ ,  $(X^M) = (x^m, x^5)$ ,  $(\eta^{MN}) = \text{diag}(-1, 1, 1, 1, 1)$  and the symbol " $*$ " means the complex conjugate operation. From the *completeness* property of  $e^{ikx}$ , we know

$$\begin{aligned} \int \frac{d^4 k}{(2\pi)^4} \frac{1}{2l} \sum_{k_5} \langle X | K \rangle \langle K | Y \rangle &\equiv \int d^5 K \langle X | K \rangle \langle K | Y \rangle \\ &= \delta^4(x - y) \hat{\delta}(x^5 - y^5) \equiv \delta^5(X - Y) , \end{aligned} \quad (16)$$

$$\begin{aligned} \int \frac{d^4 x}{(2\pi)^4} \frac{1}{2l} \int_{-l}^l dx^5 \langle K | X \rangle \langle X | P \rangle &\equiv \frac{1}{2l} \int d^5 X \langle K | X \rangle \langle X | P \rangle \\ &= \delta^4(k - p) \delta_{k_5 p_5} \equiv \frac{1}{2l} \delta^5(K - P) , \end{aligned} \quad (17)$$

where  $\hat{\delta}(x^5 - y^5) \equiv \frac{1}{2l} \sum_{n \in \mathbf{Z}} \exp\{-i\frac{n\pi}{l}(x^5 - y^5)\}$  and  $\hat{\delta}(k_5 - p_5) \equiv 2l \delta_{k_5 p_5}$  are used. We *require* the orthogonality between the coordinate states  $|X\rangle$ , and the momentum states  $|K\rangle$ .

$$\langle X | Y \rangle = \delta^5(X - Y) , \quad \langle K | P \rangle = \delta^5(K - P) , \quad (18)$$

---

<sup>3</sup> Note that the arguments in  $\Delta_F$  should not be  $X - Y$ , because P-part is the function of  $x^5 + y^5$ , not of  $x^5 - y^5$ .

then the *completeness*,

$$\int d^5K |K><K| = 1 \quad , \quad \int d^5X |X><X| = 1 \quad , \quad (19)$$

is deduced.

The 5D flat propagator  $\Delta_F(X, Y)$  of the previous section can be expressed as

$$\begin{aligned} \Delta_F(X, Y) &= \frac{1}{2l} \sum_{n \in \mathbf{Z}} \int \frac{d^4k}{(2\pi)^4} \frac{e^{-ik(x-y)}}{k^2 + (\frac{n\pi}{l})^2 - i\epsilon} \times \frac{1}{2} (e^{-i\frac{n\pi}{l}(x^5-y^5)} + Pe^{-i\frac{n\pi}{l}(x^5+y^5)}) \\ &= \int d^5K \frac{1}{K^2 - i\epsilon} \frac{1}{2} (e^{-iK(X-Y)} + Pe^{-iK(X-\tilde{Y})}) \quad , \end{aligned} \quad (20)$$

where  $\tilde{Y}^M \equiv (y^m, -y^5)$ . This can be further expressed as

$$\begin{aligned} \Delta_F(X, Y) &= \frac{1}{2} \int d^5K \frac{<X|K><K|Y> + P <X|K><K|\tilde{Y}>}{K^2 - i\epsilon} \\ &= \frac{1}{2} <X| \int d^5K \frac{|K><K|}{K^2 - i\epsilon} |Y> + \frac{1}{2} P <X| \int d^5K \frac{|K><K|}{K^2 - i\epsilon} |\tilde{Y}> \quad . \end{aligned} \quad (21)$$

Note that  $Z_2$  parity property is naturally presented by the  $Z_2$ -parity changed states  $|\tilde{Y}>$ . From the relation  $\partial_M \partial^M \Delta_F(X, y) = -\frac{1}{2} \{ \delta^5(X - Y) + P \delta^5(X - \tilde{Y}) \}$ , we can see the consistency with (15).

$$\partial_M \partial^M <X|K> = -K^2 <X|K> \quad . \quad (22)$$

We will see, in Sec.6, this formalism holds true also for the *warped* case.

## 4 Position/Momentum Propagator Approach

Let us do the previous analysis in the way free from the eigen-mode expansion.

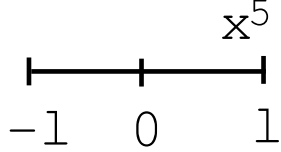
### 4.1 P/M propagator Approach

Although the extra coordinates are not observed at present, the coordinates could be different from others as its role in the quantum field theory (QFT). The treatment of Sec.2 and Sec.3 is just the 5 dimensional generalization of the ordinary (4 dimensional) QFT. We have treated there the extra coordinate on the equal footing with others. We introduce, in this section, the new approach to the propagator where the extra coordinate is differently treated with others.

We start from eq.(10).

$$\partial_M \partial^M \Phi(X) = -J(X) \quad . \quad (23)$$

Figure 2: The interval  $[-l, l]$  in which the propagator is defined



As for the region of the extra-coordinate and the boundary on  $\Phi$ , we take different ones. The extra space is the *interval*<sup>4</sup>  $[-l, l]$ , and  $Z_2$  symmetry only is imposed.<sup>5</sup> (Note that we do *not* consider the periodicity in this section.) We take odd one,  $P=-1$ , for the explicit presentation.

$$Z_2\text{-property (5D parity)} \quad \Phi(x, x^5) = -\Phi(x, -x^5), \quad J(x, x^5) = -J(x, -x^5) \quad , \quad (24)$$

The extra space manifold is shown in Fig.2. We will take into account the extension to  $\mathbf{R}=\{ -\infty < x^5 < \infty \}$  and the periodicity later(Sec.5). In order to solve (23) we define the 5D propagator  $\Delta(X, X')$  as follows.

$$\Phi(X) = \int d^5 X' \Delta(X, X') J(X') \quad ,$$

$$\partial_M \partial^M \Delta(X, X') = \partial_{M'} \partial^{M'} \Delta(X, X') = -\frac{1}{2}(\delta^5(X - X') + P\delta^5(X - \tilde{X}')) \quad , \quad P = -1 \quad , \quad (25)$$

where  $(\tilde{X}) \equiv (x^m, -x^5)$  and  $\Delta(X, X')$  is defined in the symmetric way w.r.t.  $X \leftrightarrow X'$ . Now we introduce the position/momentum propagator  $G_p(y \equiv x^5, y' \equiv x^{5'})$  as follows.

$$\Delta(X, X') \equiv \int \frac{d^4 p}{(2\pi)^4} e^{ip(x-x')} G_p(y, y') \quad ,$$

$$(-p^2 + \frac{\partial^2}{\partial y^2}) G_p(y, y') = (-p^2 + \frac{\partial^2}{\partial y'^2}) G_p(y, y') = -\frac{1}{2}(\delta(y - y') + P\delta(y + y')) \quad , \quad P = -1 \quad ,$$

$$p^2 \equiv p_m p^m \quad . \quad (26)$$

The symmetries of the defining equation of  $G_p(y, y')$  above are

**Sym(A)**  $y \leftrightarrow y'$

**Sym(B)**  $y \rightarrow -y$  and  $y' \rightarrow -y'$  ,  $P = (-1) \times (-1) = 1$

**Sym(C)**  $y \rightarrow -y$  ,  $P = -1$

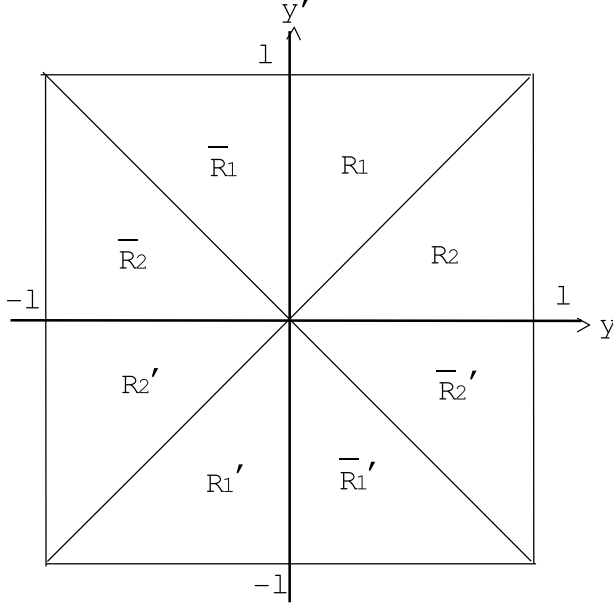
**Sym(C')**  $y' \rightarrow -y'$  ,  $P = -1$

---

<sup>4</sup>finite real region

<sup>5</sup> The approach of Sec.2 is called "orbifold picture" or "up-stairs picture", while that of this section "interval (boundary) picture" or "down-stairs picture". [10, 11] For the recent discussion on the super-symmetric case, see Ref.[15, 16]

Figure 3: 8 regions



Corresponding to the specific choice of  $Z_2$ -parity,  $P=-1$  in (24), we must take the Dirichlet boundary condition (b.c.) at  $x^5=0$ . We also take the same one at  $x^5=l$ .<sup>6</sup>

$$\begin{aligned} G_p(y=0, y') &= 0 \quad , \quad G_p(y, y'=l) = 0 \quad \text{for } 0 \leq y < y' \leq l \quad , \\ G_p(y, y'=0) &= 0 \quad , \quad G_p(y=l, y') = 0 \quad \text{for } 0 \leq y' < y \leq l \quad . \end{aligned} \quad (27)$$

The corresponding conditions for others ( $y, y' = -l$ ) are assumed in the same way. (When we take the even case of  $Z_2$ -parity in (24), the Neumann b.c. is imposed at  $x^5=0$ . See App.C.1.).

We consider first the case  $p^2 > 0$ , that is,  $p^m$  is the *space-like* 4-momentum.

We divide the whole region into 8 ones  $R_1, R_2, R'_1, R'_2, \bar{R}_1, \bar{R}_2, \bar{R}'_1$  and  $\bar{R}'_2$  as in Fig.3.

**Step 1.** Region  $R_1$  and  $R_2$

We start by solving (26) for the region  $0 \leq y, y' \leq l$ .

(i)  $y \neq y'$ .

In this case the equation (26) reduces to the *homogeneous* one.

$$(-\tilde{p}^2 + \frac{\partial^2}{\partial y^2})G_p(y, y') = (-\tilde{p}^2 + \frac{\partial^2}{\partial y'^2})G_p(y, y') = 0 \quad , \quad \tilde{p} \equiv \sqrt{p^2} \quad . \quad (28)$$

The general solution is given by

$$K_p(y, y') = A(y') \cosh \tilde{p}y + B(y') \sinh \tilde{p}y = C(y) \cosh \tilde{p}(y' - l) + D(y) \sinh \tilde{p}(y' - l) \quad , \quad (29)$$

<sup>6</sup> We may take the Neumann b.c. at  $x^5 = l$ . This choice is excluded in the case of Sec.2 (up-stairs picture), because the periodicity and the continuity requires the vanishing of the function at  $x^5 = l$ . See App.C.2 for this case.

where  $A(y'), B(y'), C(y)$  and  $D(y)$  are to be fixed by the boundary conditions. We take the solution as

$$\begin{aligned} G_p(y, y') &= K_p(y, y') = A(y') \cosh \tilde{p}y + B(y') \sinh \tilde{p}y \quad \text{for } R_1 : 0 \leq y < y' \leq l \\ G_p(y, y') &= K_p(y', y) = C(y') \cosh \tilde{p}(y - l) + D(y') \sinh \tilde{p}(y - l) \quad \text{for } R_2 : 0 \leq y' < y \leq l \end{aligned} \quad (30)$$

where we have used the  $\text{Sym}(A)$  of (26). Note that the lower equation is the  $y \leftrightarrow y'$  exchanged one of the upper equation. This will be utilized in the inhomogeneous case below. Applying the b.c. (27) to the above result, we see

$$A(y') = 0, \quad C(y) = 0, \quad (31)$$

in (29).

(ii)  $|y - y'| < +0$

We must take into account the *inhomogeneous* term, the singularity  $\frac{1}{2}\delta(y - y')$  in (26). To do it, we note the following fact. The absolute-value function  $\frac{1}{2}|y - y'|$  satisfies the following relation.

$$\begin{aligned} v(y, y') &\equiv \frac{1}{2}|y - y'| = \begin{cases} \frac{1}{2}(y' - y) & \text{for } y < y' \\ \frac{1}{2}(y - y') = y \leftrightarrow y' \text{ in the above} & \text{for } y > y' \end{cases}, \\ -\frac{\partial v(y, y')}{\partial y} &= +\frac{\partial v(y, y')}{\partial y'} = \frac{1}{2}\epsilon(y' - y) \equiv \begin{cases} +\frac{1}{2} & \text{for } y < y' \\ 0 & \text{for } y = y' \\ -\frac{1}{2} & \text{for } y > y' \end{cases}, \\ \frac{\partial^2}{\partial y^2}v(y, y') &= \frac{\partial^2}{\partial y'^2}v(y, y') = \frac{1}{2}\frac{\partial}{\partial y'}\epsilon(y' - y) = -\frac{1}{2}\frac{\partial}{\partial y}\epsilon(y' - y) = \delta(y - y') \quad , \\ \frac{\partial^2}{\partial y \partial y'}v(y, y') &= -\delta(y - y') \quad , \end{aligned} \quad (32)$$

where  $\epsilon(y)$  is the *sign function*. With the above relations and  $\text{Sym}(A)$ , we take the following b.c..

$$\text{Jump Condition: } \left[ -\frac{\partial G_p(y, y')}{\partial y} + \frac{\partial G_p(y, y')}{\partial y'} \right] \Big|_{y' \rightarrow y+0} = \frac{1}{2} \quad \text{for } y < y' \quad . \quad (33)$$

(This b.c., *in combined with the  $y \leftrightarrow y'$  exchanged definition for  $y' < y$  in (30)*, simply demands  $G_p(y, y') \sim +\frac{1}{4}|y - y'| = \frac{1}{2}v(y, y')$  for  $|y - y'| \ll 1$ . ) This condition and the *continuity* of the 2nd and 3rd equation of (29) at  $y = y'$  fix the remaining two functions  $B$  and  $D$ .<sup>7</sup> Finally we get

$$\begin{aligned} B(y') &= \frac{\sinh \tilde{p}(y' - l)}{2\tilde{p} \sinh \tilde{p}l} \quad , \quad D(y) = \frac{\sinh \tilde{p}y}{2\tilde{p} \sinh \tilde{p}l} \quad , \\ G_p(y, y') &= \begin{cases} \frac{1}{2} \sinh \tilde{p}y \sinh \tilde{p}(y' - l) / \tilde{p} \sinh \tilde{p}l \equiv \tilde{K}_p(y, y') & \text{for } 0 \leq y < y' \leq l \\ \frac{1}{2} \sinh \tilde{p}(y - l) \sinh \tilde{p}y' / \tilde{p} \sinh \tilde{p}l \equiv \tilde{K}_p(y', y) & \text{for } 0 \leq y' < y \leq l \end{cases} \end{aligned} \quad (34)$$

<sup>7</sup> Putting  $y = y'$  in (29), the continuity condition leads to  $B(y) \sinh \tilde{p}y = D(y) \sinh \tilde{p}(y - l)$ . As for the Jump condition (33), two  $G_p(y, y')$ 's appear in the left hand side. We take  $B(y') \sinh \tilde{p}y$  as the first  $G_p(y, y')$  and  $D(y) \sinh \tilde{p}(y - l)$  as the second  $G_p(y, y')$ . Then it leads to  $-B(y)\tilde{p} \cosh \tilde{p}y + D(y)\tilde{p} \cosh \tilde{p}(y - l) = 1$ .

We can view the result of Step 1 as follows. The solution for Region  $R_1$  ( $0 \leq y < y' \leq l$ ) can be expressed as

$$\begin{aligned}\bar{K}_p(y, y') &= \sinh \tilde{p}y \sinh \tilde{p}(y' - l) / 2\tilde{p} \sinh \tilde{p}l \\ &= \frac{1}{4\tilde{p} \sinh \tilde{p}l} [\{\cosh \tilde{p}(y' + y) - \cosh \tilde{p}(y' - y)\} \cosh \tilde{p}l \\ &\quad + \{-\sinh \tilde{p}(y' + y) + \sinh \tilde{p}(y' - y)\} \sinh \tilde{p}l] \quad .\end{aligned}\quad (35)$$

As for the Region  $R_2$ , the solution is given by  $\bar{K}_p(y', y)$ , which is given by changing  $\sinh \tilde{p}(y' - y)$  in (35) by  $\sinh \tilde{p}(-y' + y)$ . In the combined region  $R_1$  and  $R_2$ , this change is equivalent to change  $\sinh \tilde{p}(y' - y)$  by  $\sinh \tilde{p}|y' - y|$ . This procedure of *taking the absolute value* of  $(y' - y)$ , at the same time, makes the solution have the singularity  $\delta(y - y')$  and satisfy the *inhomogeneous* equation. (See eq.(32))

Here we stress the *requirement* of the exchange symmetry (A) and the  $Z_2$  symmetry, with the Jump Condition (33), *demand* the delta-function source at the fixed point(s). We should compare this with the situation of the KK-expansion approach in Sec.2 and 3, where the singularity  $\delta(y - y')$  comes from the *completeness* of the eigen functions  $\hat{\delta}(y - y') \equiv \frac{1}{2l} \sum_{n \in \mathbf{Z}} \exp\{-i\frac{n\pi}{l}(y - y')\}$ . ( This situation is represented in the mathematical relation (37) derived below.)

### Step 2. Extension to Region $R'_1$ and $R'_2$

Here we extend the solution to Regions  $R'_1$  and  $R'_2$ . We make use of the symmetry  $\text{Sym}(B)$ . In order to make the solution (35) have the symmetry  $\text{Sym}(B)$ , we must *take the absolute value* of  $(y' + y)$  in  $-\sinh \tilde{p}(y' + y)$  besides  $(y' - y)$  in  $\sinh \tilde{p}(y' - y)$ .

$$\begin{aligned}G_p(y, y') &= \frac{1}{4\tilde{p} \sinh \tilde{p}l} [\{\cosh \tilde{p}|y' + y| - \cosh \tilde{p}|y' - y|\} \cosh \tilde{p}l \\ &\quad + \{-\sinh \tilde{p}|y' + y| + \sinh \tilde{p}|y' - y|\} \sinh \tilde{p}l] \\ &= \frac{1}{4\tilde{p} \sinh \tilde{p}l} \{\cosh \tilde{p}(|y' + y| - l) - \cosh \tilde{p}(|y' - y| - l)\} \quad .\end{aligned}\quad (36)$$

This expression is valid for  $R'_1$  and  $R'_2$  besides for  $R_1$  and  $R_2$ .

Taking the limit  $\tilde{p} \rightarrow +0$  in the above and (13), we obtain an interesting formula.

$$\sum_{n \in \mathbf{Z}, n \neq 0} \frac{1}{(\frac{n\pi}{l})^2} \sin \frac{n\pi}{l} y \sin \frac{n\pi}{l} y' = \frac{1}{8l} \{(|y' + y| - l)^2 - (|y' - y| - l)^2\} \quad .\quad (37)$$

In this  $P = -1$  case, we can take the limit  $\tilde{p} \rightarrow +0$  which means there is no massless mode.

### Step 3. Extension to Region $\bar{R}_1$ , $\bar{R}_2$ , $\bar{R}'_1$ and $\bar{R}'_2$

The solution (36) have the symmetries:  $\text{Sym}(C)$  ( $y \rightarrow -y$ ) and  $\text{Sym}(C')$  ( $y' \rightarrow -y'$ ) with  $P=-1$  property. These allow us to use (36) in *all regions*.

The appearance  $|y' + y|$  in (36) makes the solution have the singularity  $\delta(y + y')$  and satisfy the inhomogenous equation.

We notice, in this 5D propagator treatment, the extra coordinate behaves as a *directed* axis like the *temperature*. This is because the whole regions of  $(y, y')$ -plane reduces to the

fundamental region  $R_1(0 \leq y < y' \leq l)$ . The property comes from the requirement of  $Z_2$  symmetry (and the singularity at  $y = \pm y'$ ). Wave propagation in the continuum medium with the delta-function sources have a *fixed direction* in order to satisfy  $Z_2$  symmetry.<sup>8</sup>

For the time-like 4-momentum case,  $p^2 < 0$ , the solution is obtained in the same way and is given by

$$\begin{aligned} G_p(y, y') &= -\frac{1}{4\hat{p}\sin\hat{p}l} [\{\cos\hat{p}|y' + y| - \cos\hat{p}|y' - y|\} \cos\hat{p}l \\ &\quad + \{\sin\hat{p}|y' + y| - \sin\hat{p}|y' - y|\} \sin\hat{p}l] \quad , \\ &= -\frac{1}{4\hat{p}\sin\hat{p}l} \{\cos\hat{p}(|y' + y| - l) - \cos\hat{p}(|y' - y| - l)\} \quad , \end{aligned} \quad (38)$$

where  $\hat{p} = \sqrt{-p^2}$ .

Later, in Sec.9.1, we will show the graphs of (36) and of (38) and examine their behaviour.

## 4.2 Systematic treatment of symmetries of $G_p(y, y')$

The defining equation of  $G_p(y, y')$ , (26), has the symmetries Sym(A),(B),(C) and (C'). The *fundamental region* is  $R_1$ , and the solution in other regions can be expressed by some change of arguments  $y, y'$  in the P/M propagator in the fundamental region,  $\bar{K}_p(y, y')$ .

In the previous subsection, we have done the procedure of taking the absolute value of  $y' - y$  for the singularity  $\delta(y' - y)$  and of  $y' + y$  for  $\delta(y' + y)$ . This procedure says that the P/M propagator valid in all regions can be obtained by changing arguments  $y, y'$  in  $\bar{K}_p(y, y')$ , which is the P/M propagator defined in the fundamental region  $R_1$  and has no absolute-value quantities, in the following way.<sup>9</sup>

$$\begin{aligned} y &= \frac{1}{2}(y + y') - \frac{1}{2}(y' - y) \rightarrow Y(y, y') = \frac{1}{2}|y + y'| - \frac{1}{2}|y' - y| = \begin{cases} y & \text{for } R_1, \bar{R}_1 \\ -y' & \text{for } \bar{R}_2, R'_2 \\ -y & \text{for } R'_1, \bar{R}'_1 \\ y' & \text{for } \bar{R}'_2, R_2 \end{cases} \\ y' &= \frac{1}{2}(y + y') + \frac{1}{2}(y' - y) \rightarrow Y'(y, y') = \frac{1}{2}|y + y'| + \frac{1}{2}|y' - y| = \begin{cases} y' & \text{for } R_1, \bar{R}_1 \\ -y & \text{for } \bar{R}_2, R'_2 \\ -y' & \text{for } R'_1, \bar{R}'_1 \\ y & \text{for } \bar{R}'_2, R_2 \end{cases} \end{aligned} \quad (39)$$

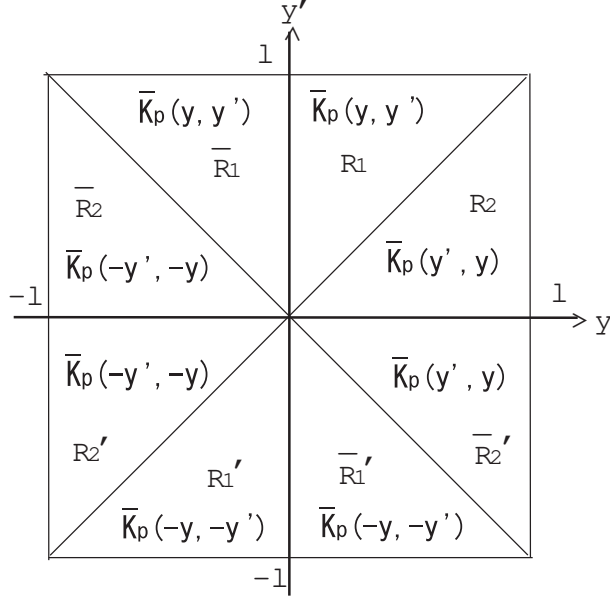
Hence P/M propagator has the following form, for the space-like 4D momentum case, in each region.

$$\begin{aligned} \bar{K}_p(y, y') &= \frac{\sinh\tilde{p}y \sinh\tilde{p}(y'-l)}{2\tilde{p}\sinh\tilde{p}l} \quad \text{for } R_1 \text{ and } \bar{R}_1 \quad , \\ \bar{K}_p(-y', -y) &= \frac{\sinh\tilde{p}y' \sinh\tilde{p}(y+l)}{2\tilde{p}\sinh\tilde{p}l} \quad \text{for } \bar{R}_2 \text{ and } R'_2 \quad , \\ \bar{K}_p(-y, -y') &= \frac{\sinh\tilde{p}y \sinh\tilde{p}(y'+l)}{2\tilde{p}\sinh\tilde{p}l} \quad \text{for } R'_1 \text{ and } \bar{R}'_1 \quad , \\ \bar{K}_p(y', y) &= \frac{\sinh\tilde{p}y' \sinh\tilde{p}(y-l)}{2\tilde{p}\sinh\tilde{p}l} \quad \text{for } \bar{R}'_2 \text{ and } R_2 \quad . \end{aligned} \quad (40)$$

<sup>8</sup> Similar situation is stressed in the analysis of the fermion chiral determinant.[17]

<sup>9</sup> This substitution is useful particularly in the warped case. See Sec.7, (98).

Figure 4: Arguments Arrangement for Propagators in 8 regions. The explicit expressions are given in (40).



In Fig.4, the arrangement of above propagators is shown. We surely see the symmetries (A),(B),(C) and (C') are satisfied. Using the new variables  $Y(y, y')$ ,  $Y'(y, y')$ , the solution (36) (space-like momentum case) is equivalently expressed as

$$G_p(y, y') = \bar{K}_p(Y(y, y'), Y'(y, y')) \quad , \quad (41)$$

where  $\bar{K}_p$  is given in (35). For the time-like case,  $\bar{K}_p$  is given by  $\bar{K}_p(Y, Y') = \frac{\sin \hat{p}Y \sin \hat{p}(Y' - l)}{2\hat{p} \sin \hat{p}l}$ ,  $\hat{p} = \sqrt{-p^2}$ .

As for the periodic property and the extension to  $-\infty < y < \infty$ , we examine in the next section.

We have given the P/M propagator in the flat 5D scalar theory (with  $P = -1$ ) in the two ways: (1) eq.(36) or eq.(38) (compactly by (41)) where absolute functions appear, and this expression is valid for all regions; (2) eq.(40) where *no* absolute-value function appears and the arguments within  $\bar{K}_p$  change depending on each region. Both ways are important. The first way is indispensable for analyzing the propagator at singular points. Practically it is necessary to draw a graph which has singular behaviour, while the second one stresses the importance of  $Z_2$ -symmetry. (See the  $\delta(0)$ -problem in Sec.10.)

## 5 KK-expansion approach versus P/M propagator approach

We have examined the same propagator equation (14) and (25) in two approaches. One is utilizing the expansion with the eigen functions (KK-modes) of  $\exp(i\frac{n\pi}{l}x^5)$ . The other

makes use of the P/M propagator  $G_p(y, y')$  in (26). In the former, the extra space is  $\mathbf{R} = (-\infty < x^5 < \infty)$  and the periodic b.c. and  $Z_2$  symmetry are imposed. The 4D space-time propagator is Feynman's. This is the orbifold approach. In the latter case, the extra space is the interval  $[-l, l]$ .  $Z_2$  symmetry only is imposed. This is the interval approach. We now connect the two results.

The P/M propagator for  $0 \leq y < y' \leq l$  (Region  $R_1$ ) is given by

$$\begin{cases} \frac{\sinh \tilde{p}y \sinh \tilde{p}(y'-l)}{2\tilde{p} \sinh \tilde{p}l} = \frac{1}{4\tilde{p} \sinh \tilde{p}l} \{ \cosh \tilde{p}(y'+y-l) - \cosh \tilde{p}(y'-y+l) \}, \tilde{p} = \sqrt{p^2} & \text{for } p^2 > 0 \\ \frac{\sin \hat{p}y \sin \hat{p}(y'-l)}{2\hat{p} \sin \hat{p}l} = \frac{1}{4\hat{p} \sin \hat{p}l} \{ -\cos \hat{p}(y'+y-l) + \cos \hat{p}(y-y'+l) \}, \hat{p} = \sqrt{-p^2} & \text{for } p^2 < 0 \end{cases} \quad (42)$$

Using the *Fourier expansion* formulae,

$$\begin{aligned} \frac{\pi}{2a} \frac{\cosh a(\pi - x)}{\sinh a\pi} &= \frac{1}{2a^2} + \sum_{n=1}^{\infty} \frac{\cos nx}{n^2 + a^2}, \quad 0 \leq x \leq 2\pi, \quad a : \text{arbitrary constant.} \\ \frac{\pi}{2a} \frac{\cos ax}{\sin a\pi} &= \frac{1}{2a^2} + \sum_{n=1}^{\infty} (-1)^{n-1} \frac{\cos nx}{n^2 - a^2}, \quad -\pi \leq x \leq \pi, \quad a : \text{non-integer arbitrary constant.} \end{aligned} \quad (43)$$

we obtain

$$\bar{K}_p(y, y') = \begin{cases} -\frac{1}{l} \sum_{n=1}^{\infty} \frac{1}{\tilde{p}^2 + (\frac{n\pi}{l})^2} \sin \frac{n\pi}{l} y \sin \frac{n\pi}{l} y' & \text{for } p^2 > 0 \\ \frac{1}{l} \sum_{n=1}^{\infty} \frac{1}{\tilde{p}^2 - (\frac{n\pi}{l})^2} \sin \frac{n\pi}{l} y \sin \frac{n\pi}{l} y' & \text{for } p^2 < 0 \end{cases} \quad (44)$$

This propagator satisfies the all symmetries (A),(B),(C) and (C') and is periodic ( $y \rightarrow y + 2l$ ), hence we may take it as the propagator valid for  $y, y' \in \mathbf{R}$  where  $\mathbf{R} = (-\infty, \infty)$ . The last procedure is taking the *universal covering* of  $S_1$ . Both the space-like case and the time-like case are just the result (13) with  $P = -1$ .

We reemphasize the following points. In the periodic approach of Sec.2, the delta function singularity comes from the *completeness* of the eigen-functions  $e^{in\pi y/l}$ . In the interval approach of Sec.4, the singularity comes from the exchange symmetry (A) and  $Z_2$ -symmetry (, that is, taking the absolute values of  $(y \mp y')$ ). The *position space* treatment gives the intimate relation between the wave propagation with symmetries and its source (singularity).

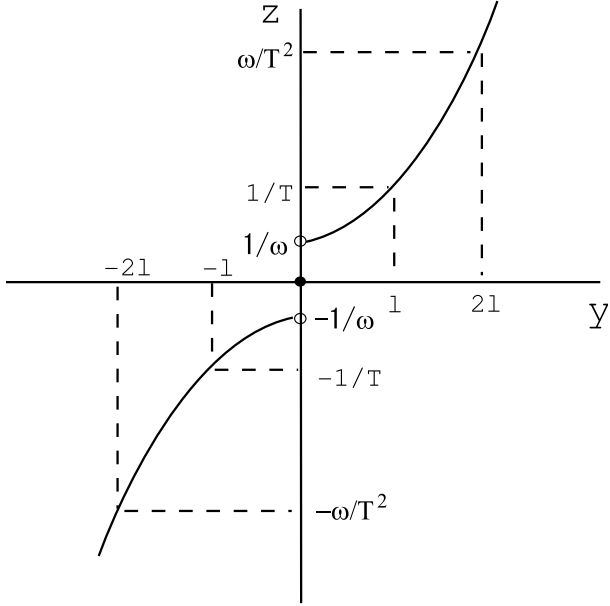
## 6 5D QFT on warped geometry $\text{AdS}_5$

Let us consider the warped case. The space-time is  $\text{AdS}_5$  manifold.

$$\begin{aligned} ds^2 &= e^{-2\sigma(y)} \eta_{ab} dx^a dx^b + dy^2, \quad -\infty < y < \infty, \\ (\eta_{ab}) &= \text{diag}(-1, 1, 1, 1), \quad \sigma(y) = \omega|y|, \quad \omega > 0 \end{aligned} \quad (45)$$

The manifold has the negative cosmological constant and is maximally symmetric with the curvature  $\omega$ . In the limit  $\omega \rightarrow 0$ , the line element (45) goes to the flat one of Sec.2. We can consider the symmetries.

Figure 5: Relation between coordinates  $z$  and  $y$



(1) **Periodicity**  $y \rightarrow y + 2l$

(2)  **$Z_2$ -property**  $y \leftrightarrow -y, P = \pm 1$

as in Sec.2. When the periodicity condition (1) is assumed,  $|y|$  in (45) is the periodic absolute-linear function[18]. Instead of  $y$ -coordinate, another one  $z$ , defined below, is also important.

$$z = \begin{cases} \frac{1}{\omega} e^{\omega y} & \text{for } y > 0 \\ 0 & \text{for } y = 0 \\ -\frac{1}{\omega} e^{-\omega y} & \text{for } y < 0 \end{cases} = \epsilon(y) \frac{e^{\omega|y|}}{\omega} \quad (46)$$

See Fig.5.

In terms of  $z$ , the metric can be expressed as

$$ds^2 = \frac{1}{\omega^2 z^2} (\eta_{ab} dx^a dx^b + (dz)^2) \quad , \quad z > \frac{1}{\omega} \text{ or } z < -\frac{1}{\omega} \quad ,$$

$$\frac{dz}{\omega z} = \begin{cases} dy & \text{for } y > 0 \\ -dy & \text{for } y < 0 \end{cases} \quad (47)$$

$(-\frac{1}{\omega}, 0) \cup (0, \frac{1}{\omega})$  is the 'prohibited' region whose values the  $z$ -coordinate *cannot* take. This metric is *conformal flat*.

The advantage of the choice (46) is as follows: (a)  $z$  is the monotonously increasing function of  $y$ ; (b) one-to-one ; (c) the  $Z_2$  symmetry is expressed in the same way as  $y$ .

(2') **Z<sub>2</sub>-property**     $z \leftrightarrow -z$ ,     $P = \pm 1$

The periodicity is expressed as

$$\begin{aligned}
 & z \rightarrow ze^{2\omega l} (> 0) & \text{for } z > \frac{1}{\omega} \\
 & z = 0 \rightarrow z = \frac{e^{2\omega l}}{\omega} = \frac{\omega}{T^2} & \text{for } z = 0 \\
 & (1') \text{ Periodicity } y \rightarrow y + 2l & z (< 0) \rightarrow -ze^{2\omega l} (> 0) \quad \text{for } -\frac{\omega}{T^2} = -\frac{e^{2\omega l}}{\omega} < z < -\frac{1}{\omega} \\
 & z = -\frac{e^{2\omega l}}{\omega} = -\frac{\omega}{T^2} \rightarrow z = 0 & \text{for } z = -\frac{e^{2\omega l}}{\omega} = -\frac{\omega}{T^2} \\
 & z \rightarrow ze^{-2\omega l} (< 0) & \text{for } z < -\frac{e^{2\omega l}}{\omega} = -\frac{\omega}{T^2}
 \end{aligned}$$

The *translation* in  $y$ -coordinate is the *scale* transformation in  $z$ -coordinate. In the conformal coordinate (47), we can *not* obtain the *flat limit* simply by  $\omega \rightarrow 0$ .

We take 5D massive scalar theory as a simple example. The Lagrangian and the field equation is written as

$$\begin{aligned}
 \mathcal{L} &= \sqrt{-G} \left( -\frac{1}{2} \nabla^A \Phi \nabla_A \Phi - \frac{1}{2} m^2 \Phi^2 + J \Phi \right) , \quad G \equiv \det G_{AB} , \\
 ds^2 &= G_{AB} dX^A dX^B , \quad \nabla^A \nabla_A \Phi - m^2 \Phi + J = 0 ,
 \end{aligned} \tag{48}$$

where  $\Phi(X) = \Phi(x^a, z)$  is the 5D scalar field and  $J(X) = J(x^a, z)$  is the external source field. The background geometry is AdS<sub>5</sub> which takes the following form, in terms of  $z$ ,

$$\begin{aligned}
 (G_{AB}) &= \begin{pmatrix} \frac{1}{\omega^2 z^2} \eta_{ab} & 0 \\ 0 & \frac{1}{\omega^2 z^2} \end{pmatrix} , \quad \sqrt{-G} = \frac{1}{(\omega|z|)^5} \\
 -\frac{1}{T} \leq z \leq -\frac{1}{\omega} \quad \text{or} \quad \frac{1}{\omega} \leq z \leq \frac{1}{T} \quad (-l \leq y \leq l) , \quad \frac{1}{T} &\equiv \frac{1}{\omega} e^{\omega l} ,
 \end{aligned} \tag{49}$$

where, at present, we take into account *only*  $Z_2$  symmetry in the interval  $y \in [-l, l]$ . Later we will discuss the periodicity condition. The field equation (48) leads to

$$\omega^2 z^2 \partial_a \partial^a \Phi + (\omega z)^5 \partial_z \left( \frac{1}{(\omega z)^3} \partial_z \Phi \right) - m^2 \Phi + J = 0 , \tag{50}$$

which is  $Z_2$ -symmetric. We can consider two cases:

$$\begin{aligned}
 \Phi(x, z) &= P \Phi(x, -z) , \quad J(x, z) = P J(x, -z) , \\
 P &= +1 \text{ (even)} , \quad P = -1 \text{ (odd)} ,
 \end{aligned} \tag{51}$$

Let us first solve the above equation by the KK-expansion method as in Sec.2.

$$\Phi(x^a, z) = \sum_n \phi_n(x) \psi_n(z) , \quad J(x^a, z) = \sum_n j_n(x) \psi_n(z) , \quad \psi_n(z) = P \psi_n(-z) , \quad P = \mp 1 , \tag{52}$$

where  $\psi_n(z)$  is the eigen-functions of the Bessel differential equation. The variable region of  $z$  is the intervals defined in (49).

$$\begin{aligned}
 (\omega z)^3 \partial_z \left( \frac{1}{(\omega z)^3} \partial_z \psi_n \right) - \frac{m^2}{(\omega z)^2} \psi_n &= -M_n^2 \psi_n \\
 \left( \int_{-\frac{1}{T}}^{-\frac{1}{\omega}} + \int_{\frac{1}{\omega}}^{\frac{1}{T}} \right) \frac{dz}{(\omega|z|)^3} \psi_n(z) \psi_k(z) &= 2 \int_{\frac{1}{\omega}}^{\frac{1}{T}} \frac{dz}{(\omega z)^3} \psi_n(z) \psi_k(z) = \delta_{nk} ,
 \end{aligned} \tag{53}$$

where  $M_n$  is the eigenvalues to be determined by the b.c.. The above equation is obtained by the requirement that the 4D field  $\phi_n(x)$ ,  $j_n(x)$  in (52) satisfy the ordinary massive scalar field equation.<sup>10</sup>

$$\partial_a \partial^a \phi_n - M_n^2 \phi_n + j_n = 0 \quad . \quad (54)$$

From eq.(52),  $\psi_n(z)$  are odd or even functions of  $z$ .  $z$  varies in  $-1/T \leq z \leq -1/\omega$  and  $1/\omega \leq z \leq 1/T$ . Hence instead of *ordinary* Bessel functions  $(\mathbf{J}_\nu(z), \mathbf{N}_\nu)$  where  $z > 0$ , it is better to introduce *odd or even* Bessel functions where the argument  $z$  is valid even for the negative region of  $z$ .<sup>11</sup> It can be done as follows because the *Bessel equation is invariant for  $Z_2$  symmetry*:  $z \rightarrow -z$ .

$$\begin{aligned} \tilde{\mathbf{J}}_\nu(z) &\equiv \epsilon(z) \mathbf{J}_\nu(|z|) & \tilde{\mathbf{N}}_\nu(z) &\equiv \epsilon(z) \mathbf{N}_\nu(|z|) & \text{for } P = -1 \\ \hat{\mathbf{J}}_\nu(z) &\equiv \mathbf{J}_\nu(|z|) & \hat{\mathbf{N}}_\nu(z) &\equiv \mathbf{N}_\nu(|z|) & \text{for } P = 1 \end{aligned} \quad (55)$$

where  $\epsilon(z)$  is the sign function introduced in(32).<sup>12</sup> Taking the case  $P = -1$ , eq.(53) has two "intermediate" solutions.

$$\varphi^{(1/\omega)}(z) = \frac{(\omega z)^2}{N^{(1/\omega)}} \left[ \tilde{\mathbf{J}}_\nu(Mz) + b_\nu(M) \tilde{\mathbf{N}}_\nu(Mz) \right], \quad (56)$$

$$\varphi^{(1/T)}(z) = \frac{(\omega z)^2}{N^{(1/T)}} \left[ \tilde{\mathbf{J}}_\nu(Mz) + b_\nu(\omega M/T) \tilde{\mathbf{N}}_\nu(Mz) \right], \quad (57)$$

where  $N^{(1/\omega)}$  and  $N^{(1/T)}$  are some normalization constants to be determined. Similarly for the case  $P = 1$ .  $b_\nu$  is given by

$$b_\nu(t) \equiv \begin{cases} -\mathbf{J}_\nu(t/\omega)/\mathbf{N}_\nu(t/\omega), & \text{for } P = -1, \\ -\mathbf{J}'_\nu(t/\omega)/\mathbf{N}'_\nu(t/\omega), & \text{for } P = 1, \end{cases} \quad (58)$$

and

$$\nu = \sqrt{4 + \frac{m^2}{\omega^2}}. \quad (59)$$

These solutions  $\varphi^{(1/\omega)}(z)$  and  $\varphi^{(1/T)}(z)$  satisfy the following boundary conditions at  $z = \frac{1}{\omega}$  and  $\frac{1}{T}$ , respectively.

$$\begin{aligned} \text{Dirichlet b.c.} \quad & \varphi^{(1/\omega)}(z)|_{z=1/\omega} = 0 & \varphi^{(1/T)}(z)|_{z=1/T} = 0 & \text{for } P = -1 \\ \text{Neumann b.c.} \quad & \frac{d}{dz} \varphi^{(1/\omega)}(z)|_{z=1/\omega} = 0 & \frac{d}{dz} \varphi^{(1/T)}(z)|_{z=1/T} = 0 & \text{for } P = 1 \end{aligned} \quad (60)$$

<sup>10</sup> Note that we assume here the "4D part" satisfy  $M_n^2 \geq 0$ . If  $M_n^2 < 0$ , the modified Bessel functions, instead of the Bessel functions, appear in the following sentences.

<sup>11</sup> The Bessel equation  $\frac{d^2\psi}{dz^2} + \frac{1}{z} \frac{d\psi}{dz} + (1 - \frac{\nu^2}{z^2})\psi = 0$  has two independet solutions: Bessel function of the first kind  $J_\nu(z)$  and that of the second kind (Neumann function)  $N_\nu(z)$ .

<sup>12</sup> The odd or even Bessel functions (55) satisfy (53) as far as  $z$  is in the variable region  $-1/T \leq z \leq -1/\omega$  or  $1/\omega \leq z \leq 1/T$ .

The "final" solution which satisfies the b.c. both at  $z = 1/\omega$  and  $z = 1/T$  is obtained by the condition that these two solutions are *not* independent.

$$\begin{aligned} b_\nu(M_n) &= b_\nu(\omega M_n/T) \equiv b_\nu^{(n)}, \\ \frac{\mathbf{J}_\nu(\frac{M_n}{\omega})}{\mathbf{N}_\nu(\frac{M_n}{\omega})} &= \frac{\mathbf{J}_\nu(\frac{M_n}{T})}{\mathbf{N}_\nu(\frac{M_n}{T})}, \quad \text{for } P = -1, \\ \frac{\mathbf{J}'_\nu(\frac{M_n}{\omega})}{\mathbf{N}'_\nu(\frac{M_n}{\omega})} &= \frac{\mathbf{J}'_\nu(\frac{M_n}{T})}{\mathbf{N}'_\nu(\frac{M_n}{T})}, \quad \text{for } P = 1, \end{aligned} \quad (61)$$

which makes them identified,

$$\varphi^{(1/\omega)}(z)|_{M=M_n} = \varphi^{(1/T)}(z)|_{M=M_n} \equiv \psi_n(z), \quad (62)$$

and determines the eigenvalues  $M_n$ . The normalization constants are then expressed as

$$N_n^{(1/\omega)2} = N_n^{(1/T)2} = \int_{1/\omega}^{1/T} \omega z dz \left[ \mathbf{J}_\nu(M_n z) + b_\nu^{(n)} \mathbf{N}_\nu(M_n z) \right]^2 \equiv N_n^2. \quad (63)$$

The solution of (54) is given by

$$\begin{aligned} \phi_n(x) &= \int \Delta_F^n(x - x') j_n(x') d^4 x' \quad , \quad \Delta_F^n(x - x') = \int \frac{d^4 k}{(2\pi)^4} \frac{e^{-ik(x-x')}}{k^2 + M_n^2 - i\epsilon} \quad , \\ (\partial_a \partial^a - M_n^2) \Delta_F^n(x - x') &= -\delta^4(x - x') \quad . \end{aligned} \quad (64)$$

5D propagator can be expected to be <sup>13</sup>, in the analogy of Sec.2's result (13),

$$\begin{aligned} \Phi(X) &= \int d^5 X' \Delta_W(X, X') \sqrt{-G'} J(X') \quad , \\ \Delta_W(X, X') &\equiv \sum_n \Delta_F^n(x - x') \times \frac{1}{2} \{ \psi_n(z) \psi_n(z') + P \psi_n(z) \psi_n(\tilde{z}') \} \quad , \quad \tilde{z}' \equiv -z' \quad . \end{aligned} \quad (65)$$

In fact we can confirm the following propagator equation.

$$\begin{aligned} (\nabla^A \nabla_A - m^2) \Delta_W(X, X') &= \{ \omega^2 z^2 \partial_a \partial^a + (\omega z)^5 \frac{\partial}{\partial z} \frac{1}{(\omega z)^3} \partial_z - m^2 \} \Delta_W(X, X') \\ &= \sum_n \omega^2 z^2 (\partial_a \partial^a - M_n^2) \Delta_F^n(x - x') \frac{1}{2} \{ \psi_n(z) \psi_n(z') + P \psi_n(z) \psi_n(\tilde{z}') \} \\ &= -(\omega|z|)^5 \delta^4(x - x') \frac{1}{2} (\hat{\delta}(z - z') + P \hat{\delta}(z - \tilde{z}')) \quad , \end{aligned} \quad (66)$$

where some relations in (53), (64) and the *completeness* relation:

$$(\omega|z|)^{-3} \sum_n \psi_n(z) \psi_n(z') \equiv \begin{cases} \epsilon(z) \epsilon(z') \hat{\delta}(|z| - |z'|) & \text{for } P = -1 \\ \hat{\delta}(|z| - |z'|) & \text{for } P = 1 \end{cases} \quad , \quad (67)$$

---

<sup>13</sup> General proof of this propagator form is given in App.B.

are used.

Now we have obtained 5D propagator  $\Delta_W(x^a, y; x'^a, y')$  which satisfies  $Z_2$  symmetry and is valid for  $y, y' \in [-l, l]$ . When we want to extend this to  $y, y' \in \mathbf{R}$  and impose the periodicity, we may take the *universal covering* of  $\Delta_W(x^a, y; x'^a, y')$  as in the flat case. That is, first we Fourier-expand<sup>14</sup>  $\Delta_W(x^a, y; x'^a, y')$  within  $y, y' \in [-l, l]$ , and then, confirming the non-singular behaviour, extend the variable region to  $\mathbf{R}$ .

The above relations can be expressed in the Dirac's bra and ket vector formalism. Let us introduce bra and ket vectors as follows.

$$\psi_n(z) \equiv (n|z) = (z|n) \quad , \quad e^{-ikx} \equiv < x|k > \quad , \quad e^{ikx} \equiv < k|x > \quad , \quad (68)$$

Depending on the  $Z_2$ -property of  $\psi_n(z)$ ,  $|z)$  and  $(z|$  have the following properties.

$$|-z) = P|z) \quad , \quad (-z| = P(z| \quad , \quad P = \mp 1 \quad . \quad (69)$$

From the orthogonality relation (53), we know

$$\left( \int_{-\frac{1}{\omega}}^{-\frac{1}{\omega}} + \int_{\frac{1}{\omega}}^{\frac{1}{\omega}} \right) \frac{dz}{(\omega|z|)^3} (n|z)(z|k) = 2 \int_{\frac{1}{\omega}}^{\frac{1}{\omega}} \frac{dz}{(\omega z)^3} (n|z)(z|k) = \delta_{n,k} \quad . \quad (70)$$

We require the orthogonality between  $(n|$  and  $|k)$ ,

$$(n|k) = \delta_{n,k} \quad . \quad (71)$$

then the completeness relation between the coordinate states  $|z)$

$$\left( \int_{-\frac{1}{\omega}}^{-\frac{1}{\omega}} + \int_{\frac{1}{\omega}}^{\frac{1}{\omega}} \right) \frac{dz}{(\omega|z|)^3} |z)(z| = 2 \int_{\frac{1}{\omega}}^{\frac{1}{\omega}} \frac{dz}{(\omega z)^3} |z)(z| = \mathbf{1} \quad . \quad (72)$$

is deduced.

The completeness relation (67) is expressed as

$$\sum_n (z|n)(n|z') = \begin{cases} (\omega|z|)^3 \epsilon(z)\epsilon(z') \hat{\delta}(|z| - |z'|) & \text{for } P = -1 \\ (\omega|z|)^3 \hat{\delta}(|z| - |z'|) & \text{for } P = 1 \end{cases} \quad . \quad (73)$$

If we require the orthogonality between the coordinate states  $(z|$  and  $|z')$ :

$$(z|z') = \begin{cases} (\omega|z|)^3 \epsilon(z)\epsilon(z') \hat{\delta}(|z| - |z'|) & \text{for } P = -1 \\ (\omega|z|)^3 \hat{\delta}(|z| - |z'|) & \text{for } P = 1 \end{cases} \quad , \quad (74)$$

then the completeness:

$$\sum_n |n)(n| = \mathbf{1} \quad , \quad (75)$$

---

<sup>14</sup> Ordinary one using periodic functions. Not Bessel Fourier-expansion.

is deduced. The 5D propagator (65) can be expressed as

$$\begin{aligned}
\Delta_W(X, X') &= \sum_n \int \frac{d^4 k}{(2\pi)^4} \frac{< x|k > < k|x' >}{k^2 + M_n^2 - i\epsilon} \times \frac{1}{2} \{ (z|n)(n|z') + P(z|n)(n|\tilde{z}') \} \\
&= 2l \int d^5 K \frac{1}{2} \left\{ \frac{(X|K)(K|X') + P(X|K)(K|\tilde{X}')}{K^2 - i\epsilon} \right\} , \\
(X) &\equiv (x^a, z) , \quad (X') \equiv (x^{a'}, z') , \quad (\tilde{X}') \equiv (x^{a'}, -z') , \\
(K) &\equiv (k_a, M_n) , \quad \int d^5 K \equiv \frac{1}{2l} \sum_n \int \frac{d^4 k}{(2\pi)^4} . \quad (76)
\end{aligned}$$

where 5D bra and ket vectors are introduced as

$$(X|K) \equiv < x|k > (z|n) , \quad (K|X') \equiv < k|x' > (n|z') . \quad (77)$$

This is the same form as in the flat case of Sec.3. The generalized points are the appearance of the extra-space 'measure factor'  $(\omega|z|)^{-3}$  in (70), (72), (73), (74) and, in the extra dimensional part, the periodic eigen functions are replaced by the Bessel ones  $(n|z) = (z|n) = \psi_n(z)$ .

In this section we have shown the basic quantum structure of the warped system, in the Dirac's bra and ket vector formalism, is the same as the flat one. In this sense, the warped system can be regarded as a *deformation* of the flat theory with the *deformation parameter*  $\omega$ . We will again point out the same interpretation from the propagator behaviour in Sec.10.

## 7 P/M Propagator approach to 5D QFT on AdS<sub>5</sub>

Let us solve the field equation (50) in the P/M propagator approach.

$$\begin{aligned}
\nabla^A \nabla_A \Phi - m^2 \Phi + J &= \\
\omega^2 z^2 \partial_a \partial^a \Phi + (\omega z)^5 \partial_z \left( \frac{1}{(\omega z)^3} \partial_z \Phi \right) - m^2 \Phi + J &= 0 . \quad (78)
\end{aligned}$$

We consider the Z<sub>2</sub>-parity odd case:

$$\text{Z}_2\text{-property (5D parity)} \quad \Phi(x, z) = P\Phi(x, -z) , \quad J(x, z) = P J(x, -z) , \quad P = -1 , \quad (79)$$

The P/M propagator  $G_p(z, z')$  is introduced as

$$\begin{aligned}
\Phi(X) &= \int d^5 X' \Delta_W(X, X') \sqrt{-G'} J(X') , \\
(\nabla^A \nabla_A - m^2) \Delta_W(X, X') &= -\frac{1}{\sqrt{-G}} \delta^4(x - x') \frac{1}{2} (\delta(z - z') + P\delta(z - \tilde{z}')) , \quad P = -1 , \\
\Delta_W(X, X') &= \int \frac{d^4 p}{(2\pi)^4} e^{ip(x-x')} G_p(z, z') , \quad (80)
\end{aligned}$$

where  $(X^A) = (x^a, z)$ ,  $(X^{A'}) = (x^{a'}, z')$  and  $G = \det G_{AB}$ . In Sec.6, we have derived  $\Delta_W$  in the KK-expansion approach. Here we rederive it in the P/M propagator approach. From the propagator equation above,  $G_p(z, z')$  must satisfy

$$\begin{aligned} & \left\{ -\omega^2 z^2 p^2 + (\omega z)^5 \frac{\partial}{\partial z} \frac{1}{(\omega z)^3} \partial_z - m^2 \right\} G_p(z, z') \\ &= -\frac{1}{2} (\omega |z|)^5 (\delta(z - z') + P \delta(z - \tilde{z}')) \quad , \end{aligned} \quad (81)$$

(The absolute value  $|z|$  comes from the space-time volume measure  $\sqrt{-G} = \sqrt{-\det G_{AB}}$ .) Hence  $G_p$  is determined by the Bessel differential equation.<sup>15</sup>

$$\begin{aligned} \left\{ -p^2 + \partial_z^2 - \frac{3}{z} \partial_z - \frac{m^2}{\omega^2 z^2} \right\} G_p(z, z') &= -\frac{1}{2} (\omega |z|)^3 (\delta(z - z') + P \delta(z - \tilde{z}')) \quad , \\ -\frac{1}{T} \leq z, z' \leq -\frac{1}{\omega} \quad \text{or} \quad \frac{1}{\omega} \leq z, z' \leq \frac{1}{T} \end{aligned} \quad (83)$$

The above equation has the symmetries.

**Sym(A)**  $z \leftrightarrow z'$

**Sym(B)**  $z \rightarrow -z$  and  $z' \rightarrow -z'$  ,  $P = (-1) \times (-1) = 1$

**Sym(C)**  $z \rightarrow -z$  ,  $P = -1$

**Sym(C')**  $z' \rightarrow -z'$  ,  $P = -1$

Corresponding to the choice of  $P = -1$  in (79), we take the Dirichlet b.c. at the fixed points:  $z, z' = \pm \frac{1}{\omega}, \pm \frac{1}{T}$ . Now let us solve (83) in the same way as in Sec.4. We consider  $p^2 > 0$  (space-like) case first.

We divide the whole region into 8 ones,  $R_1, R_2, R'_1, R'_2, \bar{R}_1, \bar{R}_2, \bar{R}'_1$  and  $\bar{R}'_2$  as in Fig.6.

**Step 1.** Region  $R_1$  and  $R_2$

We start by solving (83) for the region  $\frac{1}{\omega} \leq z, z' \leq \frac{1}{T}$ .

(i)  $z \neq z'$ .

In this case the equation (83) reduces to the *homogeneous* one.

$$\begin{aligned} & \left( -\tilde{p}^2 + \partial_z^2 - \frac{3}{z} \partial_z - \frac{m^2}{\omega^2 z^2} \right) G_p(z, z') \\ &= \left( -\tilde{p}^2 + \partial_{z'}^2 - \frac{3}{z'} \partial_{z'} - \frac{m^2}{\omega^2 z'^2} \right) G_p(z, z') = 0 \quad , \quad \tilde{p} \equiv \sqrt{p^2} \quad . \end{aligned} \quad (84)$$

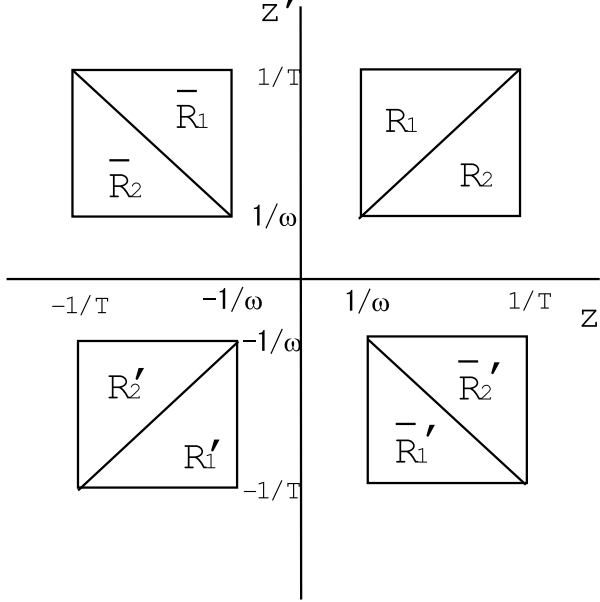
---

<sup>15</sup> For the high energy region  $\sqrt{|p^2|} \gg \omega$ , we expect (83) approaches the 'flat' (z-)space equation:

$$\left\{ -p^2 + \partial_z^2 \right\} G_p(z, z') = -\frac{1}{2} (\omega |z|)^3 (\delta(z - z') + P \delta(z - \tilde{z}')) \quad . \quad (82)$$

This corresponds to the 'flat space' limit (6.16) of Ref.[9]. Note that the warp parameter  $\omega$  remains in this limit and it is different from the flat case of Sec.2. See Fig.35 and App.C.3(3S). See also Fig.41 and App.C.5(3S).

Figure 6: 8 regions in the  $z$ -coordinates plane. This is the transformed version of Fig.3 through the relation (46)



The general solution is given by

$$K_p(z, z') = A(z')z^2 \mathbf{K}_\nu(\tilde{p}z) + B(z')z^2 \mathbf{I}_\nu(\tilde{p}z) = C(z)z'^2 \mathbf{K}_\nu(\tilde{p}z') + D(z)z'^2 \mathbf{I}_\nu(\tilde{p}z') \quad ,$$

$$\nu = \sqrt{4 + \frac{m^2}{\omega^2}} \quad (85)$$

where  $A(z')$ ,  $B(z')$ ,  $C(z)$  and  $D(z)$  are to be fixed by the boundary conditions. We consider the special case <sup>16</sup> which is important in the supersymmetry requirement[19].

$$m^2 = -4\omega^2 \quad , \quad \nu = 0 \quad . \quad (86)$$

We take the solution as

$$G_p(z, z') = K_p(z, z') = A(z')z^2 \mathbf{K}_0(\tilde{p}z) + B(z')z^2 \mathbf{I}_0(\tilde{p}z) = C(z)z'^2 \mathbf{K}_0(\tilde{p}z') + D(z)z'^2 \mathbf{I}_0(\tilde{p}z') \quad ,$$

$$\text{for } \frac{1}{\omega} \leq z < z' \leq \frac{1}{T}$$

$$G_p(z, z') = K_p(z', z) = A(z)z'^2 \mathbf{K}_0(\tilde{p}z') + B(z)z'^2 \mathbf{I}_0(\tilde{p}z') = C(z')z^2 \mathbf{K}_0(\tilde{p}z) + D(z')z^2 \mathbf{I}_0(\tilde{p}z) \quad ,$$

$$\text{for } \frac{1}{\omega} \leq z' < z \leq \frac{1}{T} \quad . \quad (87)$$

<sup>16</sup> We treat the case of the general  $\nu$  in App.B.

The latter equation is the  $z \leftrightarrow z'$  exchanged one of the former equation. Here we use Sym.(A). The Dirichlet b.c. requires

$$\begin{aligned} A(z')\mathbf{K}_0\left(\frac{\tilde{p}}{\omega}\right) + B(z')\mathbf{I}_0\left(\frac{\tilde{p}}{\omega}\right) &= 0 \quad , \\ C(z')\mathbf{K}_0\left(\frac{\tilde{p}}{T}\right) + D(z')\mathbf{I}_0\left(\frac{\tilde{p}}{T}\right) &= 0 \quad . \end{aligned} \quad (88)$$

(ii)  $|z - z'| < +0$

In order to take into account the inhomogeneous term  $-\frac{1}{2}(\omega|z|)^3\delta(z - z')$  in the RHS of (83) we put the following b.c..

$$\text{Jump Condition: } -\frac{\partial G_p(z, z')}{\partial z} + \frac{\partial G_p(z, z')}{\partial z'} \Big|_{z' \rightarrow z+0} = -\frac{1}{2}(\omega z)^3 \quad \text{for } \left(\frac{1}{\omega} \leq\right) z < z' \quad . \quad (89)$$

(This b.c., *in combined with the  $z \leftrightarrow z'$  exchanged definition for  $z' < z$  in (87)*, simply demands  $G_p(z, z') \sim -\frac{1}{4}(\omega z)^3|z - z'|$  for  $|z - z'| \ll 1$ . ) Using the upper equation of (87), the above b.c. reduces to

$$\begin{aligned} -A(z')\frac{d}{dz}\{z^2\mathbf{K}_0(\tilde{p}z)\} - B(z')\frac{d}{dz}\{z^2\mathbf{I}_0(\tilde{p}z)\} + C(z)\frac{d}{dz'}\{z'^2\mathbf{K}_0(\tilde{p}z')\} + D(z)\frac{d}{dz'}\{z'^2\mathbf{I}_0(\tilde{p}z')\} \Big|_{z' \rightarrow z+0} \\ = -\frac{1}{2}(\omega z)^3 \quad . \quad (90) \end{aligned}$$

The continuity at  $z = z'$  requires, from eq.(87),

$$A(z)\mathbf{K}_0(\tilde{p}z) + B(z)\mathbf{I}_0(\tilde{p}z) = C(z)\mathbf{K}_0(\tilde{p}z) + D(z)\mathbf{I}_0(\tilde{p}z) \quad . \quad (91)$$

The 4 relations in (88), (90) and (91), fix  $A, B, C$  and  $D$  as

$$\begin{pmatrix} A(z) \\ B(z) \\ C(z) \\ D(z) \end{pmatrix} = \left\{ \frac{\omega^3 z^2}{2} / (\mathbf{K}_0\left(\frac{\tilde{p}}{\omega}\right)\mathbf{I}\left(\frac{\tilde{p}}{T}\right) - \mathbf{K}_0\left(\frac{\tilde{p}}{T}\right)\mathbf{I}_0\left(\frac{\tilde{p}}{\omega}\right)) \right\} \times \begin{pmatrix} -\mathbf{I}_0\left(\frac{\tilde{p}}{\omega}\right)\{\mathbf{I}_0\left(\frac{\tilde{p}}{T}\right)\mathbf{K}_0(\tilde{p}z) - \mathbf{K}_0\left(\frac{\tilde{p}}{T}\right)\mathbf{I}_0(\tilde{p}z)\} \\ +\mathbf{K}_0\left(\frac{\tilde{p}}{\omega}\right)\{\mathbf{I}_0\left(\frac{\tilde{p}}{T}\right)\mathbf{K}_0(\tilde{p}z) - \mathbf{K}_0\left(\frac{\tilde{p}}{T}\right)\mathbf{I}_0(\tilde{p}z)\} \\ -\mathbf{I}_0\left(\frac{\tilde{p}}{T}\right)\{\mathbf{I}_0\left(\frac{\tilde{p}}{\omega}\right)\mathbf{K}_0(\tilde{p}z) - \mathbf{K}_0\left(\frac{\tilde{p}}{\omega}\right)\mathbf{I}_0(\tilde{p}z)\} \\ +\mathbf{K}_0\left(\frac{\tilde{p}}{T}\right)\{\mathbf{I}_0\left(\frac{\tilde{p}}{\omega}\right)\mathbf{K}_0(\tilde{p}z) - \mathbf{K}_0\left(\frac{\tilde{p}}{\omega}\right)\mathbf{I}_0(\tilde{p}z)\} \end{pmatrix} \quad (92)$$

Hence  $K_p(z, z')$  is completely fixed as

$$K_p(z, z') = -\frac{\omega^3}{2} z^2 z'^2 \frac{\{\mathbf{I}_0(\frac{\tilde{p}}{\omega})\mathbf{K}_0(\tilde{p}z) - \mathbf{K}_0(\frac{\tilde{p}}{\omega})\mathbf{I}_0(\tilde{p}z)\}\{\mathbf{I}_0(\frac{\tilde{p}}{T})\mathbf{K}_0(\tilde{p}z') - \mathbf{K}_0(\frac{\tilde{p}}{T})\mathbf{I}_0(\tilde{p}z')\}}{\mathbf{I}_0(\frac{\tilde{p}}{T})\mathbf{K}_0(\frac{\tilde{p}}{\omega}) - \mathbf{K}_0(\frac{\tilde{p}}{T})\mathbf{I}_0(\frac{\tilde{p}}{\omega})} \quad .(93)$$

**Step 2.** Extension to all other regions

We now know how to extend the above solution to all other regions in the consistent way with Sym.(A)-(C'). Before that, we point out the necessity of the extension of the modified Bessel functions to the negative real axis. (same as in (55).) Following the procedure of Sec.4.2, we see the solution in  $R_1 \bar{R}_1$  is given by  $K_p(z, z')$  (93). This function must be odd for  $z \leftrightarrow -z$ . (because of Sym(C)) It demands  $\mathbf{K}_0(\tilde{p}z)$  and  $\mathbf{I}_0(\tilde{p}z)$  is the odd function of  $z$ .<sup>17</sup> Hence the modified Bessel functions, in the  $P = -1$  case, is generalized to the corresponding odd functions.<sup>18</sup>

$$\tilde{\mathbf{I}}_\nu(z) \equiv \epsilon(z)\mathbf{I}_\nu(|z|) \quad , \quad \tilde{\mathbf{K}}_\nu(z) \equiv \epsilon(z)\mathbf{K}_\nu(|z|) \quad , \quad (95)$$

where  $\mathbf{I}_\nu(z)$  and  $\mathbf{K}_\nu(z)$  are the ordinary ones defined in  $z > 0$ . Then the propagator (93) is improved to

$$\tilde{K}_p(z, z') = -\frac{\omega^3}{2} z^2 z'^2 \frac{\{\mathbf{I}_0(\frac{\tilde{p}}{\omega})\tilde{\mathbf{K}}_0(\tilde{p}z) - \mathbf{K}_0(\frac{\tilde{p}}{\omega})\tilde{\mathbf{I}}_0(\tilde{p}z)\}\{\mathbf{I}_0(\frac{\tilde{p}}{T})\tilde{\mathbf{K}}_0(\tilde{p}z') - \mathbf{K}_0(\frac{\tilde{p}}{T})\tilde{\mathbf{I}}_0(\tilde{p}z')\}}{\mathbf{I}_0(\frac{\tilde{p}}{T})\mathbf{K}_0(\frac{\tilde{p}}{\omega}) - \mathbf{K}_0(\frac{\tilde{p}}{T})\mathbf{I}_0(\frac{\tilde{p}}{\omega})} \quad .(96)$$

With these  $Z_2$ -odd quantities, the final solution is given by

$$G_p(z, z') = \begin{cases} \tilde{K}_p(z, z') & \text{for } R_1 \text{ and } \bar{R}_1 \\ \tilde{K}_p(-z', -z) & \text{for } \bar{R}_2 \text{ and } R'_2 \\ \tilde{K}_p(-z, -z') & \text{for } R'_1 \text{ and } \bar{R}'_1 \\ \tilde{K}_p(z', z) & \text{for } \bar{R}'_2 \text{ and } R_2 \end{cases} = -\frac{\omega^3 z^2 z'^2 / 2}{\mathbf{I}_0(\frac{\tilde{p}}{T})\mathbf{K}_0(\frac{\tilde{p}}{\omega}) - \mathbf{K}_0(\frac{\tilde{p}}{T})\mathbf{I}_0(\frac{\tilde{p}}{\omega})} \times \begin{cases} \{\mathbf{I}_0(\frac{\tilde{p}}{\omega})\tilde{\mathbf{K}}_0(\tilde{p}z) - \mathbf{K}_0(\frac{\tilde{p}}{\omega})\tilde{\mathbf{I}}_0(\tilde{p}z)\}\{\mathbf{I}_0(\frac{\tilde{p}}{T})\tilde{\mathbf{K}}_0(\tilde{p}z') - \mathbf{K}_0(\frac{\tilde{p}}{T})\tilde{\mathbf{I}}_0(\tilde{p}z')\} & \text{for } R_1 \cup \bar{R}_1 \cup R'_1 \cup \bar{R}'_1 \\ \{\mathbf{I}_0(\frac{\tilde{p}}{\omega})\tilde{\mathbf{K}}_0(\tilde{p}z') - \mathbf{K}_0(\frac{\tilde{p}}{\omega})\tilde{\mathbf{I}}_0(\tilde{p}z')\}\{\mathbf{I}_0(\frac{\tilde{p}}{T})\tilde{\mathbf{K}}_0(\tilde{p}z) - \mathbf{K}_0(\frac{\tilde{p}}{T})\tilde{\mathbf{I}}_0(\tilde{p}z)\} & \text{for } R_2 \cup \bar{R}_2 \cup R'_2 \cup \bar{R}'_2 \end{cases} \quad (97)$$

As in Sec.4, we can express  $G_p(z, z')$  in the compact way using the absolute functions.

$$\begin{aligned} z &= \frac{1}{2}(z + z') - \frac{1}{2}(z' - z) \rightarrow Z(z, z') \equiv \frac{1}{2}|z + z'| - \frac{1}{2}|z' - z| \\ z' &= \frac{1}{2}(z + z') + \frac{1}{2}(z' - z) \rightarrow Z'(z, z') \equiv \frac{1}{2}|z + z'| + \frac{1}{2}|z' - z| \\ G_p(z, z') &= \tilde{K}_p(Z(z, z'), Z'(z, z')) \end{aligned} \quad (98)$$

<sup>17</sup> This situation is the same as that in (55) in the previous section. In the flat case (35), the corresponding function is  $\sinh \tilde{p}y$  which is odd for  $y \leftrightarrow -y$ .

<sup>18</sup> For the case  $P = 1$ , the generalized even functions are given by

$$\hat{\mathbf{I}}_\nu(z) \equiv \mathbf{I}_\nu(|z|) \quad , \quad \hat{\mathbf{K}}_\nu(z) \equiv \mathbf{K}_\nu(|z|) \quad . \quad (94)$$

These will be used for the vector propagator.

The last expression is valid for all regions and is indispensable for the calculation in Sec.10 and is important for drawing graphs. This is because the absolute functions can properly treat the singularities.

For the time-like case  $p^2 < 0$ , the explanation goes in the same way except the modified Bessel functions are replaced by the Bessel functions. The expression of  $\tilde{K}_p(z, z')$  in (98) is given by

$$\tilde{K}_p(z, z') = -\frac{\omega^3}{2} z^2 z'^2 \frac{\{\mathbf{J}_0(\frac{\hat{p}}{\omega})\tilde{\mathbf{N}}_0(\hat{p}z) - \mathbf{N}_0(\frac{\hat{p}}{\omega})\tilde{\mathbf{J}}_0(\hat{p}z)\}\{\mathbf{J}_0(\frac{\hat{p}}{T})\tilde{\mathbf{N}}_0(\hat{p}z') - \mathbf{N}_0(\frac{\hat{p}}{T})\tilde{\mathbf{J}}_0(\hat{p}z')\}}{\mathbf{J}_0(\frac{\hat{p}}{T})\mathbf{N}_0(\frac{\hat{p}}{\omega}) - \mathbf{N}_0(\frac{\hat{p}}{T})\mathbf{J}_0(\frac{\hat{p}}{\omega})} \quad , \quad (99)$$

where  $\hat{p} = \sqrt{-p^2}$ .

(98) and (99) will be used for z-coordinate graphical representation in App.C.3. We will give the equivalent expression as the y-coordinate counter-part in Sec.9.2.

## 8 Sturm-Liouville expansion approach versus P/M Propagator approach

We have solved the propagator of the 5D warped space-time (50) or (78) both in the expanded form (Sec.6) and in the closed form (Sec.7). Here we relate them as done for the flat case in Sec.5.

Using the Sturm-Liouville expansion formula[20] ( $f(z)$ : an arbitrary continuous (real) function defined in  $a \leq z \leq b$ )

$$f(z) = \sum_{n=1}^{\infty} \frac{k_n}{\Omega'(\lambda_n)} \psi_n(z) \int_a^b r(\xi) f(\xi) \psi_n(\xi) d\xi, \\ \Omega(\lambda) \equiv p(z) (\varphi^a(z, \lambda) \varphi^b(z, \lambda)' - \varphi^b(z, \lambda) \varphi^a(z, \lambda))' \quad , \quad k_n \equiv \frac{\varphi^b(z, \lambda_n)}{\varphi^a(z, \lambda_n)} \quad , \quad \Omega(\lambda_n) = 0 \quad , \\ \psi_n(z) \equiv \varphi^a(z, \lambda_n) \propto \varphi^b(z, \lambda_n) \quad (100)$$

where  $\psi_n$  is the eigen functions of the general operator defined below ( such as appeared in (62) ), and  $\varphi^a(z, \lambda)$  and  $\varphi^b(z, \lambda)$  are "intermediate" solutions, that is, they satisfy the differential equation below but the boundary condition is imposed *only* at one of the two boundary points.

$$(\hat{L} + \lambda r(z)) \varphi^a = (\hat{L} + \lambda r(z)) \varphi^b = 0 \quad , \quad \hat{L} = \frac{d}{dz} p(z) \frac{d}{dz} - q(z) \quad ,$$

$\varphi^a(z, \lambda)$  : b.c. is satisfied only at  $z = a$  ,  $\varphi^b(z, \lambda)$  : b.c. is satisfied only at  $z = b$  (101)

where  $\hat{L}$  is the general kinetic operator (Sturm-Liouville differential operator), and  $a$  and  $b$  are the boundary points on z-axis. In the present model, they are given by

$$p(z) = \frac{1}{(\omega z)^3} \quad , \quad q(z) = \frac{m^2}{(\omega z)^5} \quad , \quad r(z) = \frac{1}{(\omega z)^3} \quad , \quad a = \frac{1}{\omega} \quad , \quad b = \frac{1}{T} \quad , \\ \sqrt{\lambda} = \sqrt{-p^2} \quad (p^2 < 0 \text{ case}) \quad . \quad (102)$$

(We also use the notation  $M$  ( $=\sqrt{\lambda}$ ) and  $M_n$  ( $=\sqrt{\lambda_n}$ .) In this case, the equation (101) is the sourceless ( $J = 0$ ) version of (50) (the homogeneous differential equation). The formula (100) reduces to the ordinary Fourier expansion formula for the flat case. See App.A .

We can deduce, from the the P/M propagator, the expansion form by applying  $G_p(z, z')$  of Sec.7, using  $K_p(z, z')$  of (99) (time-like case), to  $f(z)$  above.

$$\begin{aligned} \frac{1}{\omega} \leq z, z' \leq \frac{1}{T} , \\ G_p(z, z') &= \sum_{n=1}^{\infty} \frac{k_n \psi_n(z)}{\Omega'(\lambda)|_{\lambda=M_n^2}} \left[ \int_{\frac{1}{\omega}}^{z'} \xi^{-3} K_p(\xi, z') \psi_n(\xi) d\xi + \int_{z'}^{\frac{1}{T}} \xi^{-3} K_p(z', \xi) \psi_n(\xi) d\xi \right] \\ &= \frac{1}{2} \sum_{n=1}^{\infty} \frac{\psi_n(z) \psi_n(z') - \psi_n(z) \psi_n(-z')}{p^2 + M_n^2}, \end{aligned} \quad (103)$$

where we have used the following calculation results.

$$\begin{aligned} k_n &\equiv \frac{\varphi^{(1/T)}(z, M_n)}{\varphi^{(1/\omega)}(z, M_n)} = 1, \\ \Omega(\lambda) &\equiv z^{-3} \left\{ \varphi^{(1/\omega)}(z, \sqrt{\lambda}) \frac{\partial \varphi^{(1/T)}(z, \sqrt{\lambda})}{\partial z} - \varphi^{(1/T)}(z, \sqrt{\lambda}) \frac{\partial \varphi^{(1/\omega)}(z, \sqrt{\lambda})}{\partial z} \right\} \\ &= \frac{2\omega^4}{\pi N_n^2} \left\{ b_0(\omega\sqrt{\lambda}/T) - b_0(\sqrt{\lambda}) \right\}, b_0 \text{ is defined in (58)}. \\ \Omega'(\lambda)|_{\lambda=M_n^2} &= -\frac{2\omega^4 \{ \mathbf{J}_0^2(\frac{M_n}{T}) - \mathbf{J}_0^2(\frac{M_n}{\omega}) \}}{\pi^2 N_n^2 M_n^2 \mathbf{N}_0(\frac{M_n}{\omega}) \mathbf{N}_0(\frac{M_n}{T}) \mathbf{J}_0(\frac{M_n}{\omega}) \mathbf{J}_0(\frac{M_n}{T})}, \\ N_n^2 &= \frac{2\omega \{ \mathbf{N}_0^2(\frac{M_n}{\omega}) - \mathbf{N}_0^2(\frac{M_n}{T}) \}}{\mathbf{N}_0^2(\frac{M_n}{\omega}) \mathbf{N}_0^2(\frac{M_n}{T})}. \end{aligned} \quad (104)$$

Particularly, we have used the Lommel's formula  $\mathbf{J}_\nu(z) \mathbf{N}_{\nu+1}(z) - \mathbf{J}_{\nu+1}(z) \mathbf{N}_\nu(z) = -2/\pi z$  and the following formula of indefinite integral that makes the propagator  $1/(p^2 + M_n^2)$  appear in the final expression of(103).

$$\int \xi \mathbf{Z}_0(\alpha\xi) \mathbf{Z}_0(\beta\xi) d\xi = \frac{\xi}{\alpha^2 - \beta^2} \{ \alpha \mathbf{Z}_1(\alpha\xi) \mathbf{Z}_0(\beta\xi) - \beta \mathbf{Z}_0(\alpha\xi) \mathbf{Z}_1(\beta\xi) \}, \quad (105)$$

where  $\mathbf{Z}_\nu$  represents  $\mathbf{J}_\nu$  and  $\mathbf{N}_\nu$ .

The result (103) is valid for other regions of  $z$  and  $z'$ . The same result is obtained also for the space-like case ( $p^2 > 0$ ). In this text the equivalence between SL-expansion and P/M propagator is shown only for  $\nu=0$ . It is valid for general  $\nu$ . In App.B we give an alternative proof which is valid for general  $\nu$ .

In this warped case, both SL-expansion and P/M-propagator approaches are done in the interval  $y \in [-l, l]$ . It can be extended to  $\mathbf{R}=(-\infty, \infty)$  by the procedure of the *universal covering*: we extend the solution, obtained for the interval  $[-l, l]$ , to  $\mathbf{R}$  by *requiring the*

periodicity  $y \rightarrow y + 2l$ .

$$\begin{aligned}\Phi(x^a, z) &= \sum_n \phi_n(x) \psi_n(z) \quad , \quad \psi_n(z) = \sum_{m=1}^{\infty} c_{nm} \sin \frac{m\pi}{l} y \quad , \\ c_{nm} &\equiv \frac{1}{l} \int_{-l}^l \psi_n(z(y)) \sin \frac{m\pi}{l} y dy = \frac{2}{l} \int_0^l \psi_n(\frac{1}{\omega} e^{\omega y}) \sin \frac{m\pi}{l} y dy \quad ,\end{aligned}\quad (106)$$

where the relation (46) is used. In this way, we can introduce the orbifold picture. This is important to connect the warped solution and the flat solution by the deformation parameter  $\omega$ .

Whether we view the system in the orbifold picture or in the interval one depends on our choice of the *infrared* regularization of the extra axis. For the former case, the extra axis is basically  $\mathbf{R} = (-\infty, \infty)$  and two identifications ( $y \leftrightarrow -y$ ,  $y \rightarrow y + 2l$ ) are imposed there. On the other hand, for the latter case, the extra axis is the interval  $[-l, l]$  with  $y \leftrightarrow -y$  identification. The importance of the infrared regularization (of the extra axis) was stressed, in the context of the wall-anti-wall formation, in Ref.[21]. In (106), we see the importance of y-coordinate as well as z.

## 9 Behaviour of P/M Propagator

The P/M propagator involves all KK modes contributions. Its behaviour characteristically changes depending on the 4-momentum  $p_a$  in relation to its absolute value  $|p_a p^a| = |p^2|$  and 2 mass parameters,  $l$  (boundary parameter, periodicity) and  $\omega$  (bulk curvature). The  $p$ -dependence for the various  $(y, y')$  (or  $(z, z')$ ) was examined in Ref.[9]. Here we show the  $(y, y')$ -dependence for various  $p_a$ . Characteristic 'brane' structures manifestly appear.

Note: In all figures in the following, the vertical plot is cut at some appropriate value when the graph height is too large.

### 9.1 Flat 5D Massless Scalar Propagator ( $Z_2$ -parity Odd, Dirichlet-Dirichlet b.c.)

The behaviour of 5D massless scalar in the flat geometry, space-like case (36) and time-like case (38), is shown in Fig.7-12.  $Z_2$ -parity is taken to be odd:  $P=-1$ . Dirichlet b.c. is imposed for all fixed points  $(y, y' = 0, \pm l)$ .

We take the boundary parameter value as

$$l=\pi, \quad 1/l \sim 0.3$$

We use the following notation.

$$\tilde{p} \equiv \sqrt{p^2} \text{ for } p^2 > 0 \text{ (space-like)}; \quad \hat{p} \equiv \sqrt{-p^2} \text{ for } p^2 < 0 \text{ (time-like)}$$

In this case, the scale parameter is the periodicity parameter  $l$  only. We can characterize the behaviours by the momentum  $p$  in comparison with  $1/l$ .

(A) Space-Like

(1S)  $\tilde{p} \ll 1/l$  , Fig.7

Upheaval and downheaval surfaces front each other at sharp edges which correspond the singularities at  $y \pm y' = 0$ . The size of the slope is  $l$ . Boundary constraint is strong. This is the 'Boundary phase'. The scale  $\tilde{p}$  does not appear in the graph.

(2S)  $\tilde{p} \sim 1/l$  , Fig.8

The gross shape is similar to (1S).

(3S)  $\tilde{p} \gg 1/l$  , Fig.9

Walls and valleys run along the diagonal axes. The configuration is free from the boundary constraint. This is the 'Dynamical phase'. The size of the wall (valley) thickness is  $1/\tilde{p}$ . Absolute value of the effective height decreases clearly. In the point of the wall (valley) formation, this situation is common to the warped case. See the (3S) of Sec.9.2.

(B) Time-Like

(1T)  $\hat{p} \ll 1/l$  , Fig.10

Shape is similar to the space-like case. This is the 'Boundary phase'.

The situation that the propagator configuration, for the small  $|p|$ , is almost same both for the space-like case and for the time-like case, is generally valid in the following ( even for the warped case). <sup>19</sup>

(2T)  $\hat{p} \sim 1/l$  , Fig.11

The absolute value of the height increases and decreases by changing  $\hat{p}$  within this region. The global shape does not change.

(3T)  $\hat{p} \gg 1/l$  , Fig.12

The wavy behaviour appears. This is the contrasting point compared with the space-like case. The singularity-lines are buried in the waves. Boundary constraint is not effective. This is the 'Dynamical phase'. The size of the wave length is  $1/\hat{p}$ .

This situation of wave formation, for the large  $\hat{p}$  in the time-like case, is generally seen in the following. Compared with the space-like case, the absolute value does not so much change for the time-like case.

Other flat propagators are displayed in Appendixes C.1 and C.2.

## 9.2 Warped 5D Scalar Propagator (Z<sub>2</sub>-Odd, Dirichlet-Dirichlet b.c.)

We graphically show the P/M propagator behaviour of 5D scalar , with  $P=-1$ , in the warped geometry: (98) with (96) for  $p^2 > 0$ , (99) for  $p^2 < 0$ . <sup>20</sup> Dirichlet b.c. is imposed on all fixed points  $(y, y' = 0, \pm l)$ . As for the choice of the value of  $\omega$ , we have the following possibilities: 1)  $\omega \ll 1/l$ , 2)  $\omega < 1/l$ , 3)  $\omega \sim 1/l$ , 4)  $\omega > 1/l$ , 5)  $\omega \gg 1/l$ . Case 1) is important for approaching the flat limit from the warped geometry. Case 5) is the situation in the real world because we know Tev(Weak)-scale/Planck-scale =  $10^{-16} = \exp(-\omega l)$ . For

<sup>19</sup> A simple reason for this similarity is the relations:  $\sin x \sim \sinh x$  ,  $\cos x \sim \cosh x$  for  $|x| \ll 1$ .

<sup>20</sup> The expressions, however, are written in z-coordinate. They are equivalently rewritten in y-coordinate as in (107) for the space-like case, and in (108) for the time-like case.

Figure 7: Flat 5D Massless Scalar Propagator ( $Z_2$ -odd, Dirichlet-Dirichlet b.c.),  $\tilde{p}=0.03 \ll 1/l$ , space-like,  $S^1$ -boundary is strongly influenced. Sec.9.1(1S)

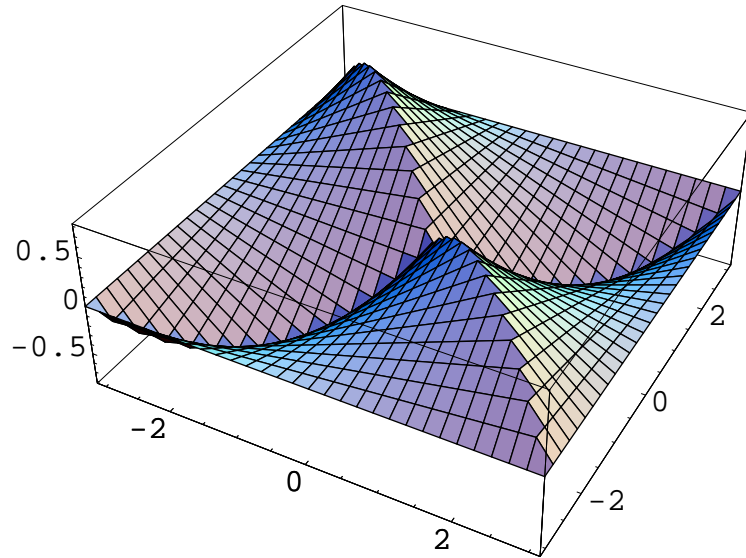


Figure 8: Flat 5D Massless Scalar Propagator ( $Z_2$ -odd, Dirichlet-Dirichlet b.c.),  $\tilde{p}=0.3 \sim 1/l$ , space-like, Sec.9.1(2S)

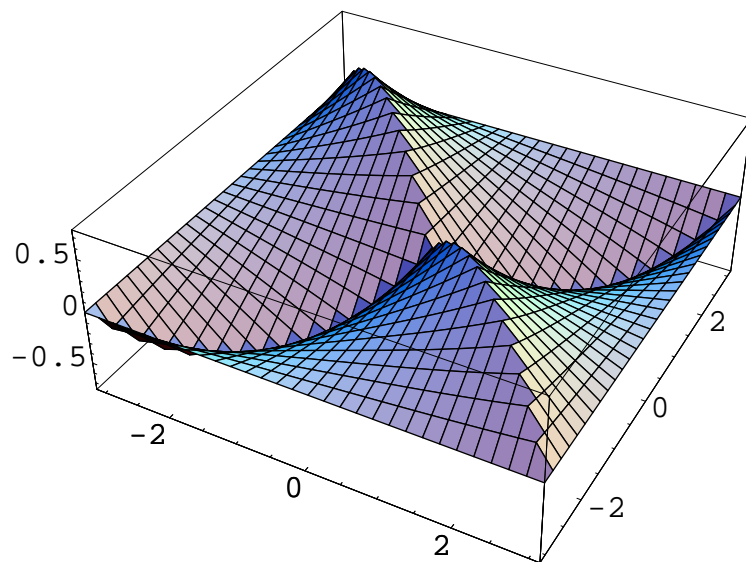


Figure 9: Flat 5D Massless Scalar Propagator ( $Z_2$ -odd, Dirichlet-Dirichlet b.c.),  $\tilde{p}=3 \gg 1/l$ , space-like,  $S^1$ -boundary is not influenced, Sec.9.1(3S)

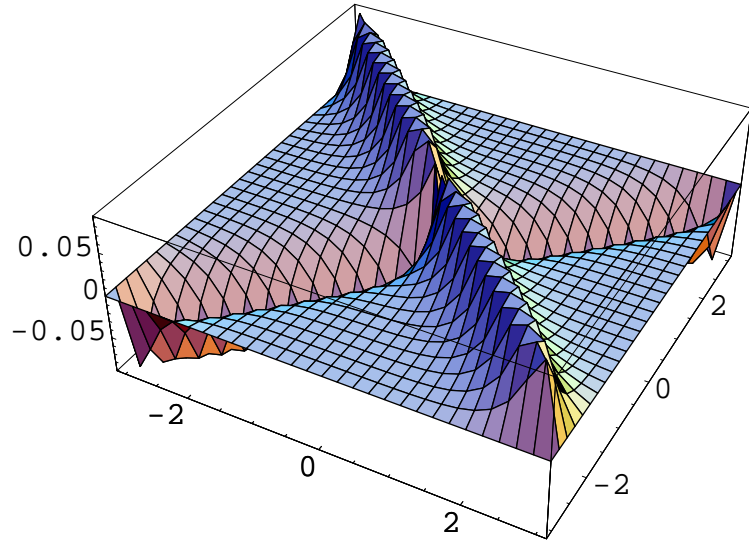


Figure 10: Flat 5D Massless Scalar Propagator ( $Z_2$ -odd, Dirichlet-Dirichlet b.c.),  $\hat{p}=0.03 \ll 1/l$ , time-like, Sec.9.1(1T),  $S^1$ -boundary is strongly influenced

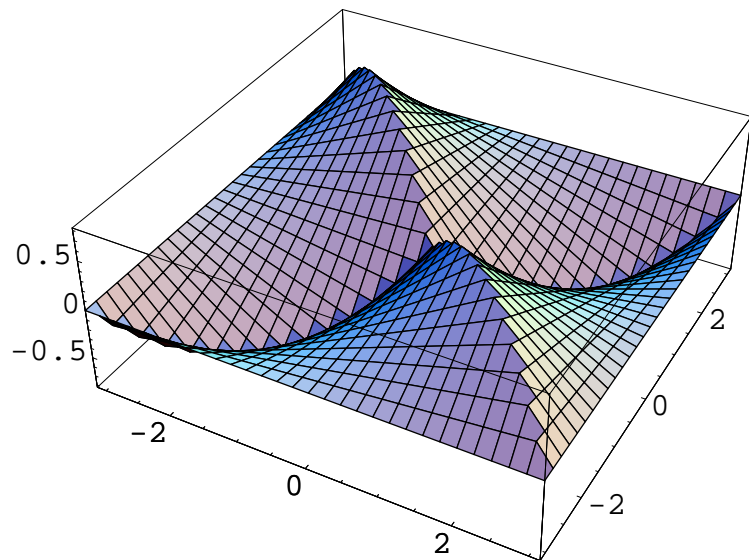


Figure 11: Flat 5D Massless Scalar Propagator ( $Z_2$ -odd, Dirichlet-Dirichlet b.c.),  $\hat{p}=0.3$   
 $\sim 1/l$ , time-like, Sec.9.1(2T)

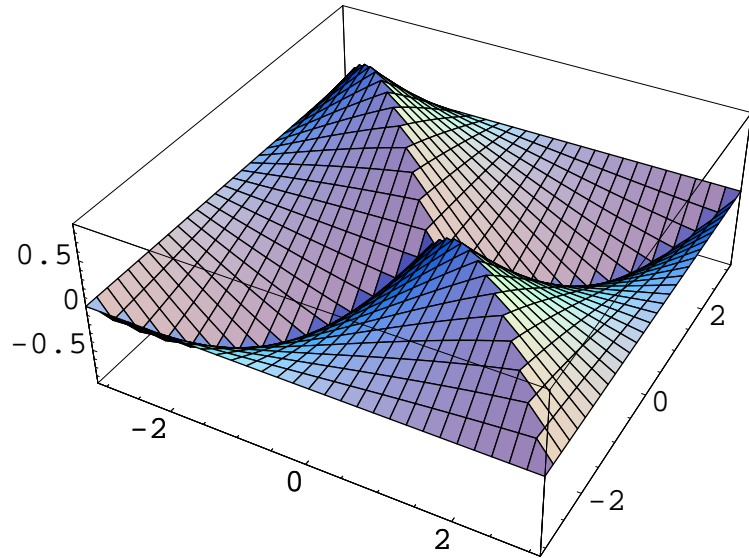
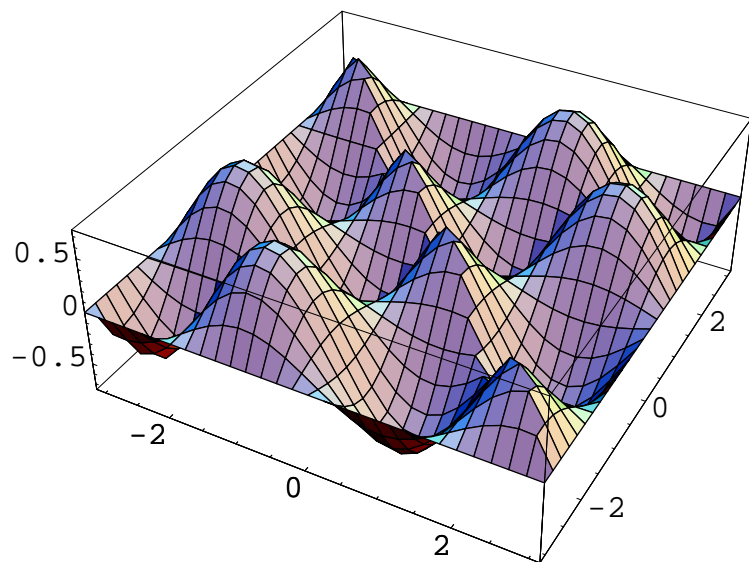


Figure 12: Flat 5D Massless Scalar Propagator ( $Z_2$ -odd, Dirichlet-Dirichlet b.c.),  $\hat{p}=1.7$   
 $> 1/l$ , time-like, Sec.9.1(3T)



simplicity, we take the case 4) for the display of graphs. The values are  
 $l=\pi$ ,  $1/l\sim 0.3$ ,  $\omega=1$ ,  $T=\omega \exp(-\omega l) \sim 0.04$

We use the following notation.

$\tilde{p} \equiv \sqrt{p^2}$  for  $p^2 > 0$  (space-like);  $\hat{p} \equiv \sqrt{-p^2}$  for  $p^2 < 0$  (time-like)

(A) Space-Like Case

For the y-coordinate presentation, we use the following propagator function.

$$G_p(y, y') = K_p(Y(y, y'), Y'(y, y')) ,$$

$$K_p(Y, Y') = \frac{1}{2\omega} \exp(2\omega|Y| + 2\omega|Y'|) \epsilon(Y) \epsilon(Y') \times$$

$$\frac{\{\mathbf{I}_0(\frac{\tilde{p}}{\omega}) \mathbf{K}_0(\frac{\tilde{p}}{\omega} e^{\omega|Y|}) - \mathbf{K}_0(\frac{\tilde{p}}{\omega}) \mathbf{I}_0(\frac{\tilde{p}}{\omega} e^{\omega|Y|})\} \{\mathbf{I}_0(\frac{\tilde{p}}{T}) \mathbf{K}_0(\frac{\tilde{p}}{\omega} e^{\omega|Y'|}) - \mathbf{K}_0(\frac{\tilde{p}}{T}) \mathbf{I}_0(\frac{\tilde{p}}{\omega} e^{\omega|Y'|})\}}{\mathbf{I}_0(\frac{\tilde{p}}{T}) \mathbf{K}_0(\frac{\tilde{p}}{\omega}) - \mathbf{K}_0(\frac{\tilde{p}}{T}) \mathbf{I}_0(\frac{\tilde{p}}{\omega})} , \quad (107)$$

where  $Y(y, y')$  and  $Y'(y, y')$  are defined in (39).

(1S)  $\tilde{p} \ll 1/l < \omega$  , Fig.13

2 sharp up-ward spikes and 2 sharp down-ward spikes appear at corners. The effective thickness of the spikes is  $1/\omega$ . (Note again that the top surface is cut at an appropriate height.) The size of the global upheaval and downheaval is  $l$ . The boundary constraint is dominant. This is the "boundary phase". There is a flat region around the center ( $y = y' = 0$ ). The propagator vanishes there. This means that the bulk propagation, near the Planck brane, gives no contribution to the amplitude. On the other hand, near the Tev brane ( $y, y' = \pm l$ ), it gives a sizable effect.

We will see the warped scale parameter  $\omega$  appears in all "phases".

(2S)  $1/l < \tilde{p} \sim \omega$  , Fig.14

2 walls with sharp edges and 2 sharp valleys develop along the diagonal axes from the corners to the center. Their thickness is  $1/\tilde{p} \sim 1/\omega$ . The flat region near the center disappears. Absolute value of the effective height decreases.

(3S)  $1/l < \omega < \tilde{p}$  , Fig.15

Walls and valleys develop from the corners almost to the center. The effective thickness of them is  $1/\tilde{p}$  near the corners and is  $1/\omega$  near the center. There is no boundary effect. This is the "dynamical phase". There is no flat region near the center, whereas in the off-diagonal region there appears the zero-value flat region. This means the bulk propagation takes place only for the case  $y' \pm y \sim 0$ . Absolute value of the effective height decreases rapidly as  $\tilde{p}$  increases.

(B) Time-Like Case

For the y-coordinate presentation, we use the following propagator function.

$$G_p(y, y') = K_p(Y(y, y'), Y'(y, y')) ,$$

$$K_p(Y, Y') = \frac{1}{2\omega} \exp(2\omega|Y| + 2\omega|Y'|) \epsilon(Y) \epsilon(Y') \times$$

$$\frac{\{\mathbf{J}_0(\frac{\hat{p}}{\omega}) \mathbf{N}_0(\frac{\hat{p}}{\omega} e^{\omega|Y|}) - \mathbf{N}_0(\frac{\hat{p}}{\omega}) \mathbf{J}_0(\frac{\hat{p}}{\omega} e^{\omega|Y|})\} \{\mathbf{J}_0(\frac{\hat{p}}{T}) \mathbf{N}_0(\frac{\hat{p}}{\omega} e^{\omega|Y'|}) - \mathbf{N}_0(\frac{\hat{p}}{T}) \mathbf{J}_0(\frac{\hat{p}}{\omega} e^{\omega|Y'|})\}}{\mathbf{J}_0(\frac{\hat{p}}{T}) \mathbf{N}_0(\frac{\hat{p}}{\omega}) - \mathbf{N}_0(\frac{\hat{p}}{T}) \mathbf{J}_0(\frac{\hat{p}}{\omega})} , \quad (108)$$

where  $Y(y, y')$  and  $Y'(y, y')$  are defined in (39).

Figure 13: Warped 5D Scalar Propagator ( $Z_2$ -odd, Dirichlet-Dirichlet b.c.),  $\tilde{p}=0.005 \ll T < 1/l < \omega$ , space-like, Sec.9.2(1S), "boundary phase"

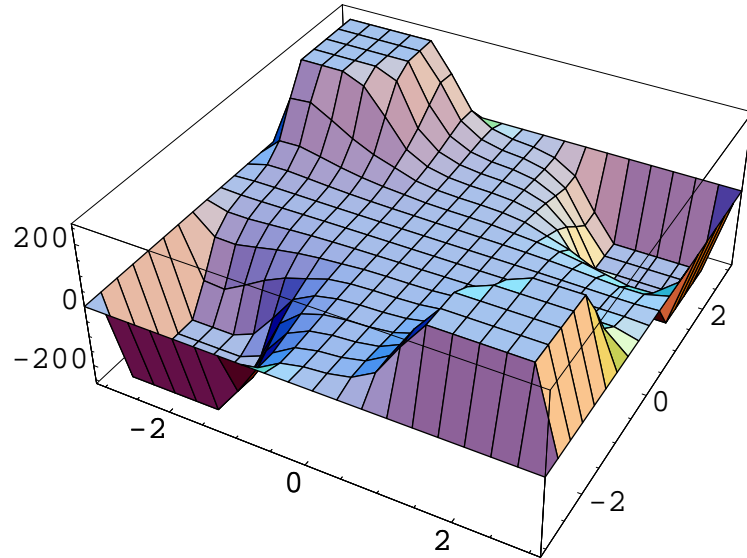


Figure 14: Warped 5D Scalar Propagator ( $Z_2$ -odd, Dirichlet-Dirichlet b.c.),  $T \ll 1/l < \tilde{p}=1=\omega$ , space-like, Sec.9.2(2S)

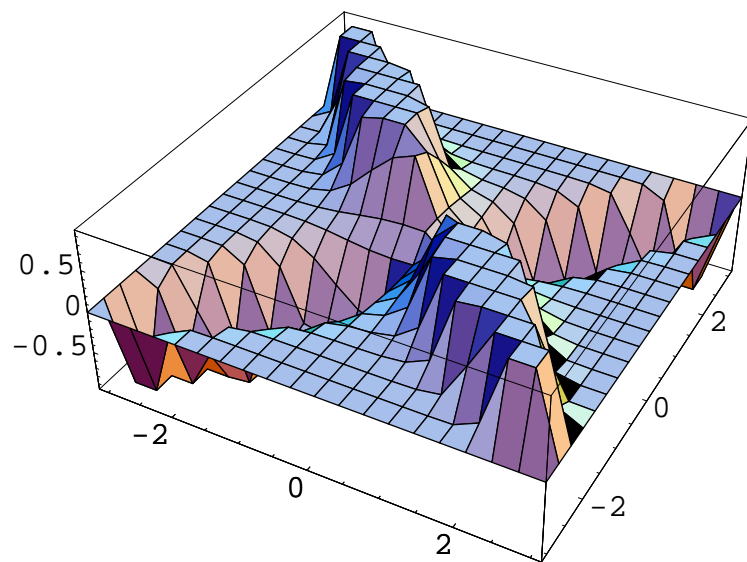
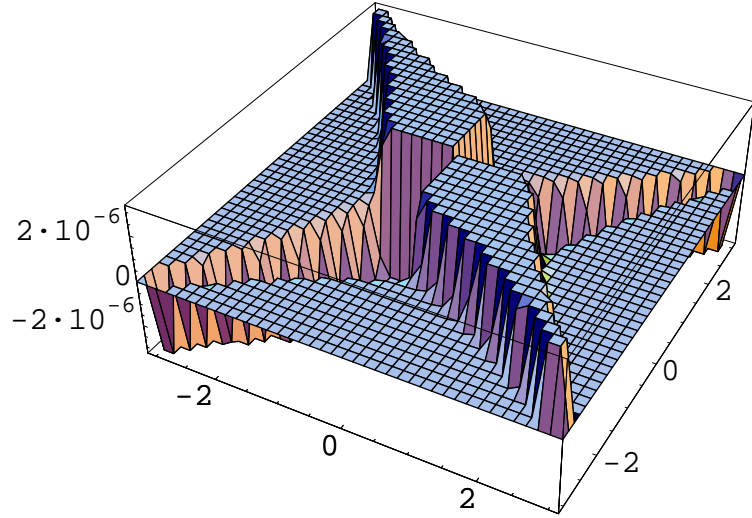


Figure 15: Warped 5D Scalar Propagator ( $Z_2$ -odd, Dirichlet-Dirichlet b.c.),  $T \ll 1/l < \omega < \hat{p}=5$ , space-like, Sec.9.2(3S)



(1T)  $\hat{p} \ll 1/l < \omega$  , Fig.16

The behaviour is quite similar to the space-like case (1S) above. The fact that, for low 4D momentum ( $\hat{p}$ ), the P/M propagator behaviours of the space-like case and of the time-like case are similar, is widely valid. See other cases below.

(2T)  $1/l < \hat{p} \sim \omega$  , Fig.17

Wavy behaviour appears. Sharp spikes gather near the 4 corners and form groups within the range of order  $1/\omega = 1/\hat{p}$ . Two types of waves are there. One type has the small wave-length of order  $1/\hat{p}=1/\omega$ , and the waves of this type appear along the 4 rims. The other type has the long wave-length of order  $l$ , which comes from the boundary constraint. It appears in the center and forms a very moderate hill. The propagator takes nearly 0 value there. This is contrasting with the space-like case. As the whole configuration,  $Z_2$  oddness disappears.

(3T)  $1/l < \omega < \hat{p}$  , Fig.18

Spikes and two types of waves are there. It is roughly similar to (2T). The plain in the center forms clearly a disk. The propagator takes nearly 0 value there. This is contrasting with the space-like case. The overall height decreases. As in (2T),  $Z_2$  oddness disappears. Although the scale  $l$  looks to appear as the radius of the plain around the center, the main configuration is free from the boundary effect. It is nearly the "dynamical phase".

From (1S) to (3S), from (1T) to (3T), the ratio  $\omega/p$  decreases. We cannot take the flat limit in this way. In fact the scale  $\omega$  remains in all "phases". The correct condition for

Figure 16: Warped 5D Scalar Propagator ( $Z_2$ -odd, Dirichlet-Dirichlet b.c.),  $\hat{p}=0.005 \ll T < 1/l < \omega$ , time-like, Sec.9.2(1T)

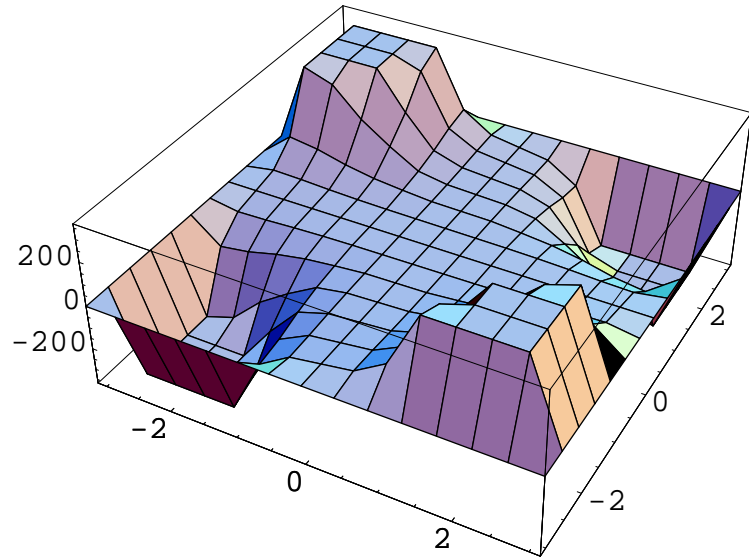


Figure 17: Warped 5D Scalar Propagator ( $Z_2$ -odd, Dirichlet-Dirichlet b.c.),  $T \ll 1/l < \hat{p}=1=\omega$ , time-like, Sec.9.2(2T)

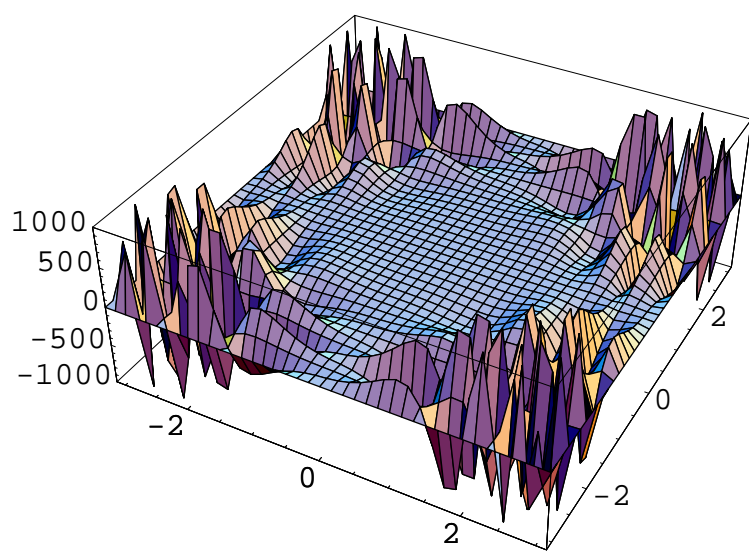
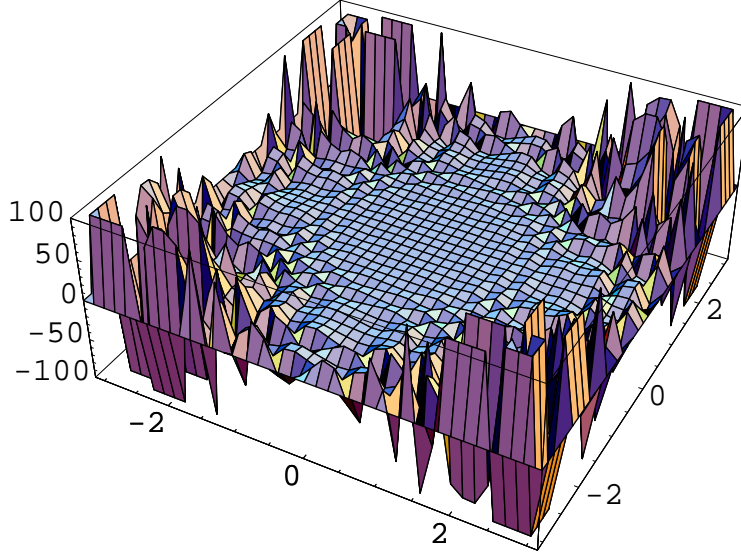


Figure 18: Warped 5D Scalar Propagator ( $Z_2$ -odd, Dirichlet-Dirichlet b.c.),  $T \ll 1/l < \omega < \hat{p}=5$ , time-like, Sec.9.2(3T)



the flat limit is both  $\omega \ll 1/l$  and  $\omega \ll p$  are satisfied. We have confirmed that, taking the values  $l = \pi$ ,  $\omega = 0.001$  ( $\omega \ll 1/l$ ), the warped propagators (107) and (108) produce graphs quite similar to the flat results of Sec.9.1 (Fig.7-12).

## 10 Solving $\delta(0)$ -problem and the deformation of propagator

P/M propagator for 5D scalar is, for the space-like 4 momentum case, given by (36). It is expressed as

$$G_p(y, y') = \frac{1}{4\tilde{p} \sinh \tilde{p}l} [\{\cosh 2\tilde{p}v_+(y, y') - \cosh 2\tilde{p}v_-(y, y')\} \cosh \tilde{p}l + \{-\sinh 2\tilde{p}v_+(y, y') + \sinh 2\tilde{p}v_-(y, y')\} \sinh \tilde{p}l] \quad . \quad (109)$$

where  $v_-$  and  $v_+$  are defined by

$$v_{\mp}(y, y') \equiv \frac{1}{2}|y' \mp y| \quad : \quad y \leftrightarrow y' \text{ symmetric} \quad . \quad (110)$$

Using the following relations:

$$\begin{aligned}
\frac{\partial v_-}{\partial y} &= -\frac{1}{2}\epsilon(y' - y) & \frac{\partial v_-}{\partial y'} &= \frac{1}{2}\epsilon(y' - y) \\
\frac{\partial v_+}{\partial y} &= \frac{1}{2}\epsilon(y' + y) & \frac{\partial v_+}{\partial y'} &= \frac{1}{2}\epsilon(y' + y) \\
\frac{\partial^2 v_-}{\partial y^2} &= \delta(y' - y) & \frac{\partial^2 v_-}{\partial y' \partial y} &= -\delta(y' - y) & \frac{\partial^2 v_-}{\partial y'^2} &= \delta(y' - y) \\
\frac{\partial^2 v_+}{\partial y^2} &= \delta(y' + y) & \frac{\partial^2 v_+}{\partial y' \partial y} &= \delta(y' + y) & \frac{\partial^2 v_+}{\partial y'^2} &= \delta(y' + y)
\end{aligned} \tag{111}$$

we obtain, for the flat case (109),

$$\begin{aligned}
\frac{\partial^2 G_p}{\partial y \partial y'} \bigg|_{y=y'=0} &= -\delta(0) + \frac{1}{2}\tilde{p} \coth \tilde{p}l & , \\
\frac{\partial^2 G_p}{\partial y \partial y'} \bigg|_{y=0, y'=\pm l} &= \frac{1}{2} \frac{\tilde{p}}{\sinh \tilde{p}l} & , \\
\frac{\partial^2 G_p}{\partial y \partial y'} \bigg|_{y=y'=\pm l} &= -\delta(0) + \frac{1}{2}\tilde{p} \coth \tilde{p}l & .
\end{aligned} \tag{112}$$

The above result says the bulk scalar propagation starting and ending at the Planck brane and that starting and ending at Tev brane are the same. The propagation starting at the Planck(Tev) brane and ending at the Tev(Planck) brane does not have  $\delta(0)$  singularity.

The  $\delta(0)$  problem first appeared in the analysis of 11D supergravity on a manifold with boundary in relation to the  $E_8 \times E_8$  heterotic string and M-theory[11]. It was shown, using a simpler model, that the problem generally occurs in the bulk-boundary theory[22]. When the bulk scalar  $\Phi$  has a derivative ( $\partial_y$ ) coupling with other field (this is the case of Mirabelli-Peskin model), the  $\Phi$  propagator part in a quantum-loop amplitude appears as the form  $\partial^2 G_p / \partial y \partial y'$ . In Ref.[22], the cancellation of  $\delta(0)$  was shown in a self energy calculation using KK-expansion. The cancellation was further confirmed in an improved way in Ref.[23, 24]. The first equation in (112) exactly coincides with the results in these papers. In the papers, however, the equation was obtained by summing all KK-modes contribution. In this paper the same equation is obtained *without* doing the KK-summation.

For the warped case, the corresponding propagator (5D scalar, space-like 4 momentum, Dirichlet b.c.) is given in (98). After calculation using (111), we obtain

$$\frac{\partial^2 G_p}{\partial y \partial y'} \bigg|_{y=y'=0} = -\delta(0) - 2\omega + \tilde{p} \frac{\mathbf{I}_0(\frac{\tilde{p}}{T})\mathbf{K}_1(\frac{\tilde{p}}{\omega}) + \mathbf{K}_0(\frac{\tilde{p}}{T})\mathbf{I}_1(\frac{\tilde{p}}{\omega})}{I_0(\frac{\tilde{p}}{T})\mathbf{K}_0(\frac{\tilde{p}}{\omega}) - \mathbf{K}_0(\frac{\tilde{p}}{T})\mathbf{I}_0(\frac{\tilde{p}}{\omega})} . \tag{113}$$

<sup>21</sup> We confirm eq.(113) leads to the first equation of eq.(112) in the limit:  $\omega/\tilde{p} \rightarrow +0$ ,  $\tilde{p}l = \text{fixed}$ . This shows the warped case is, at the propagator level, continuously connected with the

<sup>21</sup> The appearance of  $\delta(0)$  was known in Ref.[25] where KK-summation was used.

flat one. The result (113) says that the *warped version* of the Mirabelli-Peskin model does *not* suffer from the  $\delta(0)$  problem.

In Ref.[23], it is shown that the finite part of above expressions , (112) and (113), can be regarded as a "deformation" factor from the ordinary 4D theory propagator. The linear divergence, for  $\tilde{p} \rightarrow \infty$ , of the finite part just gives the UV-divergence due to 5D quantum fluctuation. Both flat and warped cases are non-renormalizable in this sense. <sup>22</sup> See Sec.11 for further discussion about the renormalizability.

## 11 Discussions and Conclusion

We have treated QFT in the 5D flat and warped space-time. The  $Z_2$ -parity is respected. The P/M propagator is closely analyzed. Its singular properties are systematically treated by the use of the absolute functions. We have obtained the visual output of various P/M propagators, which enables us to know the various "phases" depending upon the choice of fields (scalar, vector,  $\cdots$ ), boundary conditions (Dirichlet, Neumann), space-time geometry (flat, warped), the 4D momentum property(space-like, time-like) and its magnitude ( $\sqrt{|p^2|}$  in relation to  $1/l$  and  $\omega$ ). It is shown that the eigen-mode expansion approach is equivalent to the P/M propagator approach. They are related by the Fourier-expansion for the flat case and by the Sturm-Liouville expansion for the warped case. The Dirac's bra and ket vector formalism is naturally introduced for quantizing the 5D (flat and warped) space-time with  $Z_2$ -parity.

We add some comments and discussions as follows.

1) The Feynman rule for the present approach is straightforward and is given in Ref.[9]. The characteristic points are the appearance of the metric factors at vertices and the extra-axis integral form restricted by the directedness of the extra coordinate.

2) BRS structure is important for defining physical quantities in gauge theories. It is very successful in the 4D renormalizable theories. For the present model of higher dimensions, the structure is missing. The formal higher dimensional extension is possible, but the treatment of the extra dimension part is quite obscure. In Ref.[9], some Ward identities seem to work.

3) Generally the string theory is regarded advantageous over the QFT because the fundamental unit of the string tension  $\alpha'$  are there and the extendedness "softens" the singularities. The present approach is based on the higher-dimensional QFT. The extendedness parameter appears as the thickness  $\omega$ . The situation of the boundary conditions and the "brane" formation looks similar to that in the string theory. In particular, the role of the extra-axis looks to correspond to that of the open string which is used to define the D-brane. Of course, these similarities come from the fact that the original models are invented and examined, triggered by the string theory development. We point out the present approach could reveal some important *regularization* aspect of the string theory in a *simplified* way. In this respect, it is worth discussing the regularization in the present

---

<sup>22</sup> See eq.(54) of Ref.[23] for detail.

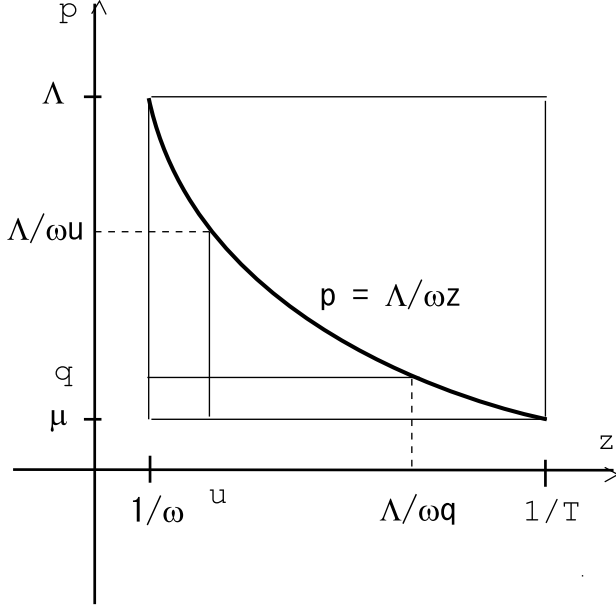
approach. In Fig.19, the integration space is shown. The horizontal axis is z-coordinate, and the range is  $1/\omega \leq z \leq 1/T$ . The vertical one is (the absolute value of) the 4D momentum. It runs in the range  $\mu (\equiv (T/\omega) \cdot \Lambda, \text{infrared cutoff}) \leq p \leq \Lambda (\text{ultraviolet cutoff})$ . What region of (z,p)-space, shown in Fig.19, should be integrated is the present discussion point. Ref.[9] proposed the region:

$$p z \leq \frac{\Lambda}{\omega} \quad , \quad \frac{1}{\omega} \leq z \leq \frac{1}{T} \quad , \quad (114)$$

based on the concrete behaviour of the P/M propagator. (See Fig.40 and Fig.41 and their explanation in App.C.5.) Adapting the region (114), the  $\beta$ -function of the gauge coupling was *finitely* obtained[9]. Clearly this procedure is still primitive and some persuasive explanation is required. We propose here a new definition of the integral region. For the explanation we look the integral region in the space of (z-coordinate, 4D coordinate  $x^a$ ), that is, the 5D coordinate space. See Fig.20. This is an equivalent description. For simplicity we take 5D Euclidean space. On the Planck-brane ( $z = 1/\omega$ ), the 4D space integral region is taken to be  $1/\Lambda \leq x \equiv \sqrt{x^a x^a} \leq 1/\mu$ . This region is 4 dimensional and forms the *thick* sphere-shell bounded by two  $S^3$ 's: one ( $S^3_{UV,Pla}$ ) has the radius  $1/\Lambda$  and the other ( $S^3_{IR,Pla}$ ) has the radius  $1/\mu$ . On the Tev-brane ( $z = 1/T$ ), the 4D space integral region is  $(1 - \varepsilon)/\mu \leq x \leq 1/\mu$ , where  $\varepsilon$  is a new regularization parameter which tends to the positive 0,  $\varepsilon \rightarrow +0$ . As on the Planck-brane, the integral region is 4 dimensional and forms the *thin* sphere-shell bounded by two  $S^3$ 's: one ( $S^3_{UV,Tev}$ ) has the radius  $(1 - \varepsilon)/\mu$  and the other ( $S^3_{IR,Tev}$ ) has the radius  $1/\mu$ . Between the two branes ( $1/\omega < z < 1/T$ ), the integral region is the 5D volume bounded by two 4D regularization surfaces,  $B_{UV}$  and  $B_{IR}$ , which can be determined by the *minimal area principle* and the boundary condition ( $S^3_{UV,Pla}$  at  $z = 1/\omega$ ,  $S^3_{UV,Tev}$  at  $z = 1/T$  for  $B_{UV}$ ;  $S^3_{IR,Pla}$  at  $z = 1/\omega$ ,  $S^3_{IR,Tev}$  at  $z = 1/T$  for  $B_{IR}$ ). Two regularization  $S^3$  spheres, the UV sphere and the IR sphere, "flow" along the z-axis changing their radii:  $B_{UV}$  describes the change of the UV sphere and  $B_{IR}$  describes the change of the IR sphere. The advantage of the new definition is that, only at the fixed points, the artificial cutoffs are introduced. This is the same situation as taken in the ordinary 4D renormalizable theories. Between the fixed points, the regularization surfaces ( $B_{UV}, B_{IR}$ ) are not introduced by hand but determined by the *bulk geometrical dynamics*. If we view this new integral region in the (z,p)-space, the similar region to (114) is expected to be obtained. It is quite interesting that the regularization surfaces,  $B_{UV}$  and  $B_{IR}$ , have similarity to the *tree propagation* of the *closed string*. The necessity of restriction on the integral region (114) strongly suggests the requirement of a new type "quantization". The integral region condition (114) looks a sort of the *uncertainty relation*. If this view is right, it is quite notable that the conjugate variable (in the quantum phase space) of the extra coordinate z is played by the absolute value of the 4D momentum,  $\sqrt{|p^2|}$ . The present standpoint described above is that the new relation comes from the *minimal area principle*. Hence the behaviour of the boundary surfaces,  $B_{UV}$  and  $B_{IR}$ , plays an important role.

4) The flat system is characterized by the cyclic functions, while the warped one is characterized by the Bessel functions. Although the periodicity is *lost* in the latter system,

Figure 19: Space of  $(z, p)$  for the integration.  $\Lambda/\omega u$  is the position-dependent cutoff[9].



both sets of functions constitute the complete orthonormal system and sufficiently deserve describing the quantum Hilbert space. The present analysis strongly suggests the Bessel function system can be regarded as a one-parameter *deformed system* of the cyclic functions.

5) As for the phenomenology application, besides the ones mentioned in the introduction, Higgs sector analysis based on 5D model is active. The Higgs field is identified with the extra-component of the bulk gauge field and the effective action is calculated under the name of "holographic pseudo-Goldstone boson"[26, 27, 28]. The form factors there correspond to P/M propagators  $G_p(y, y')$  of the present work.

## 12 App. A : Sturm-Liouville expansion formula

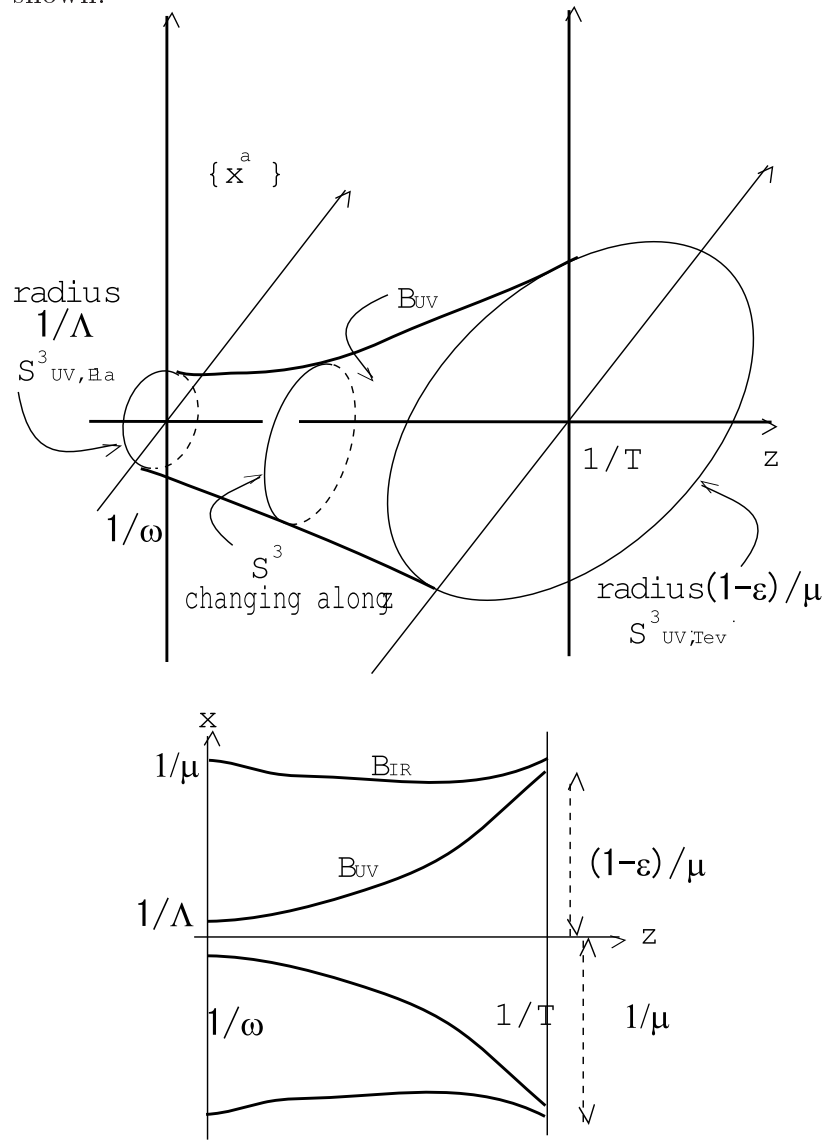
We apply the Strum-Liouville expansion formula (100) to the flat case of Sec.2 and Sec.4.

$$\begin{aligned} \partial_M \partial^M \Phi(X) &= -J(X) \quad , \\ \Phi(X) &= \int \frac{d^4 p}{(2\pi)^4} e^{ipx} \Phi_p(y) \quad , \quad J(X) = \int \frac{d^4 p}{(2\pi)^4} e^{ipx} J_p(y) \quad , \\ (-p^2 + \frac{\partial^2}{\partial y^2}) \Phi_p(y) &= -J_p(y) \quad . \end{aligned} \quad (115)$$

Hence the general operator  $\hat{L}$  (101) and the boundary points are given by

$$\begin{aligned} p(y) &= 1 \quad , \quad q(y) = 0 \quad , \quad r(y) = 1 \quad , \quad \lambda = -p^2 \quad , \\ a &= 0 \quad , \quad b = l \quad . \end{aligned} \quad (116)$$

Figure 20: Space of  $(z, x^a)$  for the integration.  $B_{IR}$ ,  $S_{IR,Pla}^3$  and  $S_{IR,Tev}^3$  can be similarly shown.



We consider the odd  $Z_2$ -parity,  $P=-1$ , as in the text. Time-like case,  $p^2 < 0$ , is taken. The homogeneous equation and its "intermediate" solutions are given as

$$\begin{aligned} (\lambda + \frac{\partial^2}{\partial y^2})\psi(y) &= 0 \quad , \quad -l \leq y \leq l \\ \varphi(y, \lambda) &= (1/\sqrt{\lambda}) \sin \sqrt{\lambda}y \quad \text{Dirichlet b.c. is satisfied at } y=0 \\ \chi(y, \lambda) &= (1/\sqrt{\lambda}) \sin \sqrt{\lambda}(l-y) \quad \text{Dirichlet b.c. is satisfied at } y=l \end{aligned} \quad (117)$$

The quantity  $\Omega$ , its zeros  $\lambda_n$  and others are obtained as

$$\begin{aligned} \Omega(\lambda) &= p(\varphi\chi' - \chi\varphi') = -(1/\sqrt{\lambda}) \sin(\sqrt{\lambda}l) \quad , \\ \Omega(\lambda_n) &= 0 \quad , \quad \lambda_n = (\frac{\pi}{l})^2 n^2, \quad n = 1, 2, \dots , \\ \Omega'(\lambda_n) &= -(l^3/2\pi^2 n^2)(-1)^n \quad , \quad k_n = \chi(y, \lambda_n)/\varphi(y, \lambda_n) = (-1)^{n+1}. \end{aligned} \quad (118)$$

Using the above results and the eigen function  $\psi_n(y) = \varphi(y, \lambda_n) = (l/\pi n) \sin(\pi ny/l)$ , the Strum-Liouville expansion formula (100) reduces to

$$f(y) = \frac{2}{l} \sum_n \left( \sin \frac{n\pi y}{l} \right) \int_0^l f(\xi) \sin \left( \frac{\pi n \xi}{l} \right) d\xi \quad . \quad (119)$$

This is the familiar Fourier expansion formula for the odd function  $f(y)$ . Its  $Z_2$  parity even version is used in (43) and the equivalence of the expansion approach and P/M approach is shown for the flat case.

## 13 App. B : General treatment of the propagator

In this appendix, we treat the propagator of  $\text{AdS}_5$  space-time (Sec.6 and Sec.7) in the general way valid for the wide-range dynamics, that is, the Strum-Liouville differential operator. The field equation (50) can be expressed, using 4D-Fourier transformed field  $\Phi_p(z), J_p(z)$  defined in (115), as

$$\begin{aligned} \left\{ \frac{d}{dz} p(z) \frac{d}{dz} - q(z) \right\} \Phi_p - p^2 r(z) \Phi_p &\equiv \hat{L} \Phi_p - p^2 r(z) \Phi_p = -\frac{J_p(z)}{(\omega z)^5} \quad , \\ p(z) &= \frac{1}{(\omega z)^3} \quad , \quad q(z) = \frac{m^2}{(\omega z)^5} \quad , \quad r(z) = \frac{1}{(\omega z)^3} \quad . \end{aligned} \quad (120)$$

This is the Strum-Liouville differential equation with source term (the inhomogeneous case). We consider  $p^2 < 0$  case (time-like). ( $p^2 > 0$  case is similarly treated.)  $Z_2$  parity is taken to be odd,  $P=-1$ , and the Dirichlet b.c. is taken both at  $z=1/\omega$  and at  $z=1/T$ . ( $P=+1$  case is similarly treated.)

(i) Homogeneous Solution ( $J_p = 0$ )

$$\hat{L}\Phi_p - p^2 r(z)\Phi_p = 0 \quad . \quad (121)$$

This is the eigenvalue equation for the operator  $r(z)^{-1}\hat{L}$ . Two independent solutions are given by <sup>23</sup>

$$(\omega z)^2 \tilde{\mathbf{J}}_\nu(Mz) \quad , \quad (\omega z)^2 \tilde{\mathbf{N}}_\nu(Mz) \quad , \quad M = \sqrt{-p^2} \quad , \quad \nu = \sqrt{4 + \frac{m^2}{\omega^2}} \quad . \quad (122)$$

We introduce two "intermediate" solutions:  $\varphi_M(z)$  which satisfies the b.c. only at  $z = 1/\omega$ , and  $\chi_M(z)$  which satisfies the b.c. only at  $z = 1/T$ .

$$\begin{aligned} \varphi_M(z) &= \frac{1}{N^{(1/\omega)}} (\omega z)^2 (\tilde{\mathbf{J}}_\nu(Mz) \mathbf{N}_\nu(\frac{M}{\omega}) - \tilde{\mathbf{N}}_\nu(Mz) \mathbf{J}_\nu(\frac{M}{\omega})) / \mathbf{N}_\nu(\frac{M}{\omega}) \quad , \\ \chi_M(z) &= \frac{1}{N^{(1/T)}} (\omega z)^2 (\tilde{\mathbf{J}}_\nu(Mz) \mathbf{N}_\nu(\frac{M}{T}) - \tilde{\mathbf{N}}_\nu(Mz) \mathbf{J}_\nu(\frac{M}{T})) / \mathbf{N}_\nu(\frac{M}{T}) \quad . \end{aligned} \quad (123)$$

The final solution is obtained by the requirement that  $\varphi_M(z)$  and  $\chi_M(z)$  become linearly-dependent each other.

$$\text{Wronskian} \quad W[\varphi_M, \chi_M] \equiv \varphi_M \frac{d}{dz} \chi_M - \chi_M \frac{d}{dz} \varphi_M \propto \left\{ \mathbf{J}_\nu(\frac{M}{\omega}) \mathbf{N}_\nu(\frac{M}{T}) - \mathbf{J}_\nu(\frac{M}{T}) \mathbf{N}_\nu(\frac{M}{\omega}) \right\} = 0 \quad (124)$$

This is because the solution must satisfy the Dirichlet b.c. at both points. The condition (124) fixes the set of eigenvalues  $\{M_n\}$ . The eigen function  $\psi_n(z)$  is obtained as

$$\begin{aligned} \psi_n(z) &= \varphi_M(z)|_{M=M_n} = \frac{1}{N_n^{(1/\omega)}} (\omega z)^2 (\tilde{\mathbf{J}}_\nu(M_n z) \mathbf{N}_\nu(\frac{M_n}{\omega}) - \tilde{\mathbf{N}}_\nu(M_n z) \mathbf{J}_\nu(\frac{M_n}{\omega})) / \mathbf{N}_\nu(\frac{M_n}{\omega}) \quad , \\ &= \chi_M(z)|_{M=M_n} \quad , \\ &2 \int_{\frac{1}{\omega}}^{\frac{1}{T}} r(z) \psi_n(z) \psi_m(z) dz = \delta_{nm} \quad (125) \end{aligned}$$

(ii) Solution of (120), Inhomogeneous solution

(iia) Expansion form

First we obtain the solution in the expansion form using the homogeneous solutions  $\{\psi_n\}$  obtained in (i).

$$\Phi_p(z) = \sum_{n=1}^{\infty} c_n(p) \psi_n(z) \quad , \quad \hat{L}\psi_n = -M_n^2 r(z) \psi_n \quad . \quad (126)$$

Putting (126) into (120), we obtain

$$\sum_{n=1}^{\infty} c_n(p) (-p^2 - M_n^2) r(z) \psi_n(z) = -\frac{J_p(z)}{(\omega z)^5} \quad . \quad (127)$$

---

<sup>23</sup> Bessel functions here are generalized as defined in (55).

From the orthogonality (125), we can read the coefficient.

$$c_n(p) = \frac{f_n}{p^2 + M_n^2} \quad , \quad f_n = \int_{1/\omega}^{1/T} \psi_n(z) \frac{J_p(z)}{(\omega z)^5} dz \quad . \quad (128)$$

Hence we obtain the solution.

$$\Phi_p(z) = \sum_{n=1}^{\infty} \frac{f_n}{p^2 + M_n^2} \psi_n(z) \quad . \quad (129)$$

This result corresponds to (65) of Sec.6.

(iib) Closed form

We can also obtain the solution in the closed form using the "intermediate" solutions  $\varphi_M(z), \chi_M(z)$  (123). The solution  $\Phi_p(z)$  of (120) can be obtained as

$$\Phi_p(z) = -\chi_M(z) \int_{1/\omega}^z \frac{\varphi_M(\xi)}{[\varphi_M(\xi), \chi_M(\xi)]} \frac{J_p(\xi)}{(\omega \xi)^5} d\xi - \varphi_M(z) \int_z^{1/T} \frac{\chi_M(\xi)}{[\varphi_M(\xi), \chi_M(\xi)]} \frac{J_p(\xi)}{(\omega \xi)^5} d\xi ,$$

$$[\varphi_M(z), \chi_M(z)] \equiv p(z)(\varphi_M(z)\chi_M'(z) - \varphi_M'(z)\chi_M(z)) \quad (130)$$

where  $p(z)$  appears in (120). Because of  $(d/dz)[\varphi_M(z), \chi_M(z)] = 0$ , we can express (130) as

$$[\varphi_M(z), \chi_M(z)] \equiv \Omega(M) \quad ,$$

$$\Phi_p(z) = -\frac{\chi_M(z)}{\Omega(M)} \int_{1/\omega}^z \varphi_M(\xi) \frac{J_p(\xi)}{(\omega \xi)^5} d\xi - \frac{\varphi_M(z)}{\Omega(M)} \int_z^{1/T} \chi_M(\xi) \frac{J_p(\xi)}{(\omega \xi)^5} d\xi \quad . \quad (131)$$

Let us here introduce the P/M propagator <sup>24</sup>

$$G_p(z, \xi) \equiv \begin{cases} -\frac{\chi_M(z)\varphi_M(\xi)}{[\varphi_M(\xi), \chi_M(\xi)]} , & \frac{1}{\omega} \leq \xi \leq z \leq \frac{1}{T} \text{ (R}_2 \text{ of Fig.6)} \\ -\frac{\varphi_M(z)\chi_M(\xi)}{[\varphi_M(\xi), \chi_M(\xi)]} , & \frac{1}{\omega} \leq z \leq \xi \leq \frac{1}{T} \text{ (R}_1 \text{ of Fig.6)} \end{cases} \quad (132)$$

where  $M = \sqrt{-p^2}$ . For other regions of Fig.6,  $G_p$  is defined following the  $Z_2$ -parity property as done in Sec.7. In terms of the above propagator, (131) can be written as

$$\Phi_p(z) = \int_{1/\omega}^{1/T} G_p(z, \xi) \frac{J_p(\xi)}{(\omega \xi)^5} d\xi \quad . \quad (133)$$

The propagator (132) is the same one that is introduced in (80) of the text. Note that  $K_p(z, \xi)$  of (99) corresponds to the lower part of (132).

---

<sup>24</sup> From the result (132), we understand the appearance of the "direction" property of the extra coordinate  $z$  (or  $y$ ), originates from the characteristic structure of the solution of the inhomogeneous (source  $J_p$  attached) differential equation.

Taking into account the expression (129) and the relation:

$$\frac{J_p(\xi)}{(\omega\xi)^5} = \sum_{n=1}^{\infty} f_n \psi_n(\xi) \quad , \quad f_n \text{ is defined in (128)} \quad , \quad (134)$$

we can read off, from (133), the following relation between the P/M propagator and the eigen functions  $\{\psi_n\}$ .

$$G_p(z, \xi) = \sum_{n=1}^{\infty} \frac{1}{p^2 + M_n^2} \frac{1}{2} (\psi_n(z)\psi_n(\xi) - \psi_n(z)\psi_n(-\xi)) \quad . \quad (135)$$

This is the same as (65) of Sec.6.

## 14 App. C : Behaviour of Various P/M propagators

The values for  $l$  (half period),  $\omega$  (thickness) are taken as

$l=\pi$ ,  $1/l \sim 0.3$ ,  $\omega=1$ ,  $T=\omega \exp(-\omega l) \sim 0.04$

We note the following notation used in the text.

$\tilde{p} \equiv \sqrt{p^2}$  for  $p^2 > 0$  (space-like);  $\hat{p} \equiv \sqrt{-p^2}$  for  $p^2 < 0$  (time-like)

### 14.1 App. C.1 : Flat 5D Massless Scalar Propagator ( $Z_2$ -parity Even, Neumann-Neumann b.c.)

The behaviour of 5D massless scalar propagator with  $Z_2$ -parity even ( $P=1$ ) is shown in Fig.21-26. Neumann b.c. is imposed for all fixed points. The P/M propagator is given by

$$G_p(y, y') = \bar{K}_p(Y(y, y'), Y'(y, y')) \quad ,$$

$$\bar{K}_p(Y, Y') = \begin{cases} -\frac{\cosh \tilde{p}Y \cosh \tilde{p}(Y'-l)}{2\tilde{p} \sinh \tilde{p}l} & \tilde{p} = \sqrt{p^2} \quad \text{for } p^2 > 0 \\ \frac{\cos \hat{p}Y \cos \hat{p}(Y'-l)}{2\hat{p} \sin \hat{p}l} & \hat{p} = \sqrt{-p^2} \quad \text{for } p^2 < 0 \end{cases} \quad (136)$$

where  $Y(y, y')$  and  $Y'(y, y')$  are defined in (39).

In this case, the scale parameter is the periodicity parameter  $l$  only. We can characterize the behaviours by the momentum  $\tilde{p}$  or  $\hat{p}$  in comparison with  $1/l$ .

(A) Space-Like

(1S)  $\tilde{p} \ll 1/l$  , Fig.21

Upheaval and downheaval surfaces front each other at sharp edges which correspond to the singularities at  $y \pm y' = 0$ . The size of the slope is  $l$ . The boundary constraint is strong. This is the 'boundary phase'. The scale  $p$  does not appear in the graph.

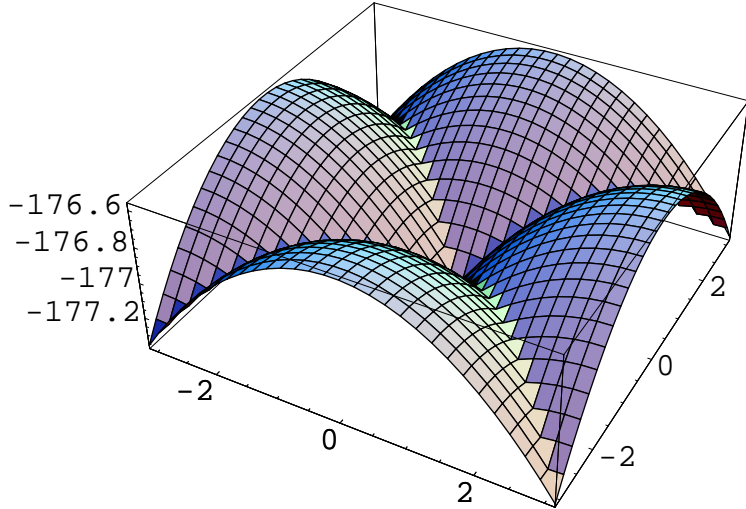
(2S)  $\tilde{p} \sim 1/l$  , Fig.22

The gross shape is similar to (1S). The height decreases.

(3S)  $\tilde{p} \gg 1/l$  , Fig.23

Valleys run along the diagonal axes. The configuration is free from the boundary constraint.

Figure 21: Flat 5D Massless Scalar Propagator (  $Z_2$ -parity even, Neumann-Neumann b.c.),  $\tilde{p}=0.03 \ll 1/l$ , space-like, App.C.1(1S). "Boundary phase".



This is the 'dynamical phase'. The size of the valley-width is  $1/\tilde{p}$ . In the off-diagonal region ( $y \pm y' \neq 0$ ), flat planes appear and the propagator takes nearly 0 there. The height decreases furthermore.

(B) Time-Like

(1T)  $\hat{p} \ll 1/l$ , Fig.24

Shape and height are similar to the space-like case. This is the 'boundary phase'.

(2T)  $\hat{p} \sim 1/l$ , Fig.25

The absolute value of the height increases and decreases. Shape is similar to the space-like case.

(3T)  $\hat{p} \gg 1/l$ , Fig.26

The wavy behaviour appears. The singularity-lines are buried in the waves. Boundary constraint is not effective. This is the 'dynamical phase'. The size of the wave length is  $1/\hat{p}$ .

Compared with the space-like case, the height does not so much change for the time-like case.

## 14.2 App. C.2 : Flat 5D Massless Scalar Propagator ( $Z_2$ -parity Odd, Dirichlet-Neumann b.c.)

The behaviour of 5D massless scalar flat propagators with the mixed b.c. are shown in Fig.27-32.  $Z_2$ -parity is taken to be odd:  $P=-1$ . Dirichlet b.c. is imposed for  $y=0$ , while

Figure 22: Flat 5D Massless Scalar Propagator (  $Z_2$ -parity even, Neumann-Neumann b.c.),  $\tilde{p}=0.3 \sim 1/l$ , space-like, App.C.1(2S)

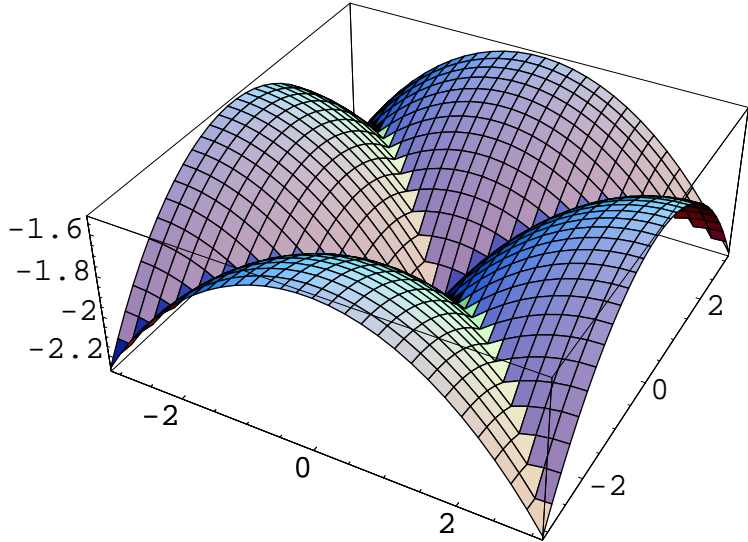


Figure 23: Flat 5D Massless Scalar Propagator (  $Z_2$ -parity even, Neumann-Neumann b.c.),  $\tilde{p}=3 \gg 1/l$ , space-like, App.C.1(3S). The "dynamical phase".

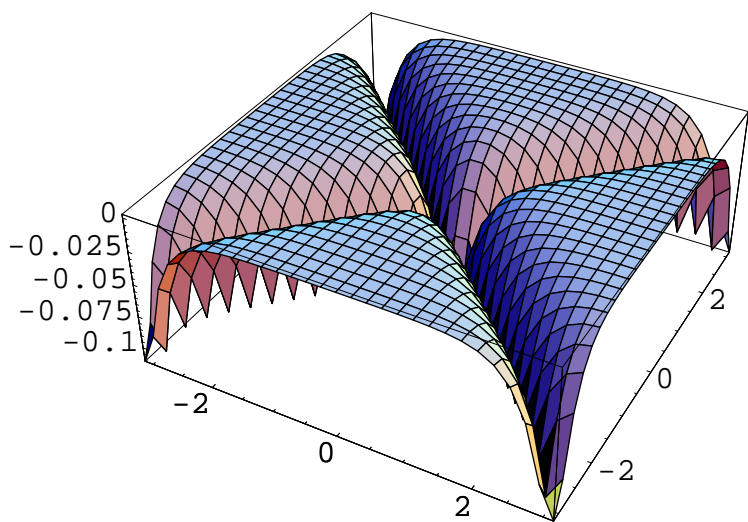


Figure 24: Flat 5D Massless Scalar Propagator (  $Z_2$ -parity even, Neumann-Neumann b.c.),  $\hat{p}=0.03 \ll 1/l$ , time-like, App.C.1(1T). The "boundary phase".

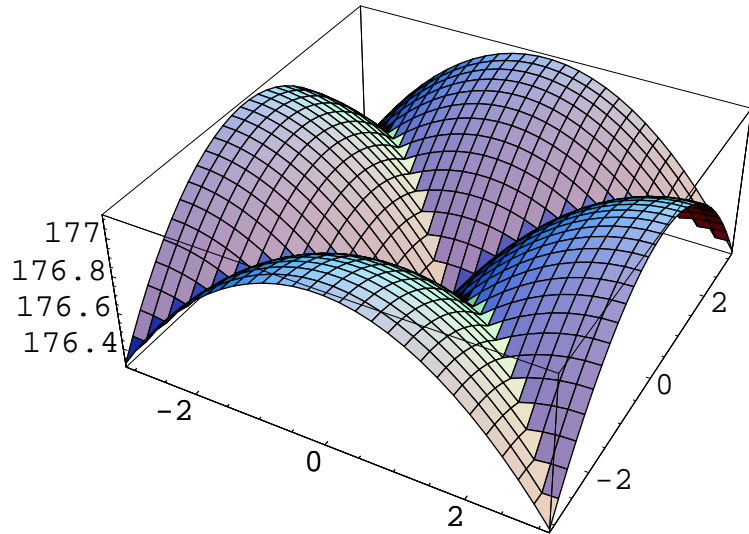


Figure 25: Flat 5D Massless Scalar Propagator (  $Z_2$ -parity even, Neumann-Neumann b.c.),  $\hat{p}=0.3 \sim 1/l$ , time-like, App.C.1(2T).

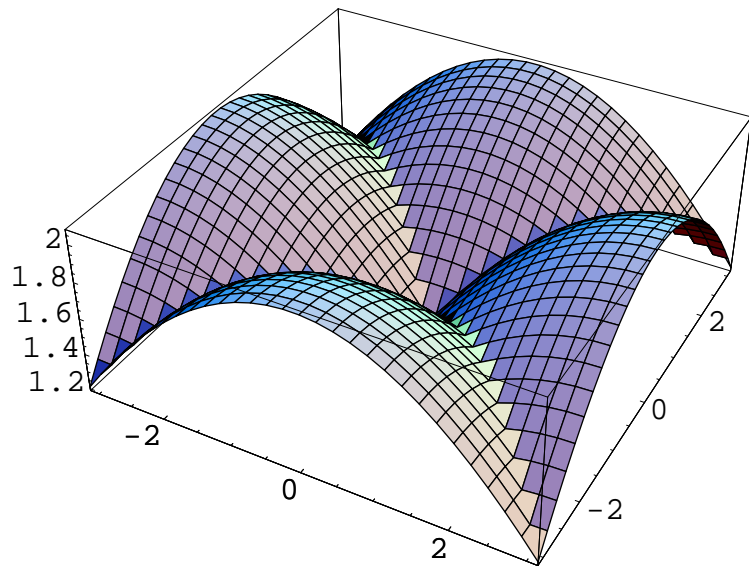
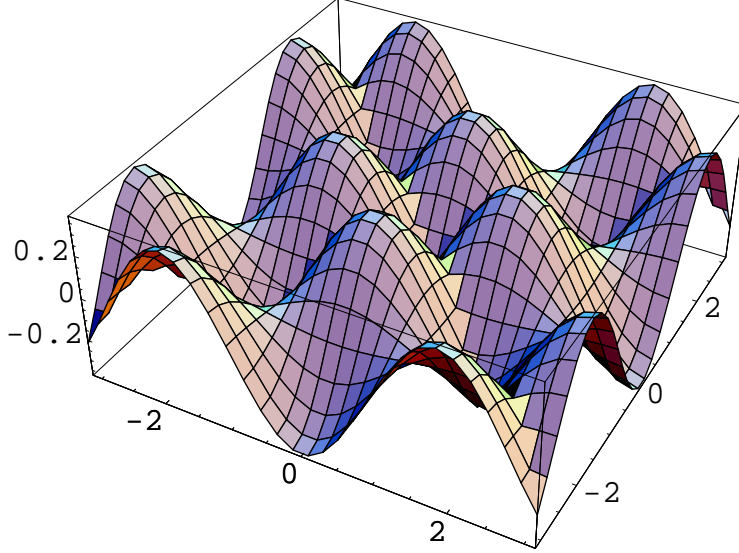


Figure 26: Flat 5D Massless Scalar Propagator (  $Z_2$ -parity even, Neumann-Neumann b.c.),  $\hat{p}=1.7 \gg 1/l$ , time-like, App.C.1(3T).



Neumann b.c. for  $y=\pm l$ . The P/M propagator is given by

$$G_p(y, y') = \bar{K}_p(Y(y, y'), Y'(y, y')) ,$$

$$\bar{K}_p(Y, Y') = \begin{cases} -\frac{\sinh \tilde{p}Y \cosh \tilde{p}(Y'-l)}{2\tilde{p} \cosh \tilde{p}l} & \tilde{p} = \sqrt{p^2} \quad \text{for } p^2 > 0 \\ -\frac{\sin \hat{p}Y \cos \hat{p}(Y'-l)}{2\hat{p} \cos \hat{p}l} & \hat{p} = \sqrt{-p^2} \quad \text{for } p^2 < 0 \end{cases} \quad (137)$$

where  $Y(y, y')$  and  $Y'(y, y')$  are defined in (39).

In this case, the scale parameter is the periodicity parameter  $l$  only. We characterize the behaviours by the momentum  $\tilde{p}$  or  $\hat{p}$  in comparison with  $1/l$ .

(A) Space-Like

(1S)  $\tilde{p} \ll 1/l$  , Fig.27

Slanted flat surfaces front each other along the diagonal lines ( $y \pm y' = 0$ , the singularities). The size of the surface is  $l$ . Boundary constraint is strong. This is the 'boundary phase'. The scale  $p$  does not appear in the graph.

(2S)  $\tilde{p} \sim 1/l$  , Fig.28

The shape and the height are similar to (1S).

(3S)  $\tilde{p} \gg 1/l$  , Fig.29

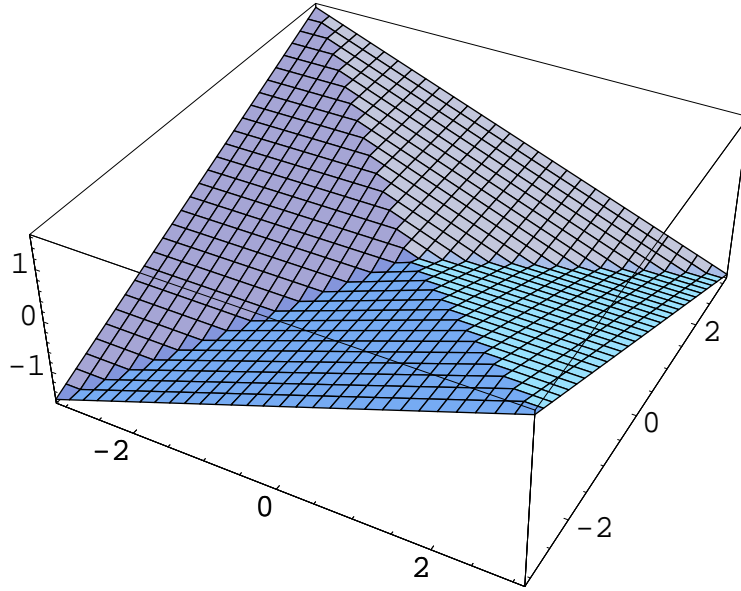
Walls and valleys run along the diagonal axes. The configuration is free from the boundary constraint. This is the 'dynamical phase'. The size of the wall (valley) thickness is  $1/p$ . Absolute value of the effective height decreases.

(B) Time-Like

(1T)  $\hat{p} \ll 1/l$  , Fig.30

Shape and height are similar to the space-like case. This is the 'boundary phase'.

Figure 27: Flat 5D Massless Scalar Propagator ( $Z_2$ -parity Odd, Dirichlet-Neumann b.c.),  $\tilde{p}=0.03 \ll 1/l$ , space-like, App.C.2(1S). The "boundary phase".



(2T)  $\hat{p} \sim 1/l$  , Fig.31

The absolute value of the height increases and decreases by changing  $p$  within this region. The global shape does not change.

(3T)  $\hat{p} \gg 1/l$  , Fig.32

The wavy behaviour appears. The singularity-lines are buried in the waves. Boundary constraint is not effective. This is the 'dynamical phase'. The size of the wave length is  $1/\hat{p}$ .

### 14.3 App. C.3 : z-Coordinate Representation and Warped 5D Scalar Propagator ( $Z_2$ -parity odd, Dirichlet-Dirichlet b.c., space-like 4-momentum)

We give here the P/M propagator behaviour in terms of z-coordinate. Its relation to y is given in (46). We take 5D scalar propagator with  $P=-1$ . Dirichlet b.c. is imposed on all fixed points. 4D momentum is space-like. The propagator function is given in (98) with (96). It can be reexpressed as follows using the ordinary Bessel functions and the sign function.

$$\begin{aligned}
 G_p(z, z') &= K_p(Z(z, z'), Z'(z, z')) \quad , \\
 K_p(Z, Z') &= \frac{\omega^3}{2} Z^2 Z'^2 \epsilon(Z) \epsilon(Z') \times \\
 &\frac{\{I_0(\frac{\tilde{p}}{\omega}) K_0(\tilde{p}|Z|) - K_0(\frac{\tilde{p}}{\omega}) I_0(\tilde{p}|Z|)\} \{I_0(\frac{\tilde{p}}{T}) K_0(\tilde{p}|Z'|) - K_0(\frac{\tilde{p}}{T}) I_0(\tilde{p}|Z'|)\}}{I_0(\frac{\tilde{p}}{T}) K_0(\frac{\tilde{p}}{\omega}) - K_0(\frac{\tilde{p}}{T}) I_0(\frac{\tilde{p}}{\omega})} \quad , \quad (138)
 \end{aligned}$$

Figure 28: Flat 5D Massless Scalar Propagator ( $Z_2$ -parity Odd, Dirichlet-Neumann b.c.),  $\tilde{p}=0.3 \sim 1/l$ , space-like, App.C.2(2S).

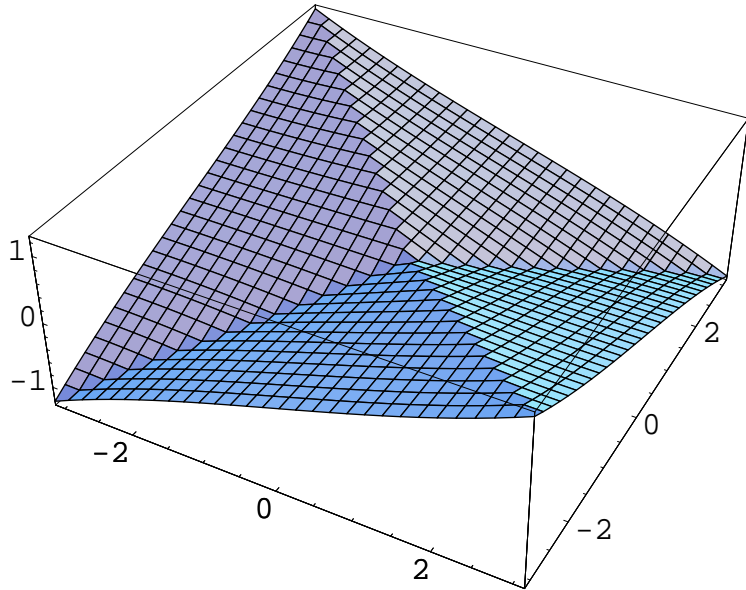


Figure 29: Flat 5D Massless Scalar Propagator ( $Z_2$ -parity Odd, Dirichlet-Neumann b.c.),  $\tilde{p}=3 \gg 1/l$ , space-like, App.C.2(3S). The "dynamical phase".

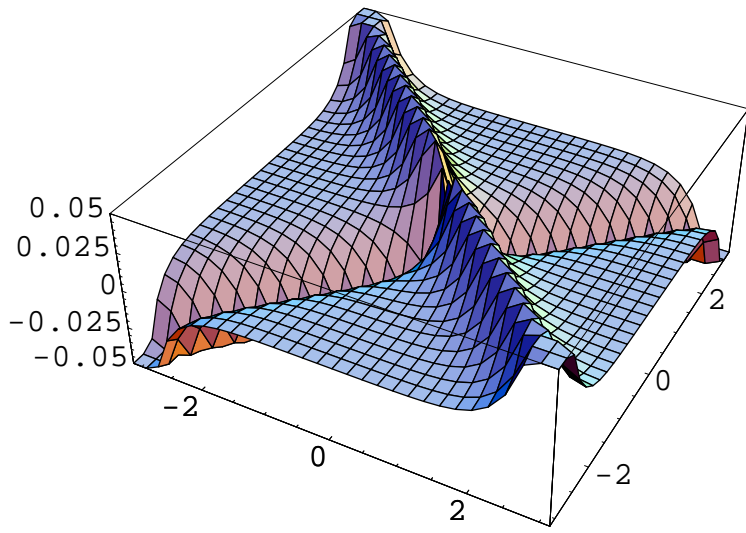


Figure 30: Flat 5D Massless Scalar Propagator ( $Z_2$ -parity Odd, Dirichlet-Neumann b.c.),  $\hat{p}=0.03 \ll 1/l$ , time-like, App.C.2(1T). The "boundary phase".

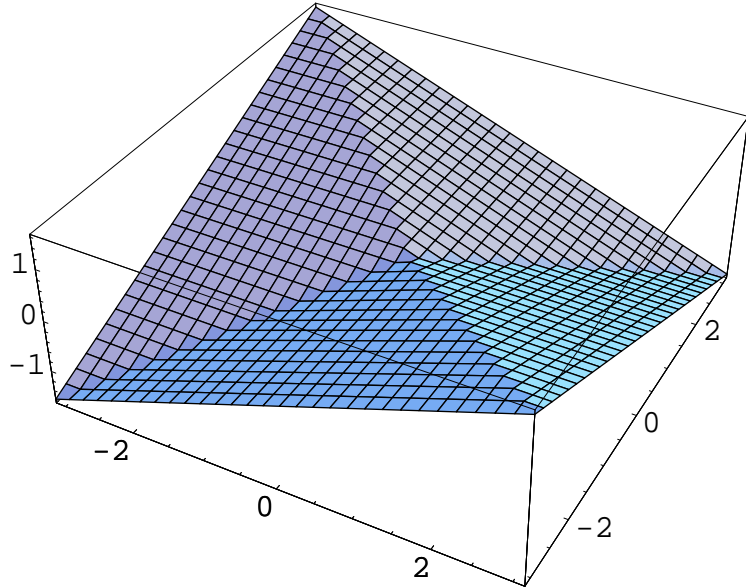


Figure 31: Flat 5D Massless Scalar Propagator ( $Z_2$ -parity Odd, Dirichlet-Neumann b.c.),  $\hat{p}=0.3 \sim 1/l$ , time-like, App.C.2(2T).

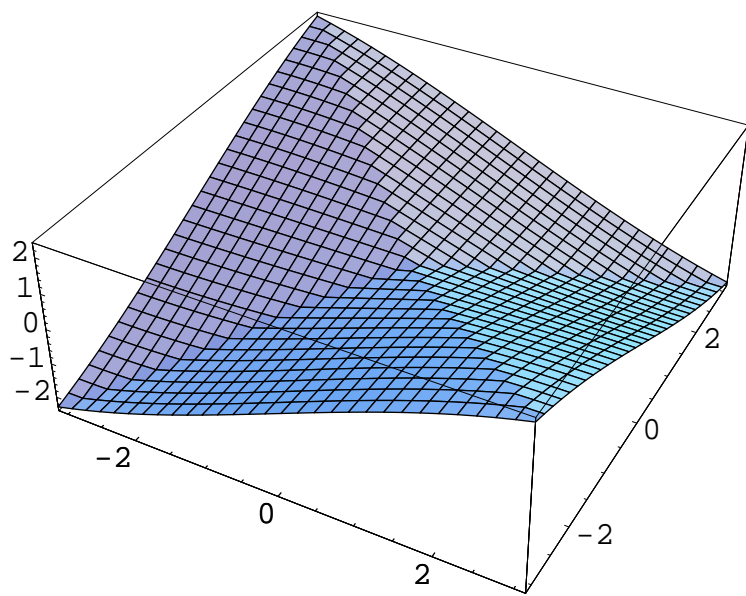
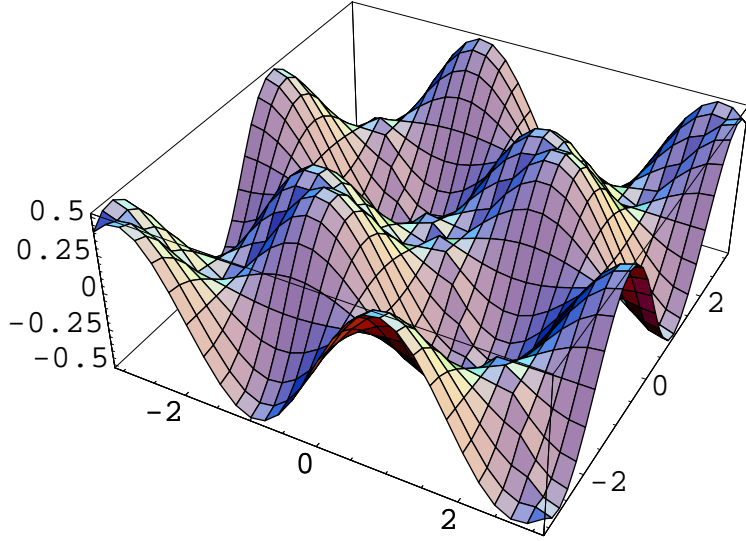


Figure 32: Flat 5D Massless Scalar Propagator ( $Z_2$ -parity Odd, Dirichlet-Neumann b.c.),  $\hat{p}=1.7 \gg 1/l$ , time-like, App.C.2(3T). The "dynamical phase".



where  $Z(z, z')$  and  $Z'(z, z')$  are defined in (98).

As we see the following graphs, large part of the whole image is naturally displayed. This means the  $z$ -coordinate is more suitable than  $y$ -coordinate for the warped geometry description. (Compare the height-region in Sec.9.2 ( $y$ -coordinate is used) and in this subsection for corresponding graphs.) From the  $z$ -coordinate property, however, it is *hard to detect characteristic scales* in the graphs.

The following graphs are re-drawing of those of Sec.9.2. They are displayed for  $\bar{R}_1 U \bar{R}_2$  region of the  $(z, z')$ -plane (See Fig.6).

(1S)  $\tilde{p} \ll 1/l < \omega$  , Fig.33

(2S)  $1/l < \tilde{p} \sim \omega$  , Fig.34

(3S)  $1/l < \omega < \tilde{p}$  , Fig.35

If we go further larger  $\tilde{p}$  ( $1/l < \omega \ll \tilde{p}$ ), the situation is the "flat ( $z$ -)space limit" represented by eq.(6.16) of Ref.[9]. Compare with Fig.9. <sup>25</sup>

<sup>25</sup> Note that the propagator in this flat limit is different from the flat propagator given in Sec.2-5 of this paper. The present flat propagator satisfies the free propagator equation in  $y$ -coordinate (26), whereas eq.(6.16) of Ref.[9] satisfies that in  $z$ -coordinate (82).

Figure 33: z-Coordinate Representation, Warped 5D Scalar Propagator ( $Z_2$ -parity odd, Dirichlet-Dirichlet b.c.,  $\tilde{p}=0.005 \ll T < 1/l < \omega$ , space-like, App.C.3(1S)).

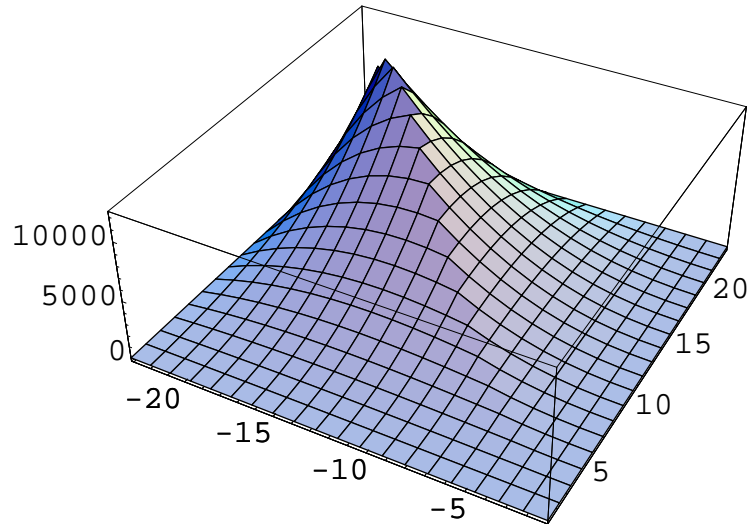


Figure 34: z-Coordinate Representation, Warped 5D Scalar Propagator ( $Z_2$ -parity odd, Dirichlet-Dirichlet b.c.,  $T \ll 1/l < \tilde{p}=1=\omega$ , space-like, App.C.3(2S)).

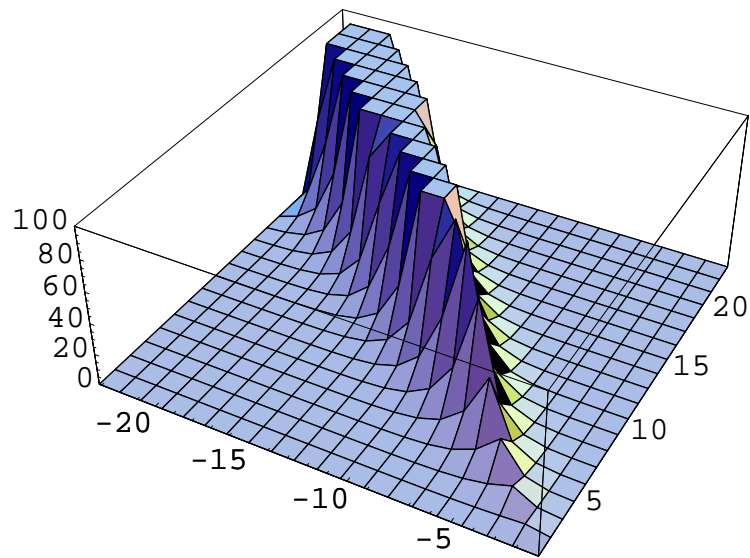
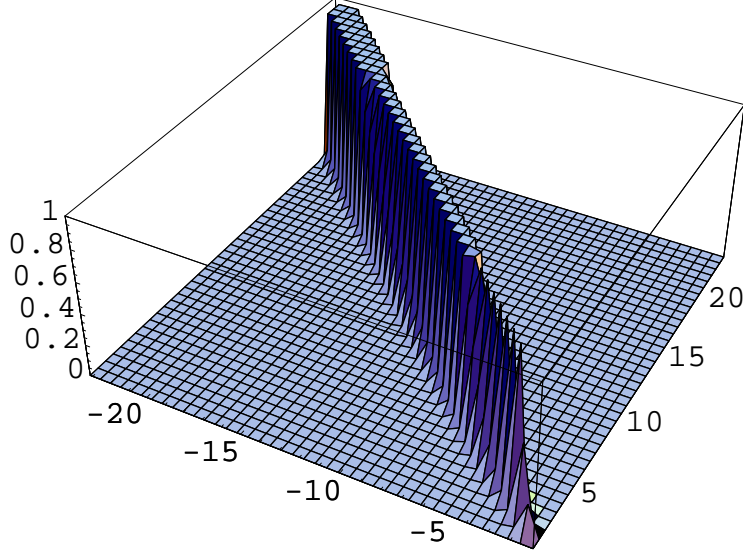


Figure 35: z-Coordinate Representation, Warped 5D Scalar Propagator ( $Z_2$ -parity odd, Dirichlet-Dirichlet b.c.),  $T \ll 1/l < \omega < \tilde{p}=5$ , space-like, App.C.3(3S).



#### 14.4 App. C.4 : Warped 5D Massless Vector ( $Z_2$ -parity Even, Neumann-Neumann b.c., space-like 4 momentum)

In the warped case the theory has two scale parameters: thickness  $\omega$  and the periodicity parameter  $l$ . The propagator behaviour is characterized by the relation between  $\sqrt{|p^2|}$ ,  $\omega$  and  $1/l$ .

In this subsection, the 5D vector propagator with  $Z_2$ -parity even ( $P=1$ ) is examined. The Neumann b.c. is imposed on all fixed points. The P/M propagator is given by

$$G_p(y, y') = K_p(Y(y, y'), Y'(y, y')) \quad ,$$

$$K_p(Y, Y') = \frac{1}{\omega} \exp(k|Y| + k|Y'|) \times$$

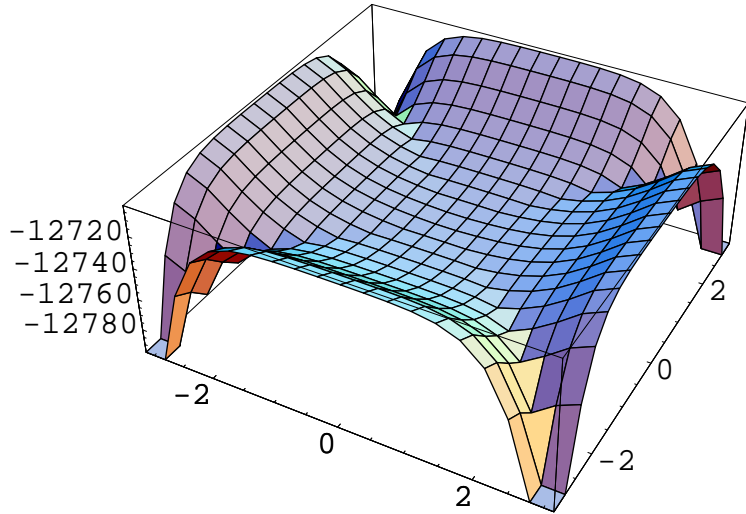
$$\frac{\{I_0(\frac{\tilde{p}}{\omega})K_1(\frac{\tilde{p}}{\omega}e^{\omega|Y|}) + K_0(\frac{\tilde{p}}{\omega})I_1(\frac{\tilde{p}}{\omega}e^{\omega|Y|})\}\{I_0(\frac{\tilde{p}}{T})K_1(\frac{\tilde{p}}{\omega}e^{\omega|Y'|}) + K_0(\frac{\tilde{p}}{T})I_1(\frac{\tilde{p}}{\omega}e^{\omega|Y'|})\}}{I_0(\frac{\tilde{p}}{\omega})K_0(\frac{\tilde{p}}{T}) - K_0(\frac{\tilde{p}}{\omega})I_0(\frac{\tilde{p}}{T})} \quad , \quad (139)$$

where  $Y(y, y')$  and  $Y'(y, y')$  are defined in (39).

(1S)  $\tilde{p} \ll 1/l < \omega$  , Fig.36

4 notches appear at 4 corners. The effective width of the notch is  $1/\omega$ . The size of the global upheaval and downheaval is  $l$ . The boundary constraint is dominant. This is the "boundary phase". There is a flat region around the center ( $y = y' = 0$ ). The propagator takes a non-zero constant there. This means that the bulk propagation, near the Planck brane, simply gives a common constant , as the extra-space contribution, to the amplitude. On the other hand, near the Tev brane ( $y, y' = \pm l$ ), it gives a "sizable" effect.

Figure 36: Warped 5D Massless Vector ( $Z_2$ -parity Even, Neumann-Neumann b.c.)  $\tilde{p}=0.005$   
 $\ll T \sim 0.04 \ll 1/l \sim 0.3 \ll \omega=1$ , space-like., App.C.4(1S)



(2S)  $1/l < \tilde{p} \sim \omega$  , Fig.37

4 valleys develop along the diagonal axes from the corners to the center. Their width is  $1/\tilde{p} \sim 1/\omega$ . The flat region near the center disappears. In the off-diagonal region ( $y \pm y' \neq 0$ ), flat planes begin to appear and the propagator takes nearly 0 value there. The height decreases.

(3S)  $1/l < \omega < \tilde{p}$  , Fig.38

Valleys develop furthermore. The width of them is  $1/\tilde{p}$  near the corners and is  $1/\omega$  near the center. There is no boundary effect. This is the "dynamical phase". There is no flat region near the center, whereas in the off-diagonal region there appears the flat region. The propagator value is 0 in this flat region. This means the bulk propagation takes place only for the case  $y' \pm y \sim 0$ . Absolute value of the effective height decreases rapidly as  $\tilde{p}$  increases. If we take further larger  $\tilde{p}$  ( $1/l < \omega \ll \tilde{p}$ ), the situation is the "flat limit". Compare with Fig.23.

Time-like case is given in App.C.6.

#### 14.5 App. C.5 : z-Coordinate Representation for Warped 5D Massless Vector ( $Z_2$ -parity Even, Neumann-Neumann b.c., space-like)

We give here the P/M vector ( $Z_2$ -parity even, Neumann-Neumann b.c., space-like) propagator behaviour in terms of z-coordinate. The propagator expression is given in (139)

Figure 37: Warped 5D Massless Vector ( $Z_2$ -parity Even, Neumann-Neumann b.c.)  $T \ll 1/l$   
 $\tilde{p} = 1 = \omega$ , space-like, App.C.4(2S)

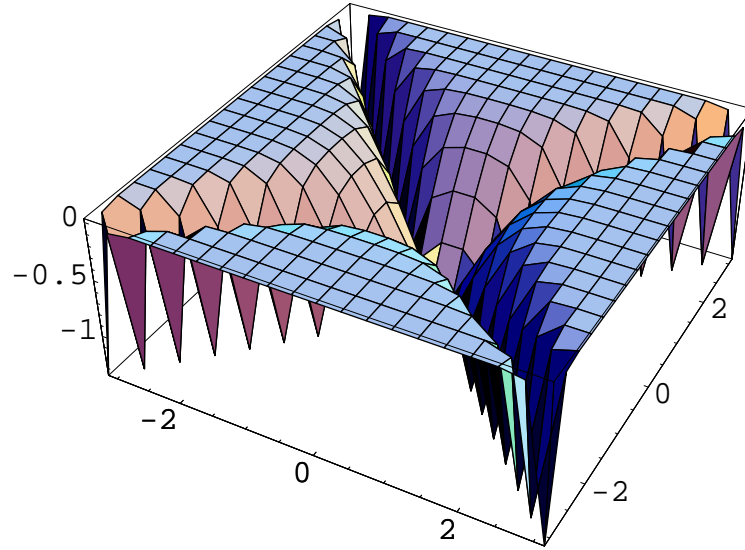


Figure 38: Warped 5D Massless Vector ( $Z_2$ -parity Even, Neumann-Neumann b.c.),  $T \ll 1/l < \omega < \tilde{p} = 5$ , space-like, App.C.4(3S).

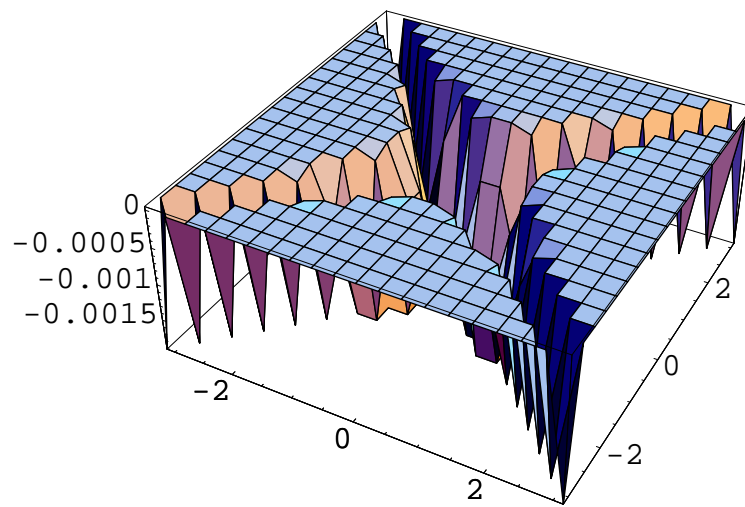
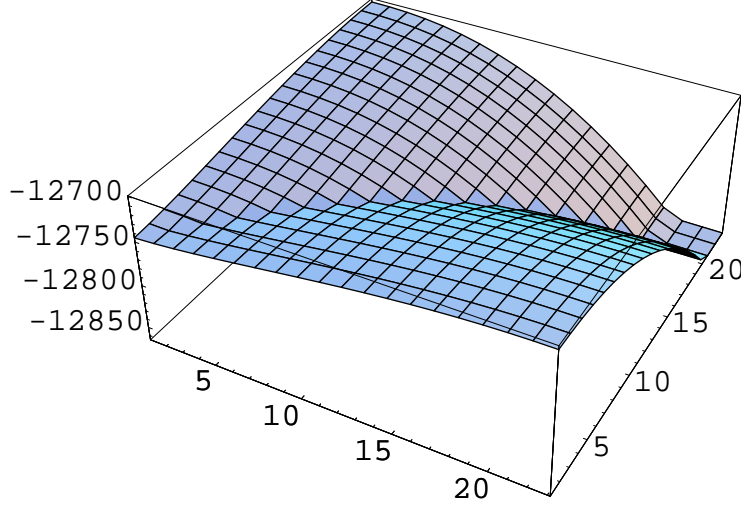


Figure 39: z-Coordinate Representation for Warped 5D Massless Vector ( $Z_2$ -parity Even, Neumann-Neumann b.c.),  $\tilde{p}=0.005 \ll T \sim 0.04 \ll 1/l \sim 0.3 \ll k=1$ , space-like, App.C.5(1S).



using the y-coordinate. Here its z-coordinate expression is given.

$$G_p(z, z') = K_p(Z(z, z'), Z'(z, z')) \quad , \\ K_p(Z, Z') = \omega |Z| |Z'| \times \\ \frac{\{\mathbf{I}_0(\frac{\tilde{p}}{\omega})\mathbf{K}_1(\tilde{p}|Z|) + \mathbf{K}_0(\frac{\tilde{p}}{\omega})\mathbf{I}_1(\tilde{p}|Z|)\}\{\mathbf{I}_0(\frac{\tilde{p}}{T})\mathbf{K}_1(\tilde{p}|Z'|) + \mathbf{K}_0(\frac{\tilde{p}}{T})\mathbf{I}_1(\tilde{p}|Z'|)\}}{\mathbf{I}_0(\frac{\tilde{p}}{\omega})\mathbf{K}_0(\frac{\tilde{p}}{T}) - \mathbf{K}_0(\frac{\tilde{p}}{\omega})\mathbf{I}_0(\frac{\tilde{p}}{T})} \quad , \quad (140)$$

where  $Z(z, z')$  and  $Z'(z, z')$  are defined in (98).

The following graphs are re-drawing of those of App.C.4 using the z-coordinate. They are displayed for  $R_1UR_2$  region of the  $(z, z')$ -plane (See Fig.6).

(1S)  $\tilde{p} \ll 1/l < \omega$  , Fig.39

(2S)  $1/l < \tilde{p} \sim \omega$  , Fig.40

(3S)  $1/l < \omega < \tilde{p}$  , Fig.41

If we take further larger  $\tilde{p}$ , the configuration becomes the "flat (z-)space limit". Compare with Fig.23. ( The same situation has already appeared for the scalar propagator case, Fig.34 and Fig.35 in App.C.3. )

In the graphs of (2S) and (3S), we see, in their off-diagonal regions, the top surfaces very gradually approach the 0-value surface as they deviate from the diagonal axis:  $G_p(z, z') \sim -\exp(-\tilde{p}|z' - z|)$ . This is the "untrusted" region pointed out in ref.[9].

Figure 40: z-Coordinate Representation for Warped 5D Massless Vector ( $Z_2$ -parity Even, Neumann-Neumann b.c.),  $T \ll 1/l < \tilde{p} = 1 = \omega$ , space-like, App.C.5(2S).

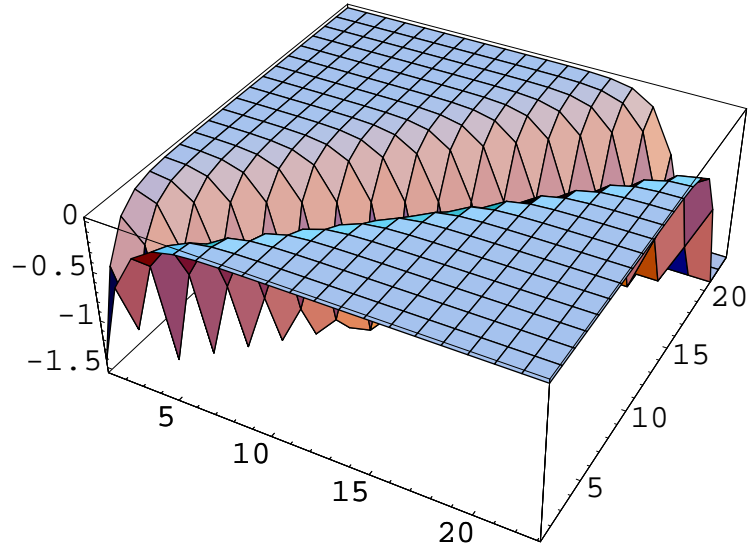
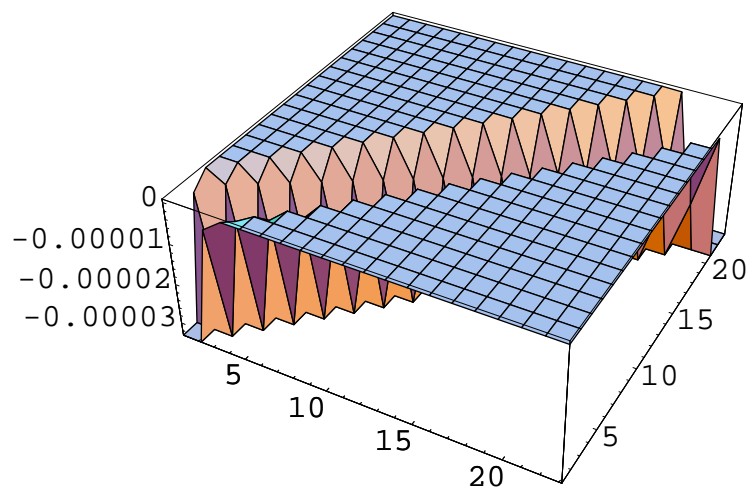


Figure 41: z-Coordinate Representation for Warped 5D Massless Vector ( $Z_2$ -parity Even, Neumann-Neumann b.c.),  $T \ll 1/l < \omega < \tilde{p} = 5$ , space-like, App.C.5(3S)



## 14.6 App. C.6 : Warped 5D Massless Vector (Z<sub>2</sub>-parity Even, Neumann-Neumann b.c., time-like 4 momentum)

Here we give the P/M propagator behaviour of the warped 5D massless vector (Z<sub>2</sub>-parity Even, Neumann-Neumann b.c., time-like 4 momentum). The propagator is given by

$$G_p(y, y') = K_p(Y(y, y'), Y'(y, y')) \quad ,$$

$$K_p(Y, Y') = -\frac{1}{\omega} \exp(k|Y| + k|Y'|) \times$$

$$\frac{\{\mathbf{N}_0(\frac{\hat{p}}{\omega})\mathbf{J}_1(\frac{\hat{p}}{\omega}e^{\omega|Y|}) - \mathbf{J}_0(\frac{\hat{p}}{\omega})\mathbf{N}_1(\frac{\hat{p}}{\omega}e^{\omega|Y|})\}\{\mathbf{N}_0(\frac{\hat{p}}{T})\mathbf{J}_1(\frac{\hat{p}}{\omega}e^{\omega|Y'|}) - \mathbf{J}_0(\frac{\hat{p}}{T})\mathbf{N}_1(\frac{\hat{p}}{\omega}e^{\omega|Y'|})\}}{\mathbf{N}_0(\frac{\hat{p}}{\omega})\mathbf{J}_0(\frac{\hat{p}}{T}) - \mathbf{J}_0(\frac{\hat{p}}{\omega})\mathbf{N}_0(\frac{\hat{p}}{T})} \quad , \quad (141)$$

where  $Y(y, y')$  and  $Y'(y, y')$  are defined in (39).

This is the time-like case of App.C.4.

(1T)  $\hat{p} \ll 1/l < \omega$  , Fig.42

The situation is quite similar to (1S) of App.C.4.

(2T)  $1/l < \hat{p} \sim \omega$  , Fig.43

Wavy behaviour appears. Two types of waves are there. One type has the small wave-length of order  $1/\hat{p}=1/\omega$ , and the waves of this type gather near the 4 corners. The other type has the long wave-length of order  $l$ , which comes from the boundary constraint. In particular, there exists a very moderate hill around the center. The propagator takes nearly 0 value there. This is contrasting with the space-like case. The overall height decreases.

(3T)  $1/l < \omega < \hat{p}$  , Fig.44

Two types of waves are there. One type has the small wave-length of order  $1/\hat{p}$ , and the waves of this type gather near the 4 corners and the 4 rims. Their heights differ so much. The other type has the long wave-length of order  $\omega$  and the very low height. These waves gather around the center and form a slightly wavy plain. The propagator takes nearly 0 value there. This is contrasting with the space-like case. The overall height decreases. Although the scale  $l$  looks to appear as the radius of the plain around the center, the main configuration is free from the boundary effect. This is the "dynamical phase". When  $\hat{p}$  becomes further larger, the configuration approaches a "flat limit". It differs from the flat result, Fig.26.

Figure 42: Warped 5D Massless Vector ( $Z_2$ -parity Even, Neumann-Neumann b.c.),  $\hat{p}=0.005$   
 $\ll T \sim 0.04 \ll 1/l \sim 0.3 \ll \omega=1$ , time-like. App.C.6(1T).

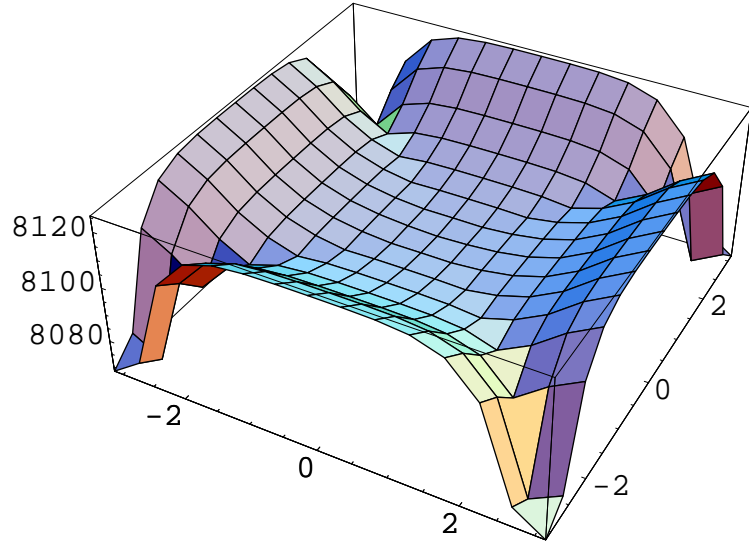


Figure 43: Warped 5D Massless Vector ( $Z_2$ -parity Even, Neumann-Neumann b.c.),  $T \sim 0.04$   
 $\ll 1/l \sim 0.3 < \hat{p} = \omega = 1$ , time-like. App.C.6(2T).

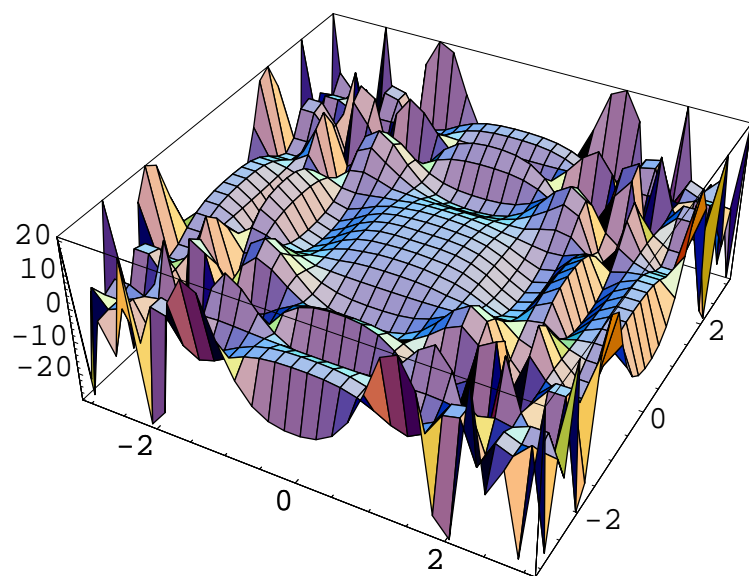
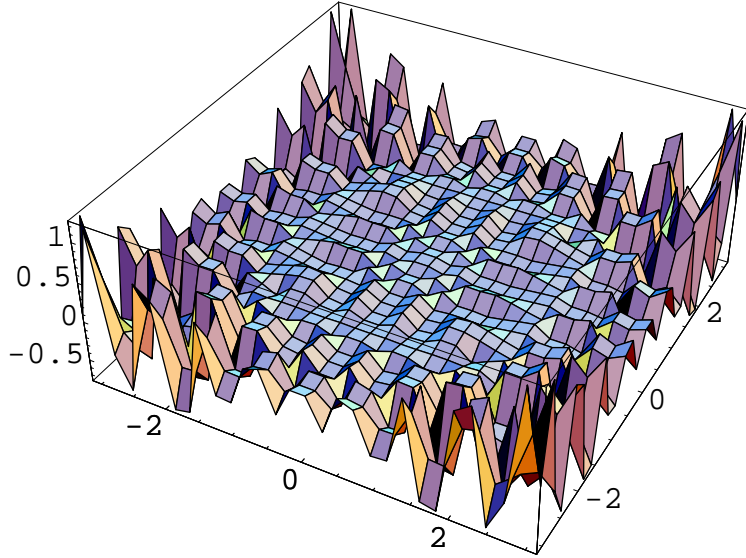


Figure 44: Warped 5D Massless Vector ( $Z_2$ -parity Even, Neumann-Neumann b.c.),  $T \sim 0.04$   
 $\ll 1/l \sim 0.3 < \omega = 1 \ll \hat{p} = 10$ , time-like. App.C.6(3T).



## 15 Acknowledgement

Parts of the content of this work have been already presented at YITP workshop on QFT and String (06.9.12, Kyoto, Japan), Joint Meeting of Pacific Region Particle Physics Communities (06.11.01, Hawaii, Honolulu, USA) and RIKEN Seminar (06.11.27, Wako, Japan). The authors thank N. Nakanishi, Hiroshi Suzuki and K. Oda for useful comments on the occasions.

## References

- [1] L.Randall and R.Sundrum, Phys.Rev.Lett.**83**(1999)3370,hep-ph/9905221
- [2] L.Randall and R.Sundrum, Phys.Rev.Lett.**83**(1999)4690,hep-th/9906064
- [3] K. Agashe, G. Perez and A. Soni, Phys.Rev.**D71**(2005)016002, hep-ph/0408134
- [4] S.J. Brodsky and G.F.de Teramond, hep-th/0702205, "AdS/CFT and QCD"
- [5] J. Garriga and T. Tanaka, Phys.Rev.Lett.**84**(2000)2778, hep-th/9911055
- [6] S.B. Giddings, E. Katz and L. Randall, JHEP**0003**(2000)023, hep-th/0002091
- [7] A. Pomarol, Phys.Rev.Lett.**85**(2000)4004, hep-ph/0005293
- [8] T. Gherghetta and A. Pomarol, Nucl.Phys.**B602**(2001)3, hep-ph/0012378

- [9] L. Randall and M.D. Schwartz, JHEP **0111** (2001) 003, hep-th/0108114
- [10] E. Witten, Nucl.Phys.**B471**(1996)135, hep-th/9602070
- [11] P. Hořava and E. Witten, Nucl.Phys.**B475**(1996)94, hep-th/9603142
- [12] Th. Kaluza, Sitzungsberichte der K.Preussischen Akademie der Wissenschaften zu Berlin. p966 (1921)
- [13] O. Klein, Z. Physik **37** 895 (1926)
- [14] P.A.M. Dirac, "The Principles of Quantum Mechanics", 4th Edition, Oxford Univ. Press, Oxford, 1958
- [15] D. V. Belyaev, hep-th/0509171, "Boundary conditions in the Mirabelli and Peskin model"
- [16] D. V. Belyaev, hep-th/0509172, "Boundary conditions in supergravity on a manifold with boundary"
- [17] S. Ichinose, Phys.Rev.**D61**(2000)055001
- [18] S. Ichinose and A. Murayama, Phys.Lett.**B596** (2004) 123, hep-th/0405065
- [19] T. Gherghetta and A. Pomarol, Nucl.Phys.**B586**(2000)141, hep-ph/0003129
- [20] E.C. Titchmarsh, "Eigenfunction Expansions Associated with Second-order Differential Equations" (Part I), Second edition, Oxford University Press, Oxford, 1962.
- [21] S. Ichinose, Phys.Rev.**D65**(2002)084038, hep-th/0008245
- [22] E.A. Mirabelli and M.E. Peskin, Phys.Rev.**D58**(1998)065002, hep-th/9712214
- [23] S. Ichinose and A. Murayama, Nucl.Phys.**B710**(2005)255, hep-th/0401011
- [24] S. Ichinose and A. Murayama, Phys.Lett.**B593**(2004)242, hep-th/0403080
- [25] S. Ichinose and A. Murayama, hep-th/0606167, "The delta(0) Singularity in the Warped Mirabelli-Peskin Model"
- [26] K. Oda and A. Weiler, Phys.Lett.**B606**(2005)408, hep-ph/0410061
- [27] K. Agashe, R. Contino and A. Pomarol, Nucl.Phys.**B719**(2005)165, hep-ph/0412089
- [28] A. Falkowski, Phys.Rev.**D75**(2007)025017